Technical Report

TR-00-05

Thermo-mechanical effects from a KBS-3 type repository

Performance of pillars between repository tunnels

Eva Hakami, Stig-Olof Olofsson
Itasca Geomekanik AB

March 2000

Svensk Kärnbränslehantering AB
Swedish Nuclear Fuel
and Waste Management Co
Box 5864
SE-102 40 Stockholm Sweden
Tel 08-459 84 00
+46 8 459 84 00
Fax 08-661 57 19
+46 8 661 57 19

Thermo-mechanical effects from a KBS-3 type repository

Performance of pillars between repository tunnels

Eva Hakami, Stig-Olof Olofsson

Itasca Geomekanik AB

March 2000

Keywords: Thermo-mechanical effects, KBS-3, numerical modelling, FLAC^{3D}, temperature, rock mass strength, stability, effective stress analysis

This report concerns a study which was conducted for SKB. The conclusions and viewpoints presented in the report are those of the author(s) and do not necessarily coincide with those of the client.

Abstract

The aim of this study has been to investigate how the rock mass, in the near field of a KBS-3 type repository, will be affected by the excavation of tunnels and deposition holes and the thermal load from the deposited waste. The three-dimensional finite difference program *FLAC*^{3D} was used to perform numerical simulation of the rock mass behaviour. The rock mass was modelled as a homogeneous and isotropic continuum. The initial area heat intensity of the repository was assumed to be 10 W/m² in all models.

The results show that in the middle of the pillar between the repository tunnels the temperature reaches a maximum of about 70 °C after 55 years of deposition. The extent of areas where the rock is predicted to yield depends on the assumed quality of the rock mass and the initial in-situ stress field. The volume of yielded rock reaches a maximum after about 200 years after deposition. For a rock mass with internal friction angle of 45° and cohesion of 5 MPa (using a Mohr-Coulomb material model), the extent of yielded rock is limited to about 1.5 m behind the excavation periphery.

The largest rock displacements are found in the tunnel floor at the upper part of the deposition holes. Tension and shear failure in the periphery of the excavations is predicted to occur during the rock excavation, with a depth extension depending on the magnitude and orientation of the in-situ stresses, as well as on the rock mass quality. Both the excavation effects and the thermo-mechanical effects are smallest when the major principal stress is oriented parallel with the deposition tunnels. The maximum convergence between tunnel walls was calculated to occur after 200 years and be about 9 mm, in the model assuming a rock mass with 5 MPa cohesion, 45° internal friction angle and maximum horizontal stress perpendicular to the tunnel. In this study confining effects from the buffer and backfill material was neglected.

The effective stress concept was used in most of the models, together with the Mohr-Coulomb yield criterion. A comparison between models with and without water pressure shows that, at repository depth, the effect from ground water pressure makes a considerable difference in the prediction of yielded areas.

The results from this study indicate that the central part of the rock pillar between repository tunnels will remain stable and keep its initial properties, on the assumption that the overall quality of the rock mass is good. However, in the rock close to the excavations (< 1 m) the stiffness and strength should be expected to reduce to some extent compared to initial properties.

The cases where major discontinuities intersect the repository area, or major changes in tectonic stresses take place, has not been investigated. Creep (time dependent deformation) in the heated rock mass has also not been considered in this study.

Contents

List of Figures

List of Tables

List of Appendices

1 Introduction

According to the KBS-3 repository concept high level radioactive waste is stored in deposition holes drilled from the floor in tunnels located 500 meters below the ground surface, see Figure 1-1. The excavation of tunnels and deposition holes, as well as the heat generated by the waste, will induce stress changes in the rock surrounding the repository. The stress changes will cause changes in the rock mass properties. The magnitude of the changes depends on magnitude of induced stresses and the rock properties. In the safety assessment of the KBS-3 concept changes in rock properties are of concern, because the changes may influence the ability of the rock mass to effectively isolate the repository waste from the environment.

A multi-phase investigation was previously performed to investigate the global thermo-mechanical aspects of a deep geological repository (Hakami et al., 1998). This investigation focused on the effects on a large scale, i.e., thermo-mechanically-induced changes in the stress-field at a large distance from the repository itself. In the global scale the effects must not be such that the permeability of fracture zones and rock mass is increased to an unacceptable degree. The investigation showed that the global thermal effects depend to a large extent on the geometrical layout of the repository, the heat intensity of the waste and on the mechanical properties of the rock mass at the repository site. Increased compressive stresses and closure of fracture zones were predicted in the region near the repository due to the heat load and at the ground surface a stress reduction and fracture opening were predicted.

Considering the high stresses expected at the repository level, one of the concerns has been the possibility of having an extensive volume of yielded rock closely surrounding the tunnels and deposition holes, as well as in the rock mass between the repository tunnels (pillars). The distance between the tunnels, the magnitude and orientation of the in-situ stress field and the thermal load determines the stress concentrations in the pillars. If the stresses in a pillar exceed the strength of the rock mass, failure may occur that gives rise to deformations and disturbed rock mass conditions.

The aim of this project has been to investigate how the rock mass, in the nearfield of the repository, will be affected by the excavation of tunnels and deposition holes and the thermal load from deposited waste.

The scope of the study is limited to one repository layout and one in-situ stress condition (two different directions for the major principal stress). Furthermore, the analyses performed require idealisation of the problem in different ways. The idealisations will be presented and discussed further in chapter 2: Model Description. Thereafter the calculation results will be presented in the form of selected plots and diagrams. Comparison of results from different models, having different rock properties, will be discussed in this context. A complete presentation of plasticity state plots, for all models and time periods analysed, is given in the appendices. In the chapter that follows, the results are discussed with reference to the idealisations inherent in the model. Finally, the conclusions that may be drawn are summarised.

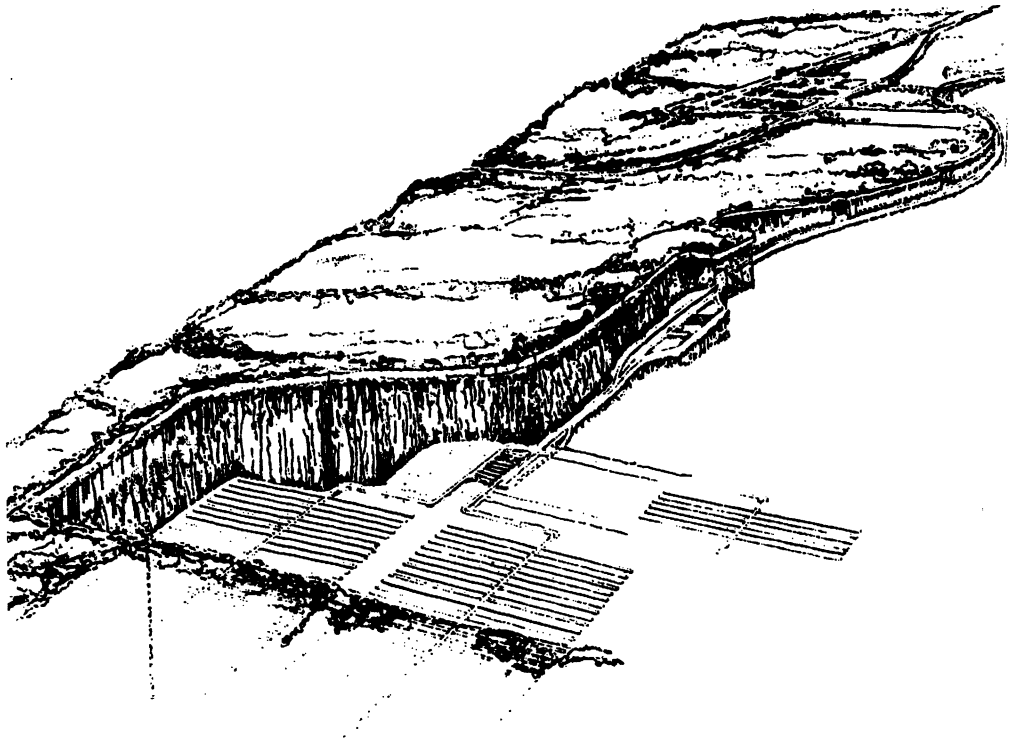

Figure 1-1 Schematic view of a KBS-3 type repository

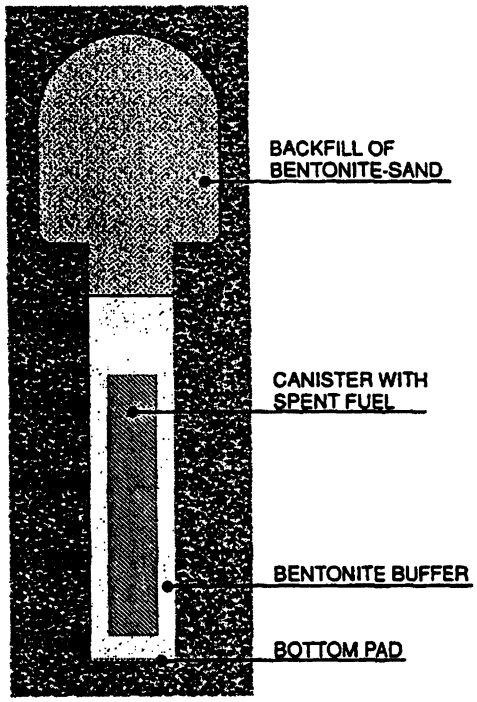

Figure 1-2 Vertical section through repository tunnel at deposition hole in a KBS-3 type repository (not in scale).

2 Model Description

2.1 General

The finite-difference program *FLAC*^{3D} (Itasca, 1997) was selected to perform thermo-mechanical analyses of rock mass behaviour. A three-dimensional analysis is required because the problem geometry (vertical deposition holes and horizontal tunnel system) can not be adequately represented in two-dimensions. *FLAC*^{3D} can be used to make both thermal and mechanical calculations. *FLAC*^{3D} solves problems assuming the rock behaves as a continuum (i.e., discontinuities are not explicitly represented). No rock mass is a true continuum, however, it is often successfully modelled as a continuum material in situations where the important discontinuities are either very widely spaced relative to the excavation size or where the discontinuities are very closely spaced relative to the excavation size, or where the discontinuities are not expected to slip or separate significantly. *FLAC*^{3D} can model a limited number (one or two) individual discontinuities, but this feature has not been used in this study. Thus, the focus of this study has not been the possible induced shearing of single large discontinuities at the repository, but rather the "smeared-out" behaviour of a fairly densely fractured crystalline rock mass, using equivalent continuum material properties.

2.2 Modelling Sequence

Although the *FLAC*^{3D} code can perform fully coupled calculations, due to runtime limitations, it was not possible to perform fully coupled thermo-mechanical calculations for the long time period studied (10 000 years) and the large model size. A partially coupled procedure was therefore adopted in which the thermal and thermo-mechanical calculations were performed stepwise in two models of different sizes. First, thermal calculations were performed using a large model to determine the temperature distribution with time. A large model is required for thermal analysis to avoid boundary effects. Therefore, this model is tall, extending from the ground surface to below the repository (see Section 2.3). Calculated temperatures for each grid point, at selected times, were then "exported" to the smaller model to perform the thermo-mechanical calculations, i.e. the calculated temperatures at the grid points in the central part of the tall model were collected and initiated in the corresponding grid points of the shorter model, giving an instantaneous increase of the temperatures at each step. The boundaries for the mechanical calculation can be much closer than for the thermal model. This step-wise procedure allows some computational economy in running the thermo-mechanical models.

The temperature change is much faster in the early stages of deposition. Therefore, to produce more-or-less equal temperature increments between each modelling step the

time intervals selected are shorter in the beginning of the time span studied. Temperatures were collected and "exported" to the thermo-mechanical models at times 0.5, 2, 6, 12, 25, 50, 200, 1 000, 2 500, 5 000 and 10 000 years after deposition. For each time interval, the stresses and displacements that result from the temperature change increment are calculated.

The thermo-mechanical response of the rock mass surrounding the repository was simulated by adopting the following modelling sequence:

1. Excavation of the repository tunnel.

2. Excavation of the deposition hole.

3. Introduction of ground water pressure (for models M1-M6, M8; see Section 2.6).

4. Initiation of temperatures at the time 0.5 years.

5. Initiation of temperatures at the time 2 years.

(6. – 13 Etc. for following times)

14. Initiation of temperatures at the time 10 000 years.

At each stage, stress changes are induced in the *FLAC*^{3D} model, due to either excavations, ground water pressure introduction or temperature changes, and the stress redistribution required to re-establish equilibrium was calculated before the next step.

2.3 Model Geometry

A KBS-3 type repository consists of a large number of equally spaced parallel tunnels in which the canisters are placed in depositions holes drilled from the floor (SKB, 1992). The distance between repository tunnels is assumed here to be 25 metres and the distance between the deposition holes to be 6 metres. The repeated pattern of parallel tunnels and deposition holes in the KBS-3 layout permits simplification of the repository geometry in a numerical model of the central part of the repository. A quarter-symmetry model was built by using *FLAC*^{3D} that included one "unit" section of a repository tunnel with a deposition hole. The repository is thus simulated as having an infinite horizontal extent. Figure 2-1 shows the assumed layout for the repository and the *FLAC*^{3D} model at the repository horizon.

The thermal and thermo-mechanical calculations were performed in two separate models, due to runtime limitations, (as described in Section 2.2). The difference in geometry between the models was only the height. The thermal calculations were made in a 2 000 meter high model containing 35 500 finite difference zones. The upper horizontal boundary corresponded to the ground surface, 500 m above the floor of the repository tunnel. The lower horizontal boundary was situated 1 500 m below the floor of the repository tunnel.

The thermo-mechanical calculations were performed in models, which were 200 meters high, with the upper surface located 100 m above the floor of the repository tunnel. These models contained 18 000 finite difference zones.

2.4 Thermal Model

2.4.1 Thermal properties

In this study some general assumptions have been made concerning the thermal load, initial conditions, thermal and mechanical properties for the rock mass. These assumptions are consistent with assumptions adopted in previous studies concerning the global thermo-mechanical effects from a KBS-3 type repository, (Hakami et al., 1998).

The thermal properties are assumed to be isotropic, homogenous and constant throughout the rock mass. Heat transfer by conduction in the rock mass is modelled. Neither heat convection by fluid flow nor fluid buoyancy was considered. The thermo-mechanical calculations involved a one-way coupling. Changes in the temperature field affect the stress field through the linear expansion coefficient, but heat generated by friction, for example, was ignored.

The excavated volumes are treated as perfect insulators (i.e. no heat transfer occurs through these volumes). Thermal properties for the rock mass are given in Table 2-1.

Table 2-1 Thermal properties for the rock mass

Property	Value
Specific heat [J/kg°C]	740.74
Thermal conductivity [W/m°C]	3.0
Linear expansion coeff. [1/°C]	8.5E-6

2.4.2 Initial and boundary conditions

The initial temperatures in the rock mass were assumed to increase with depth with a gradient of 0.016 °C per meter, from 7 °C at the ground surface to 15 °C at 500 m depth.

The horizontal boundaries were modelled as fixed temperature boundaries. The upper horizontal boundary representing the ground surface was fixed at 7 °C. The lower horizontal boundary at 1 500 m below the floor of the repository tunnel was fixed at 39 °C. Adiabatic boundary conditions are used for the symmetry planes.

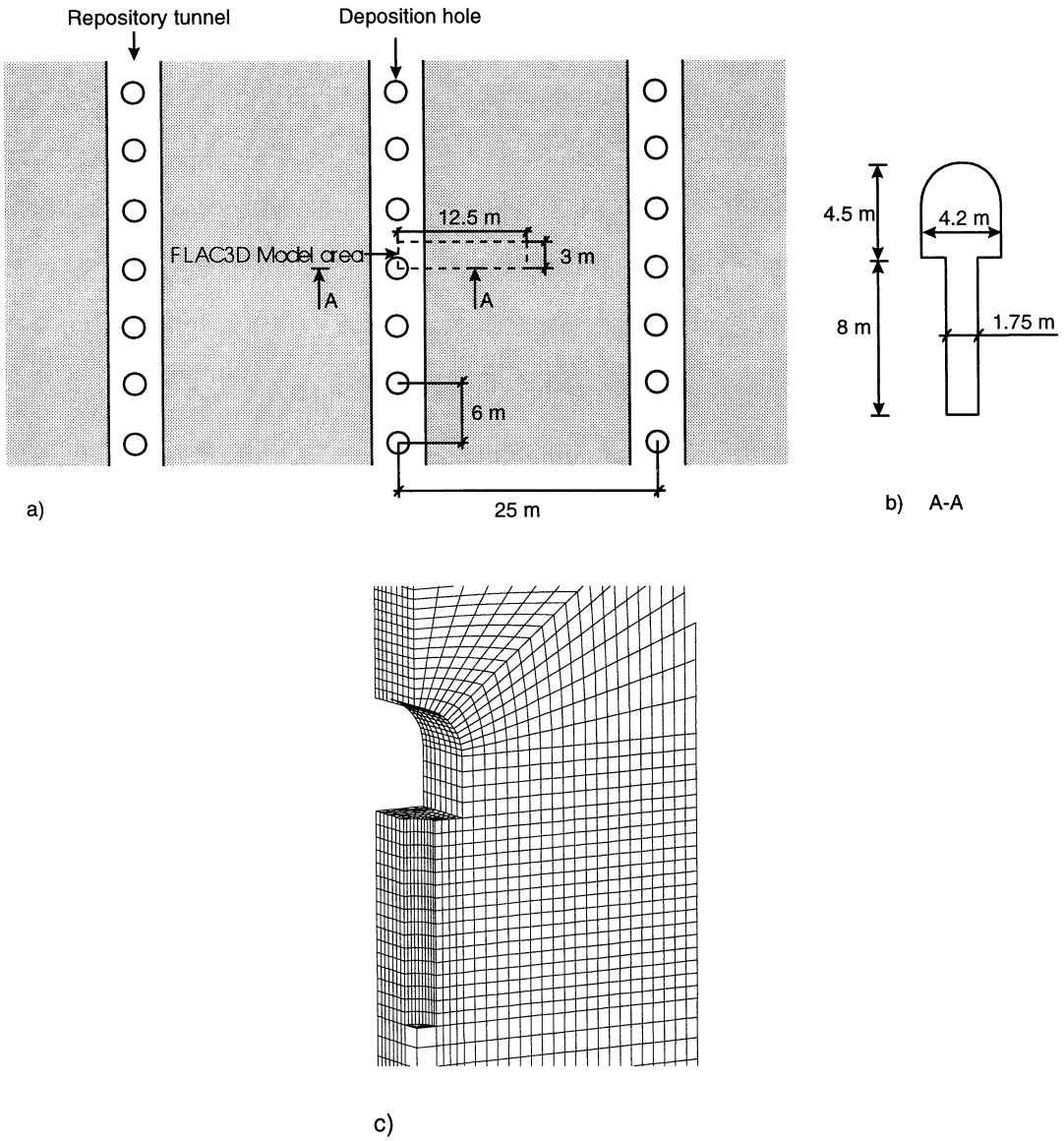

Figure 2-1 Assumed repository layout is given in (a) plan for central part of the repository and (b) section across repository tunnel. (c) FLAC^{3D} finite difference grid at the repository level in perspective. The model extends further 500 m upwards, 1500 m downwards and is totally 2000 m long.

2.4.3 Heat intensity function

Thermal calculations were carried out up to 10 000 years after waste deposition. The heat intensity function used for the first 1 000 years of deposition is defined by the following equation (Thunvik and Braester,1991):

$$Q(t)/Q_0 = \left(\alpha_1 e^{-\alpha_2 t} + (1-\alpha_1)e^{-\alpha_3 t}\right) \quad (2\text{-}1)$$

where $Q(t)$ denotes the time-dependent heat intensity,
Q_0 denotes the heat intensity at the time of the deposition,
t is the time,
$\alpha_1 = 7.531212 \times 10^{-1}$,
$\alpha_2 = 2.176060 \times 10^{-2}$, and
$\alpha_3 = 1.277985 \times 10^{-3}$.

The above function describes the decay well only up to about 1 000 years after the waste deposition. Therefore, for the time period following after 1 000 years, heat intensity ratios according to Table 2-2 were used in the modelling, see (Håkansson, 1999). A linear heat intensity function between the tabulated values was assumed.

Table 2-2 Assumed heat intensity ratios at times after 1 000 years.

t (years)	$Q(t)/Q_0$
970	0.0611
2970	0.0207
9970	0.0119
29970	0.0051

The initial heat intensity for each canister (Q_0), i.e. heat intensity at the time of waste deposition, is set to 1500 W in the models, which is considered as an upper bound for the expected canister heat intensity (Pusch & Touret, 1988; Pusch & Börgesson, 1992). With a canister spacing of 25 m by 6 m, the corresponding initial area intensity becomes 10.0 W/m^2.

Heat conduction through the buffer material was not considered in the thermal model. Thus, the thermal load is applied directly to the deposition hole boundary and the position of the thermal load represents a horizontal projection of the canister on the deposition hole boundary, see Figure 2-2. In reality the heat will spread out also from the top and the bottom of the canister and the temperature at the wall of the deposition hole is therefore somewhat overestimated. However, the total heat release from the canister is correct in the model and minor differences in position of thermal load would not significantly influence the temperature development at a distance from the wall of the deposition hole.

Using a quarter symmetry model means that the model will simulate a situation where all canisters are deposited at the same time and that they all have the same initial heat intensity. In reality, the repository will be filled with waste gradually such that some of the heat will have been already dissipated when the repository is completely filled. Also the model is based on the assumption that no heat is transferred through the vertical boundaries, but only spreads upwards and downwards. This simulates a situation where the repository has infinite horizontal extension. In reality the heat from the repository

will spread out also to the rock beside the repository, i.e. the heat front will become curved. However, for the central part of the repository, temperature analysis has shown that this approximation is reasonable for the first 1 000 years (Claesson and Probert, 1996).

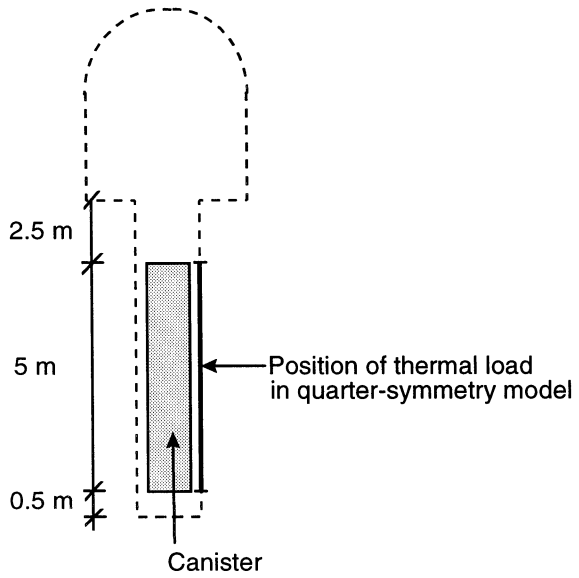

Figure 2-2 Cross section through repository tunnel showing position of applied thermal load in the numerical model.

2.5 Mechanical Model

2.5.1 Rock mass properties

The rock mass is modelled as an isotropic and homogenous elasto-plastic material with a Mohr-Coulomb yield criterion. The rock mass properties are given in Table 2-3. Cohesion values and internal friction angles were varied in different models (see Section 2.6 and Table 2-4). The possible creep (time-dependent) deformation of the heated rock mass was neglected in this study.

Table 2-3 Rock mass properties

Parameter	Value
Density [kg/m³]	2700
Young's modulus [GPa]	30
Poisson's ratio	0.22
Internal friction angle [°]	30, 45
Tensile strength	0
Cohesion [MPa]	1.0, 3.0, 5.0

2.5.2 Initial stresses and boundary conditions for the thermo-mechanical model

The *in-situ* stress state, as measured at Äspö, was taken to be the initial stress conditions of the model. The measured major principal stress is nearly horizontal, the intermediate stress is subhorizontal and the minor stress is close to vertical. Based on the measured results, the initial stresses were assumed to vary with depth, as given by Larsson (1995):

$$\sigma_H = 5.0 + 2\sigma_V \quad (3\text{-}2)$$

$$\sigma_h = 2.5 + \sigma_V \quad (3\text{-}3)$$

$$\sigma_V = \rho g z = 2700 \cdot 9.81 \cdot z \cdot 10^{-6} \quad (3\text{-}4)$$

where z is depth in meters below the ground surface, and stresses are in MPa.

The major horizontal stress (σ_H) was oriented either parallel to the repository tunnel or perpendicular to the tunnel, in different models (see Section 2.5).

The upper horizontal boundary is modelled as a constant stress boundary. The applied stress equals the vertical stress at the depth of 400 m below ground surface. The boundary condition for the symmetry planes and the lower horizontal boundary is zero normal displacement.

In seven of the thermo-mechanical models, hydrostatic water pressure resulting from a groundwater surface located at ground surface was introduced following excavation of the tunnel and deposition hole. The original ground water levels are restored immediately when the repository is sealed. A mechanical pressure equal to the hydrostatic pressure was also applied at the same time to the boundaries of the repository tunnel and deposition hole. This simulates the water pressure in the filling material. Effective stresses (i.e., total stresses minus water pressure) are then used in the analysis when comparing stress state in the rock with the specified rock strength criterion, i.e. the Mohr-Coulomb yield envelope. The swelling pressure from the compacted bentonite and the tunnel backfill was, however, not accounted for in the models of this study.

One thermo-mechanical model was run without initiating hydrostatic water pressure, model M7. This model is used to check the influence of the conservative hydraulic assumption mentioned above. Also, some previous thermo-mechanical modelling (Hakami et al., 1998) has been carried out without introducing ground water pressure.

2.6 Models analysed

The stress state around the actual repository tunnel will be dependent on many different factors such as: the initial stress conditions, water pressure distribution and the properties of the rock mass. Both cases having the major horizontal stress either perpendicular to the tunnel or parallel to the tunnel were considered. Effective stress

analysis was carried out assuming a simplified water pressure distribution. Also one analysis was performed without water pressure. Finally, the influence from differences in rock mass parameters was analysed in terms of varying the cohesion and the internal friction angle. A total of eight thermo-mechanical models were analysed as listed in Table 2-4.

The repository geometry, thermal heat load and all other rock mass parameters were kept constant in the models analysed.

Table 2-4 List of thermo-mechanical models

Model	Direction of major horizontal stress relative to repository tunnel axis	Rock mass cohesion [MPa]	Rock mass internal friction angle [°]	Water pressure introduced after sealing
M1	Parallel	5	30	Yes ('effective stress')
M2	Parallel	3	30	Yes ('effective stress')
M3	Parallel	1	30	Yes ('effective stress')
M4	Perpendicular	5	30	Yes ('effective stress')
M5	Perpendicular	3	30	Yes ('effective stress')
M6	Perpendicular	1	30	Yes ('effective stress')
M7	Parallel	5	30	No ('total stress')
M8	Parallel	5	45	Yes ('effective stress')

3 Results

3.1 Temperature Distribution

The temperature increases rapidly close to the canisters directly after the deposition. The temperature front moves outwards and the heated rock volume gets increasingly larger. Therefore, when determining maximum temperature or the temperature distribution, this would apply only for a specified point or at a specified time, respectively. As an example, the temperature contours at the repository level 50 years after deposition are shown in Figure 3-1. The temperature at the deposition hole boundary is close to maximum at this time.

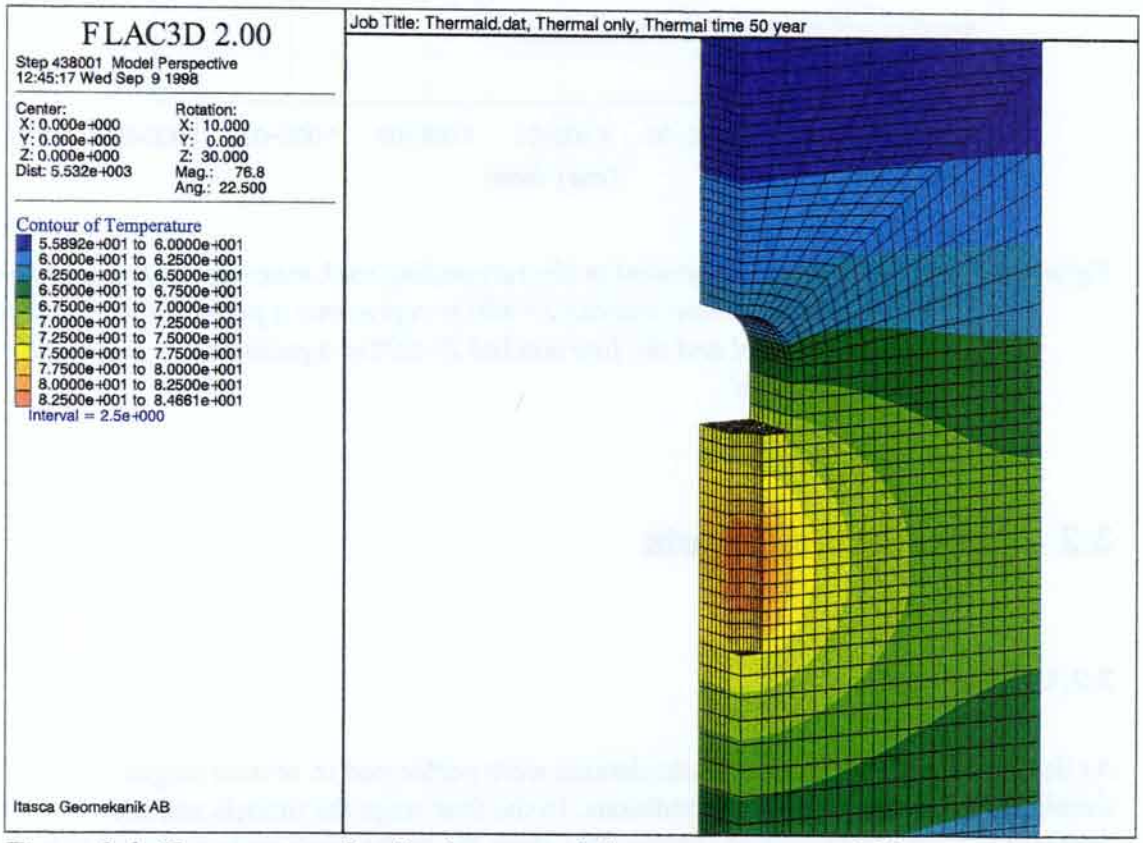

Figure 3-1 Temperature distribution around the repository tunnel 50 years after deposition. Initial area heat intensity is 10 W/m^2, corresponding to an initial canister heat intensity of 1500 W.

The temperature development with time at selected points in the model is shown in Figure 3-2. A maximum temperature of 85 °C is reached at the deposition hole boundary after approximately 44 years of heating. At point 4, situated in the pillar midway between adjacent repository tunnels, a maximum temperature of about 70 °C is reached

after 55 years, and this temperature is more or less maintained till about 800 years after deposition. At a vertical distance of 100 meters, below and above the repository tunnel (Z=400 and Z=600), the maximum temperature is reached at about 1000 years after deposition.

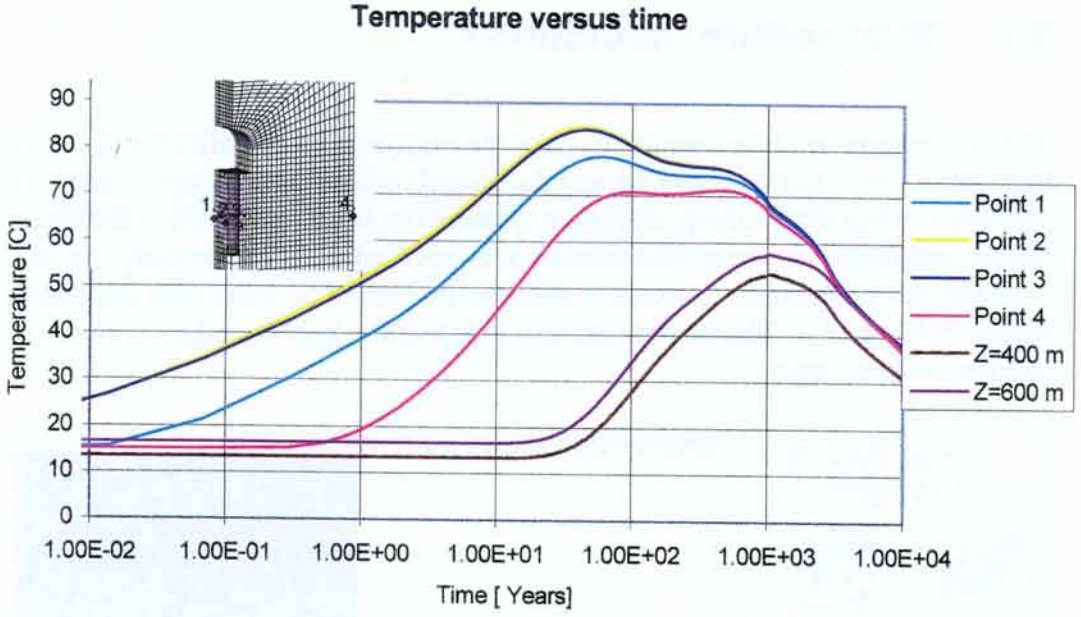

Figure 3-2 Temperature development in the surronding rock mass due to heating from the canisters. The line marked Z=400 m represents a point 100 m above the repository tunnel and the line marked Z=600 m a point 100 m below the repository tunnel.

3.2 Excavation Effects

3.2.1 General

As described in Section 2.2 the calculations were performed in several stages, simulating different repository conditions. In the first stage the tunnels and the deposition holes are excavated. During this stage the water pressure is assumed to be zero in the whole model, corresponding to a situation where the repository area is fully drained. The equilibrium state after this stage is presented first and is called "total stress analysis" (the effective stress here equals the total stress).

In next step a water pressure corresponding to the depth below ground water surface is applied in the model and a new equilibrium is calculated. These analyses, here called "effective stress analyses" are presented in the following section. The results are dependent on how the water pressure is introduced into the model, and this is discussed in the last section.

3.2.2 Total stress analysis

The excavation of repository tunnel and deposition hole gives rise to stress redistribution in the surrounding rock. As an illustration, the minor and major principal stresses for model M1 are shown in Figure 3-3 and Figure 3-4. In model M1, the major horizontal principal stress is initiated parallel to the repository tunnel. The minor principal stress decreases near the excavation boundary and is zero on the excavation boundary. (Note that compressive stresses are negative.) The initial major principal stress at the repository level is about 31.5 MPa.

The stress and boundary conditions cause the rock mass to yield (i.e., fail) around the excavation boundaries. Yielded zones have reached the shear strength and/or tensile strength as given by the Mohr-Coulomb yield envelope. (The plasticity states in individual zones of the model after excavation of repository tunnel and deposition hole are shown for the different models in Appendix A.) Yielding around the excavation boundary (see App. A-2) causes the major principal stresses to diminish. Outside the yielded volume, the major principal stresses are mainly unchanged from the initial stress level. Near the deposition hole the major principal stress rises to 40 MPa.

Stress plots for model M4 are shown in Figures 3-5 and 3-6. In model M4 the rock properties are the same as in M1, but the major horizontal principal stress is initiated perpendicular to the repository tunnel. It can be seen how the minor principal stress decreases near the excavation boundary and is zero on the excavation boundary. The major principal stress is amplified, by the excavation, in the tunnel roof and the tunnel floor. Stress levels reach 60 MPa. In the pillar between repository tunnels the major principal stress relaxes, from 31.5 MPa down to about 20 to 25 MPa.

Rock mass displacements for model M6 are given in Figure 3-7. Model M6 gives the largest excavation induced rock mass displacements among the models, because the cohesion is only 1 MPa and the direction of the major principal stress is perpendicular to the tunnel. Maximum displacement of nearly 17 mm occurs in the floor of the repository tunnel.

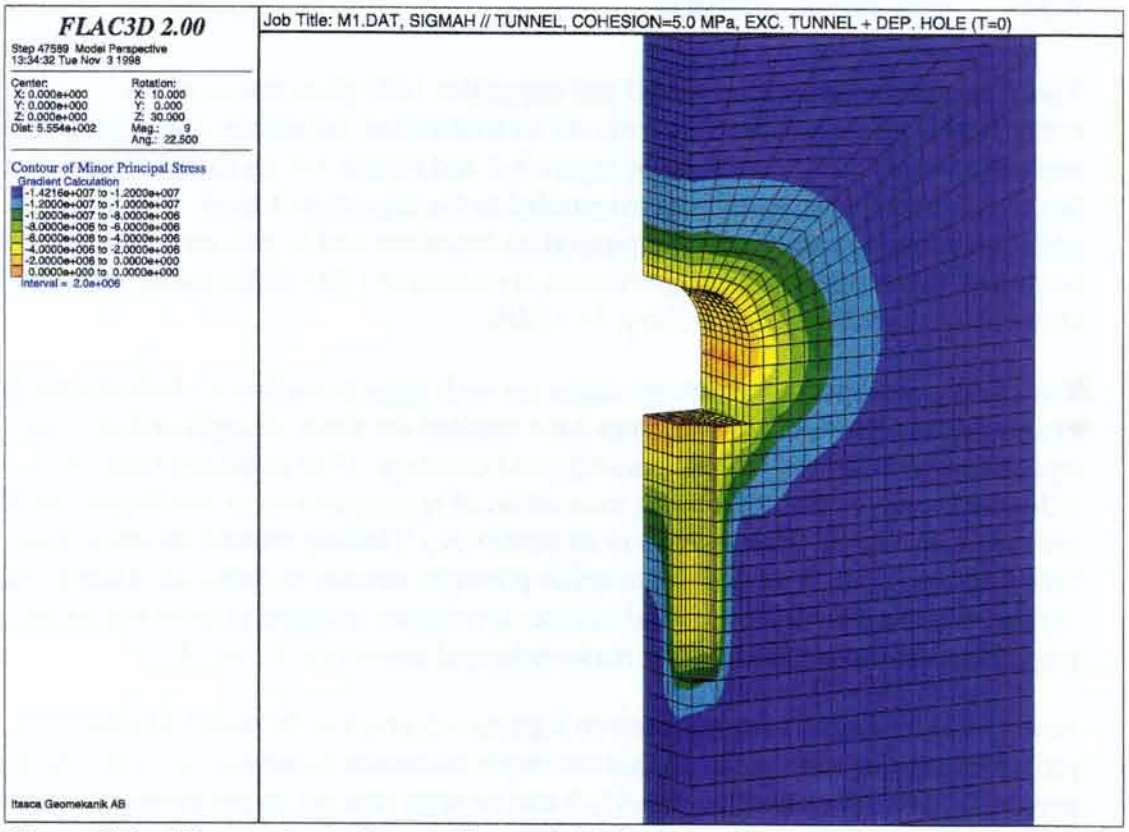

Figure 3-3 Minor principal stress for model M1. Major horizontal principal stress applied parallel to the repository tunnel in model M1.

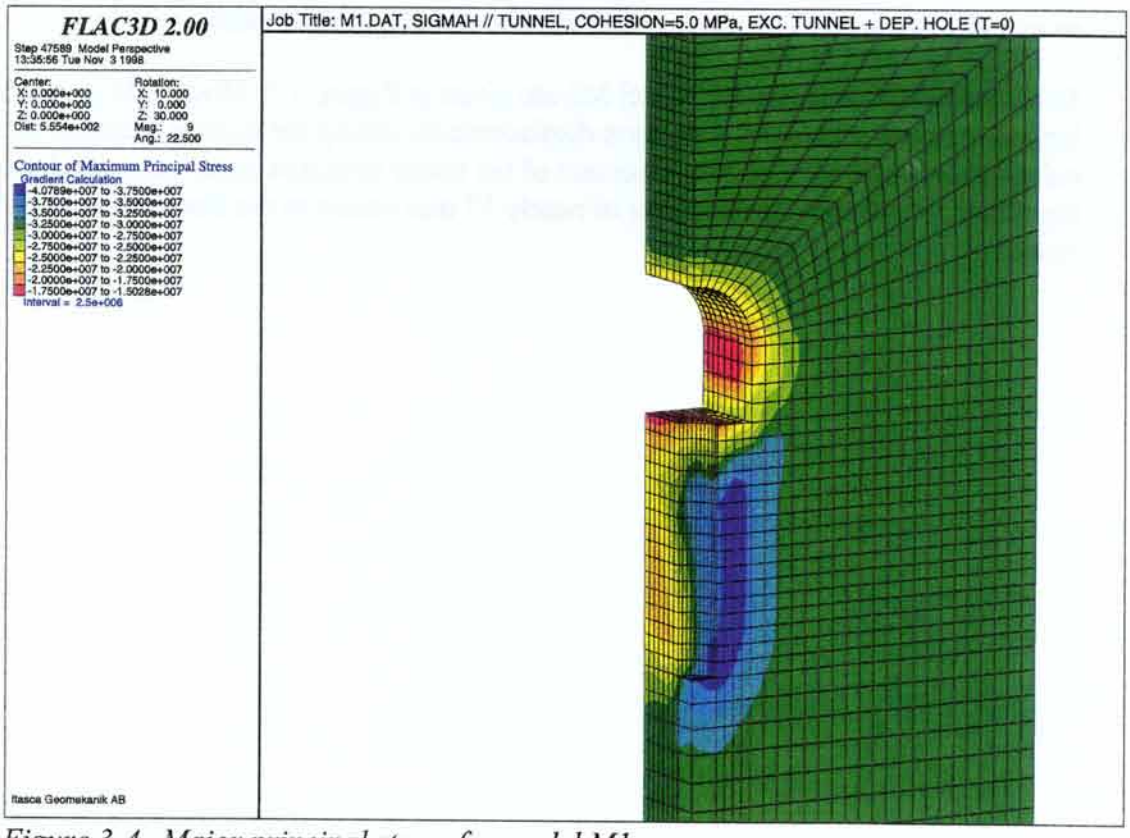

Figure 3-4 Major principal stress for model M1.

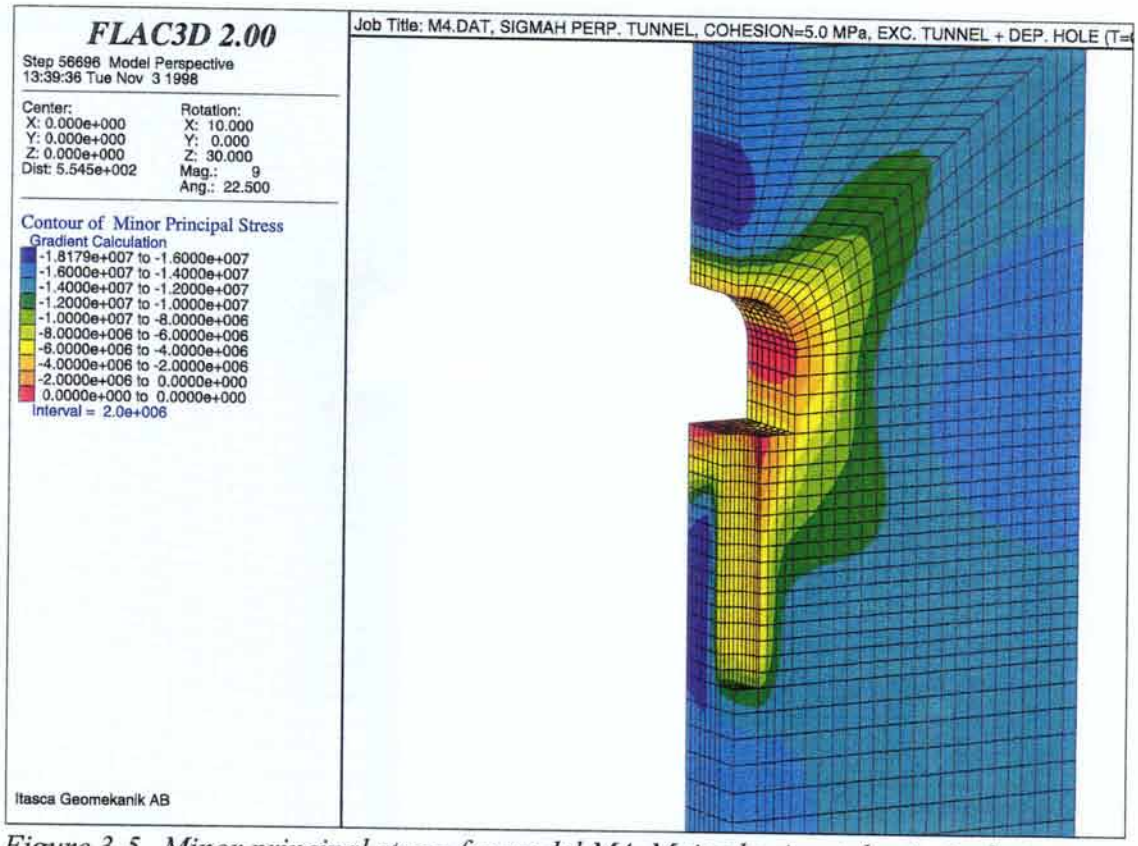

Figure 3-5 Minor principal stress for model M4. Major horizontal principal stress applied perpendicular to the repository tunnel.

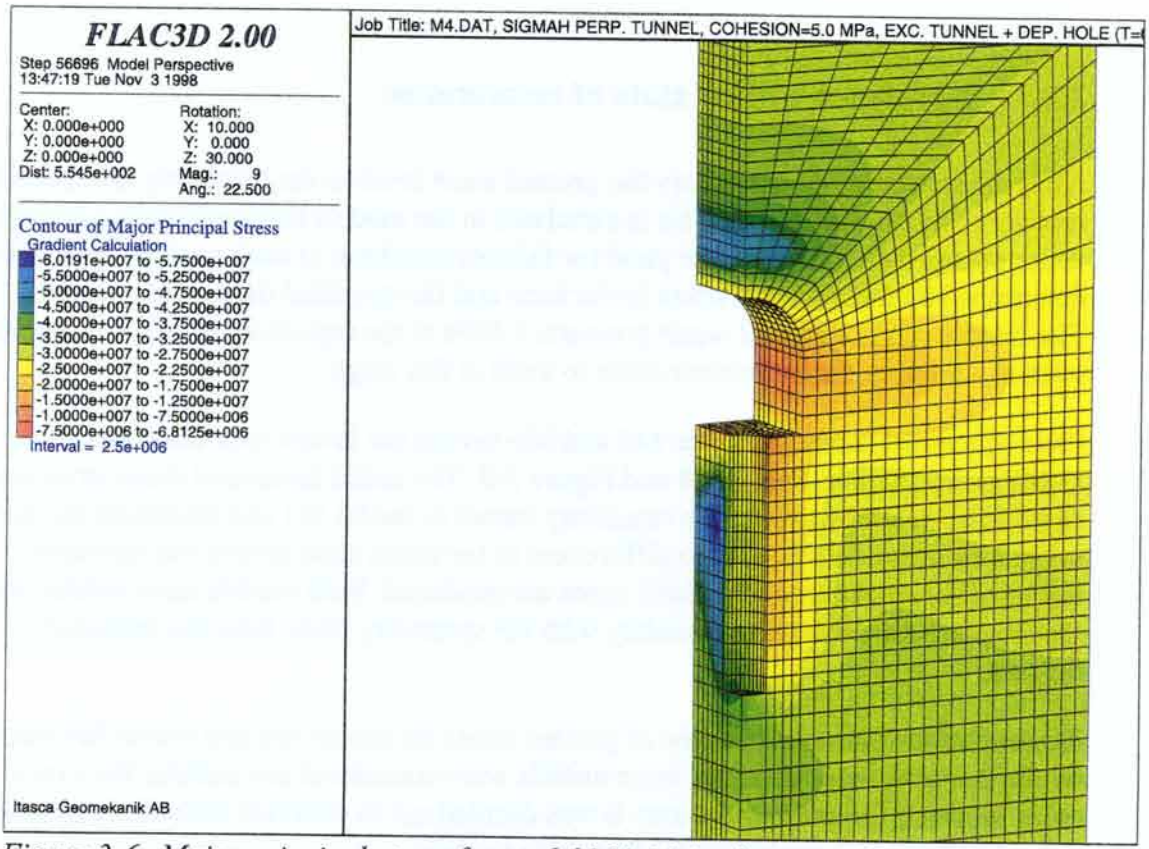

Figure 3-6 Major principal stress for model M4. Major horizontal principal stress applied perpendicular to the repository tunnel.

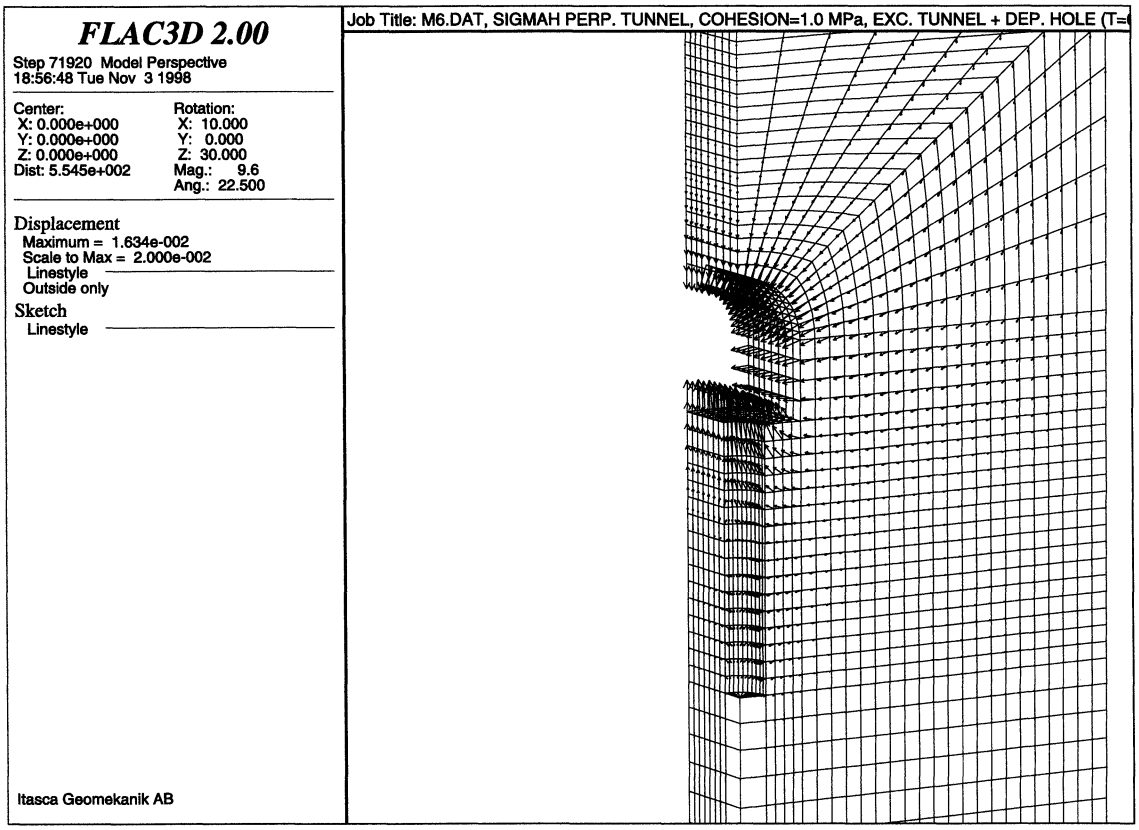

Figure 3-7 Excavation induced rock mass displacements for model M6. Displacement unit is metres.

3.2.3 Simulation of final state of resaturation

After the sealing of the repository the ground water level in the repository is expected to recover to its original levels. This is simulated in the models by introducing a ground water pressure distribution. The yield (or failure) condition of each zone of the model is determined by the effective stress in the zone and the specified rock mass properties. The introduction of ground water pressure, 5 MPa at the repository level, causes zones even at a distance from the excavation to yield at this stage.

Plots of yielded zones for model M3 and M6 having the lowest rock mass cohesion (1 MPa) are given in Figure 3-8 and Figure 3-9. The initial horizontal major principal stress is assumed parallel to the repository tunnel in model M3 and perpendicular to the repository tunnel in M6. Due to differences in the stress state around the repository tunnel different patterns of yielded zones are produced. Both models have yielded zones that connect the excavation boundary with the symmetry plane between repository tunnels.

Because of the extensive volume of yielded zones for model M3 and model M6 caused by the low rock mass strength, these models were considered not realistic for a rock mass accepted for a repository site. It was decided not to continue with the subsequent thermo-mechanical modelling for these two models.

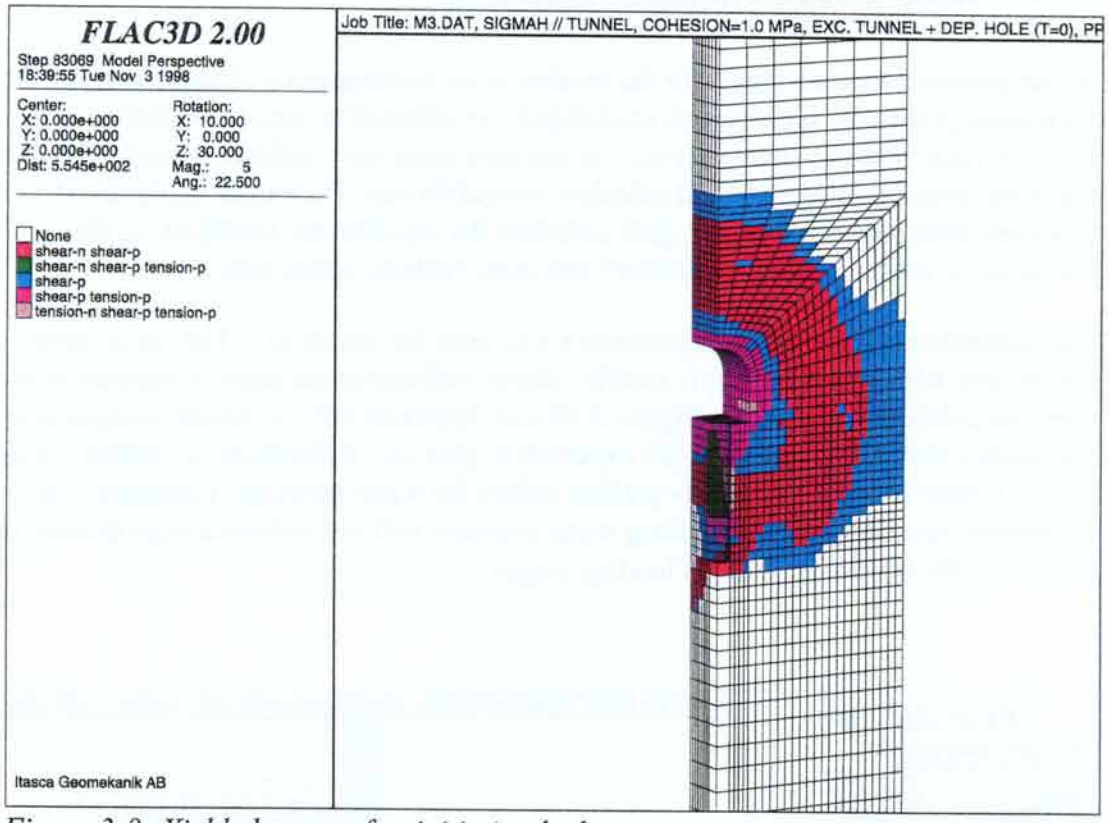

Figure 3-8 Yielded zones after initiating hydrostatic water pressures for Model M3. Major principal stress applied parallel to the repository tunnel.

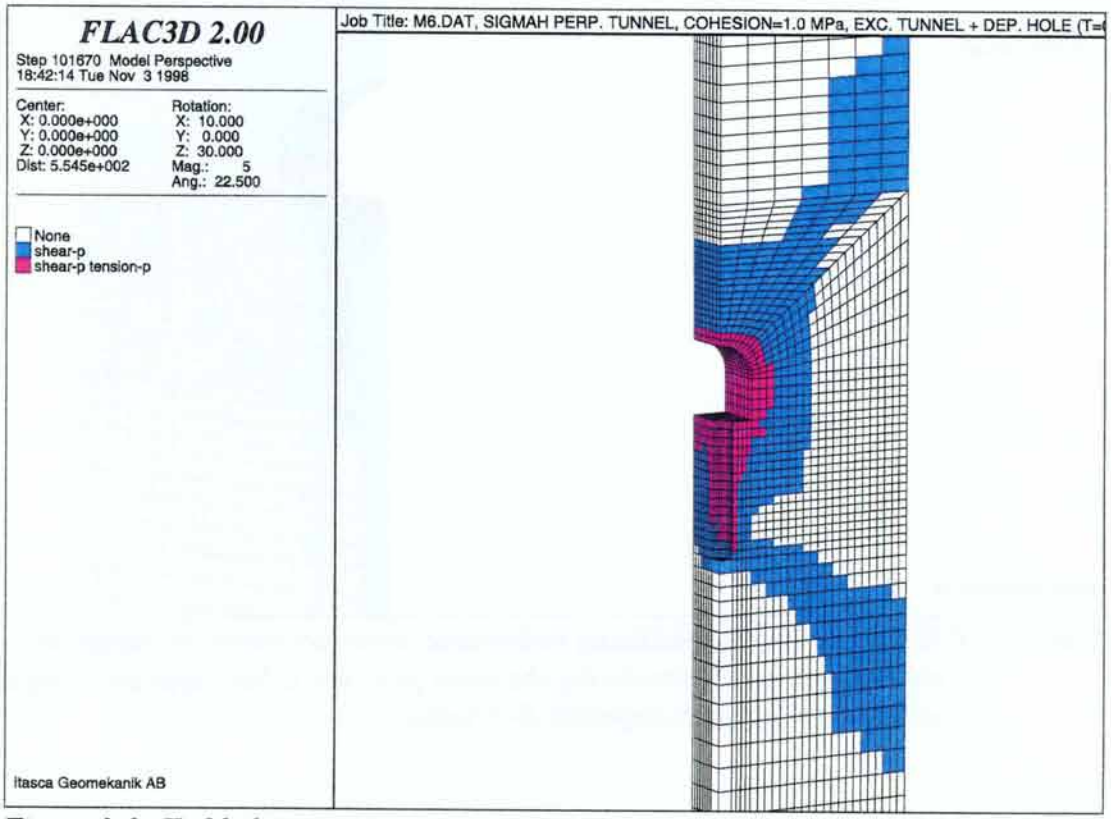

Figure 3-9 Yielded zones after initiating hydrostatic water pressures for Model M6. Major principal stress applied perpendicular to the repository tunnel.

3.2.4 Water pressure initiation procedure

Water pressure was introduced in the models as an instantaneous change, keeping the rock mass properties and strength unchanged. An alternative way of modelling is to let the rock mass respond elastically (i.e. let the rock mass have infinite strength) first when the water pressure is applied and calculate to equilibrium. Thereafter apply the Mohr-Coulomb strength criterion and again calculate the equilibrium condition. In this way the model is subjected to a "smoother" and more realistic stress path.

For comparison, the alternative procedure was used for model M1. The result shows that the volume with yielded zones is smaller, about half-maximum depth compared to the previous calculation (compare Figure 3-10 and Appendix B2). A similar comparison for the models with lower cohesion are expected to give less differences in yielded volumes because more zones have already yielded before the water pressure is initiated. The alternative procedure for introducing water pressure will not influence significantly the results for the following thermal loading stages.

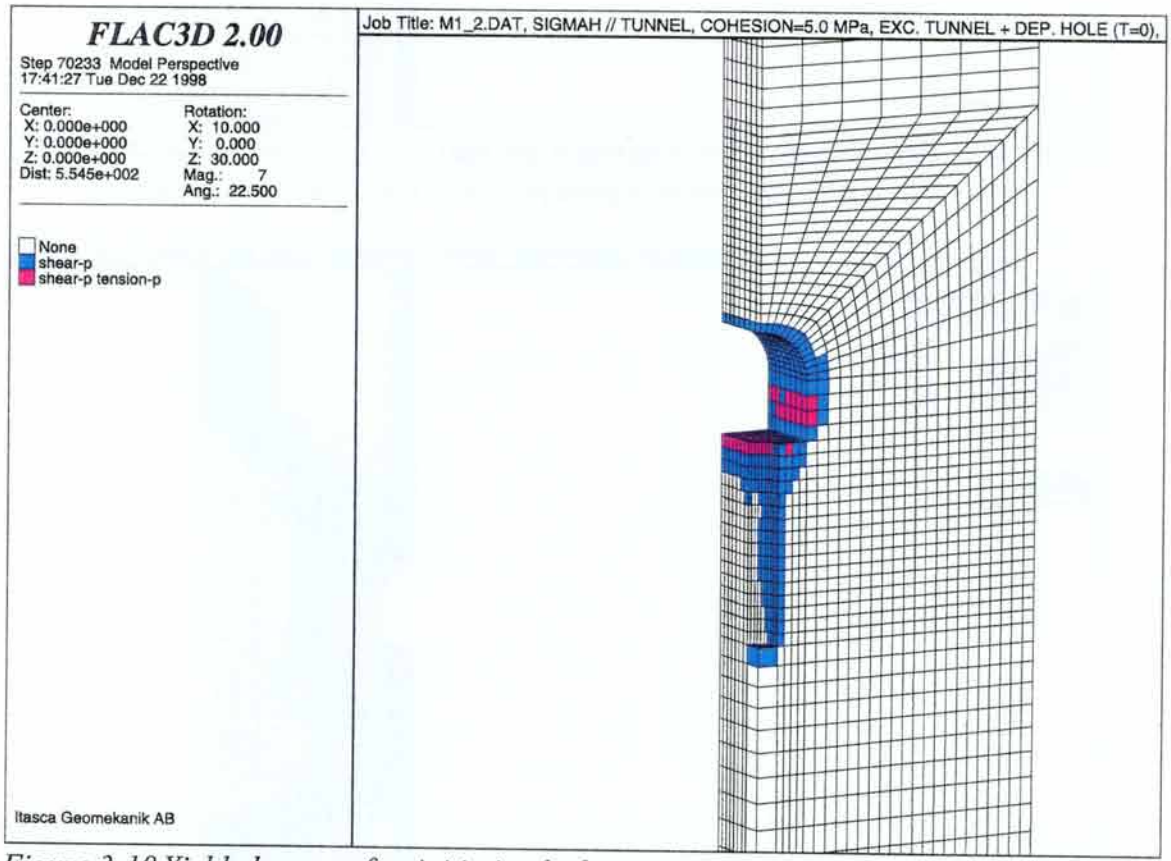

Figure 3-10 Yielded zones after initiating hydrostatic water pressures for Model M1. An alternative way of introducing the water pressure is here applied. Compare with plasticity plot in Appendix B-2 (upper).

3.3 Thermo-Mechanical Effects

3.3.1 Plasticity state of the zones

Plasticity state indicators show the condition of individual zones at selected times. Of particular interest are plasticity state indicators that show activated or yielding zones (i.e., zones that are failing) for the particular time interval. It is important to note, however, that due to stresses redistribution and changes in thermal loading a zone can be yielding for one time interval and not for another time interval.

Plots of yielded zones for model M1 and model M4 at time interval 50 - 200 years are shown in Figures 3-11 and 3-12. At this time interval, the most extensive volumes of yielded zones are produced in both models. It can be noted that the difference in the initial stress orientation between model M1 and M4 influences the yield pattern in rock mass surrounding the repository.

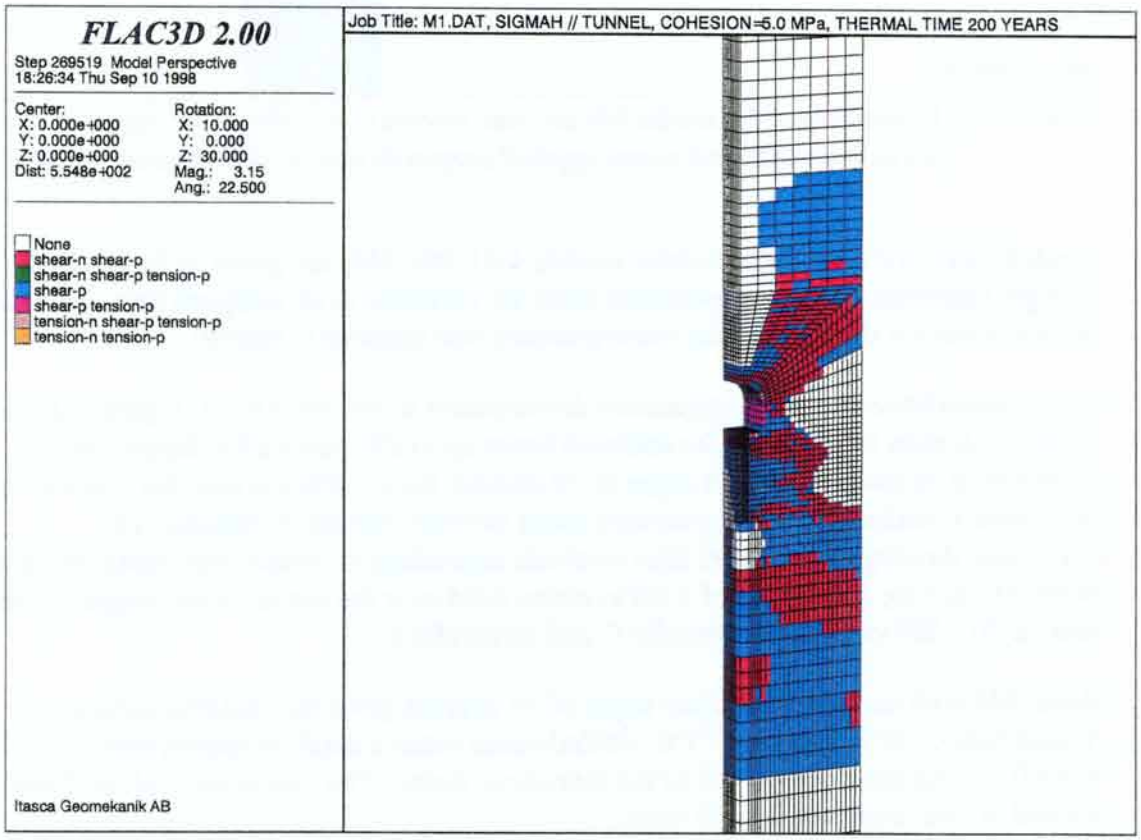

Figure.3-11 Yielded zones for model M1 for time interval 50 - 200 years. Major horizontal principal stress applied parallel to the repository tunnel.

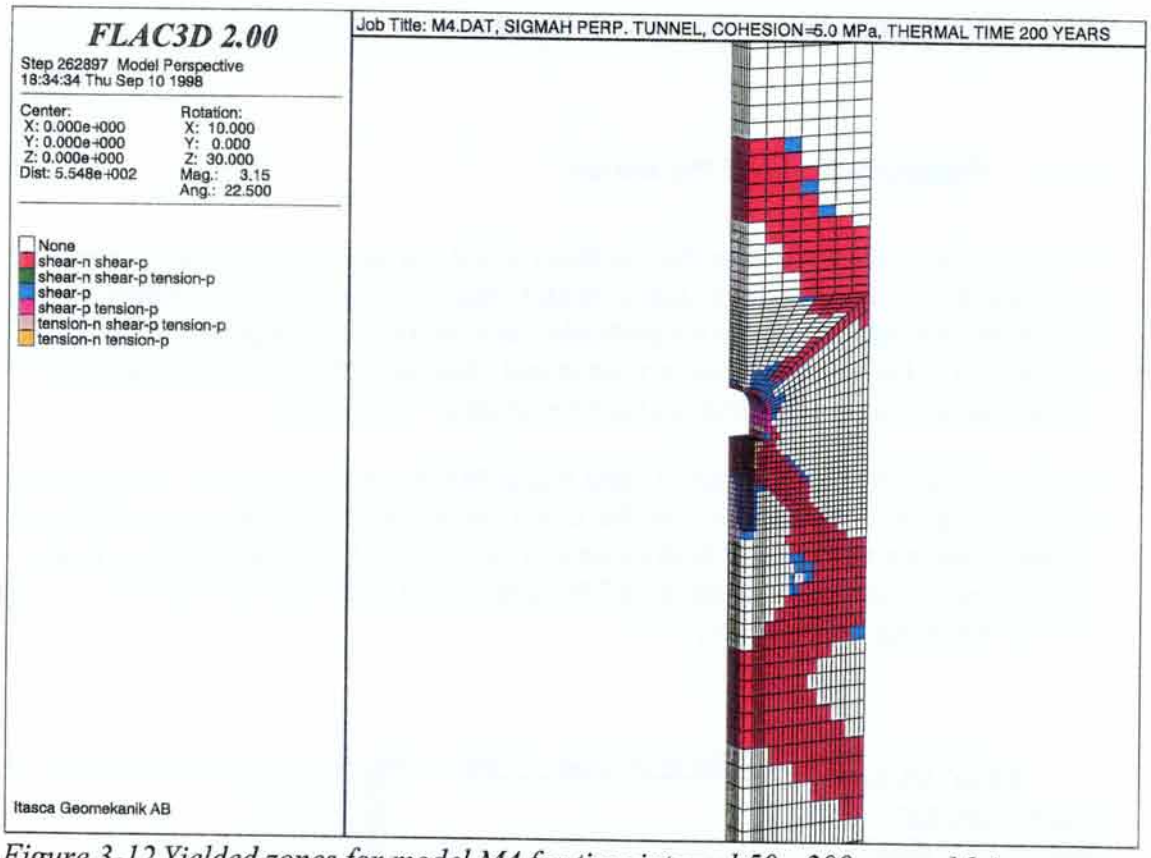

Figure 3-12 Yielded zones for model M4 for time interval 50 - 200 years. Major horizontal principal stress applied perpendicular to the repository tunnel

Yielded zones for the effective stress models (M1-M6, M8) are given in Appendix B through Appendix F. In the appendices plots are collected at all analysed times including yielded zones for the stage when water pressure was initiated (Time=0).

In correspondence with the temperature development in the models (cf. Figure 3-2), the yielding volumes increase for the analysed times up to 200 years after deposition. All models with an internal friction angle of 30 degrees have yielded zones that connect the excavation boundary with the symmetry plane between repository tunnels. The connection develops at different time intervals depending on model. For model M2 and model M5 having a cohesion of 3 MPa, zones yield over the entire model height at time interval 50 - 200 years, see Appendix C and Appendix E.

Model M8 with an internal friction angle of 45 degrees gives the smallest volume of yielded zones, see Appendix F. The yielded zones reach a depth of approximately 1.5 m in the floor and parts of the wall of the repository tunnel. The maximum yielded depth is reached at time interval 50 - 200 years.

At 1 000 years after deposition, temperatures near the repository level have started to decrease which reduces the yielding volumes near the repository level, see for example Appendix B-6 Time interval 200 - 1 000 years.

Cooling throughout the model starts after 1 000 years of deposition. For the analysed time intervals 1 000 - 2 500, 2 500 - 5 000 and 5 000 - 10 000 years, the yielding volume

is reduced and yield occurs close to the repository tunnel and the deposition hole, see for example Appendix B-6 and B-7.

3.3.2 Stress distribution

Effective principal stresses were calculated along a vertical scanline, see Figure 3-13.

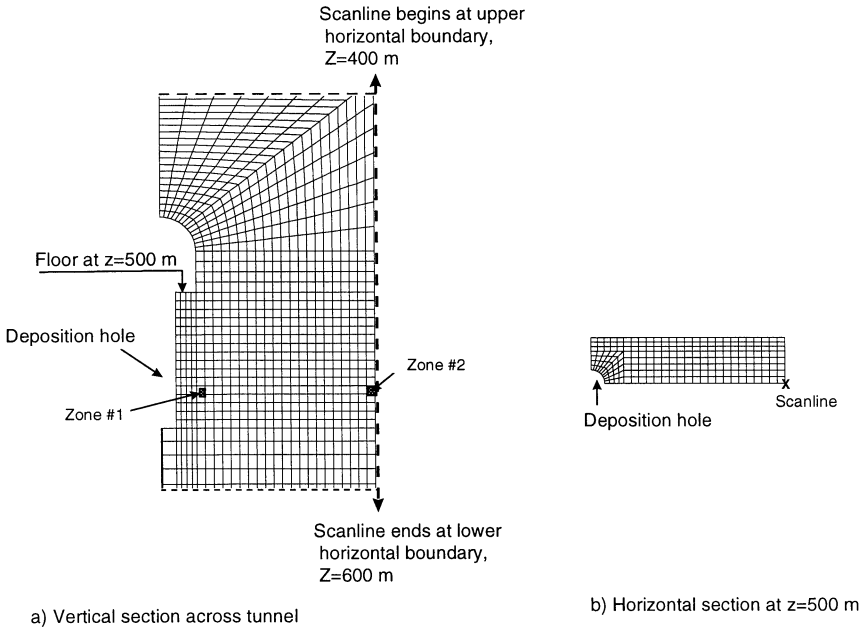

Figure 3-13 Position of scanline used to record effective principal stresses and two zones for illustration of stress paths (see Section 3.3.5).

Effective major and minor principal stresses along the scanline for model M1, M4 and M8 are given in Figures 3-14, 3-15 and 3-16. Stresses are given at elapsed times 12, 1000 and 10 000 years after deposition.

The effective major principal stress changes with thermal loading. The effective major principal stress at 1 000 years after deposition shows a stress relaxation above and below the repository level. The relaxation is caused by the yielded areas along the scanline (see Appendix B). The relaxation of the effective major principal stress is evident even at time 10 000 years when the stress levels are within the elastic regime. Note that the minor principal stresses are mainly unaffected during the thermal loading. The minor stress is vertical in most part of the model and is determined by the weight of the overlying rock.

In agreement with the yield state plot, the stress curves for M4 indicates excess stresses around the repository for model M4. Similarly, for model M8 the rock mass will also experience a increase in major effective stress of 10-15 MPa in the whole heated rock

volume, but no failure is predicted along the scanline in the pillar centre, due to the higher strength properties in this model.

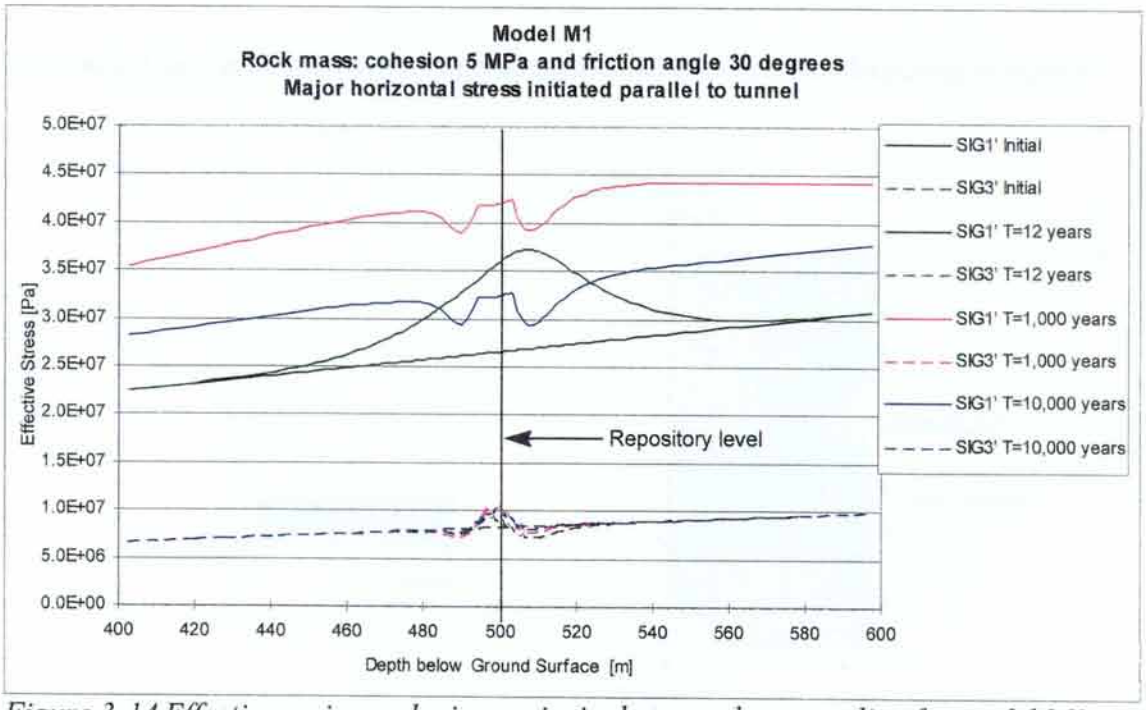

Figure 3-14 Effective major and minor principal stress along scanline for model M1. Stress situation is presented for initial stage and after 12 years, 1000 years and 10 000 years of deposition, see legend.

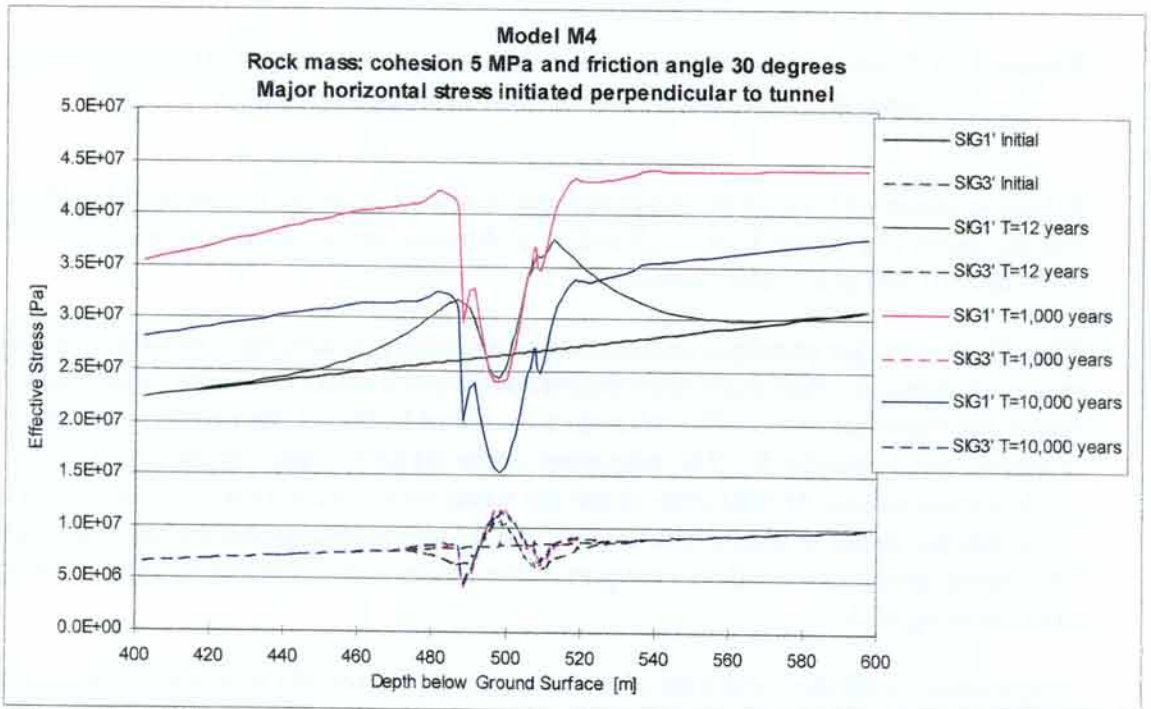

Figure 3-15 Effective major and minor principal stress along scanline for model M4 Stress situation is presented for initial stage and after 12 years, 1000 years and 10 000 years of deposition, see legend.

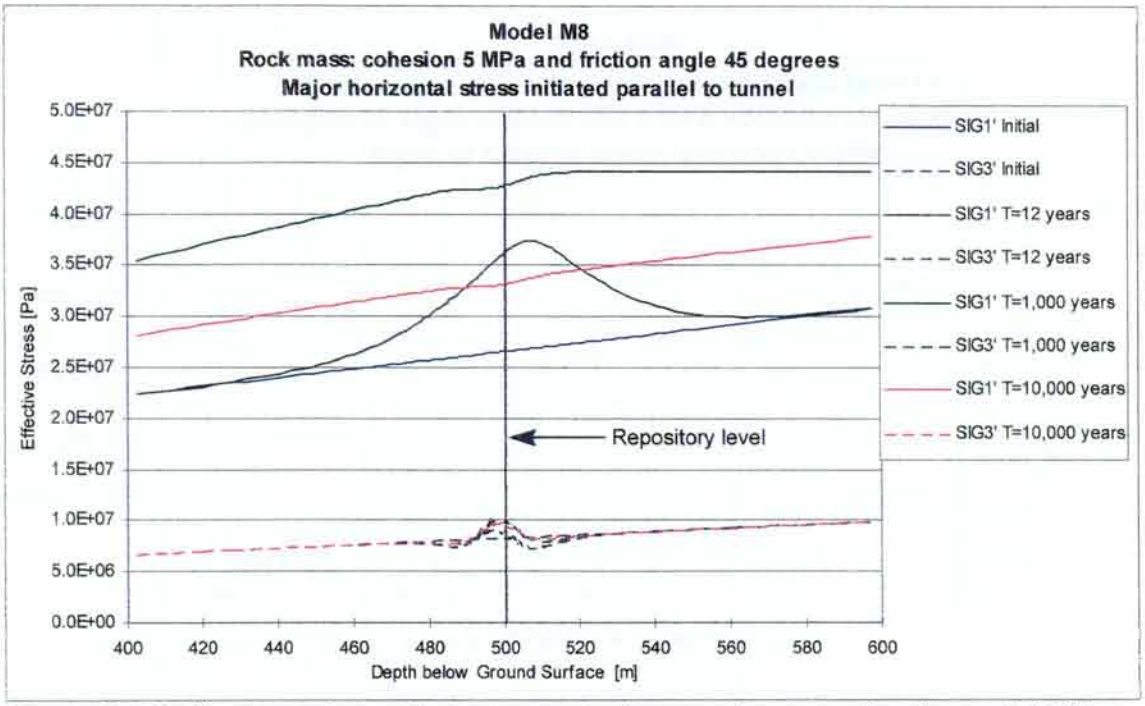

Figure 3-16 Effective major and minor principal stress along scanline for model M8. Stress situation is presented for initial stage and after 12 years, 1000 years and 10 000 years of deposition, see legend.

3.3.3 Rock mass displacement

The gradual increase in temperature causes an expansion of the rock mass and, since the rock mass is confined in all directions but upwards, the main induced displacement is a heave of the whole repository area. To illustrate this, the vertical displacements at four different times are shown in graphs below for the same scanline and models as for the stresses (see Figures 3-17, 3-18 and 3-19).

The maximum heave occurs after 1 000 years of deposition and is about 13 cm. This order of magnitude agrees with the results from the previous global study, using the *3DEC* code (Hakami et al., 1998).

The vertical displacement depends to some extent on the plasticity state of the zones in the model and therefore the slope of the displacement curves changes with depth. In areas around the repository, where yield is predicted, displacement gradients are larger, indicating larger vertical strains (see model M4).

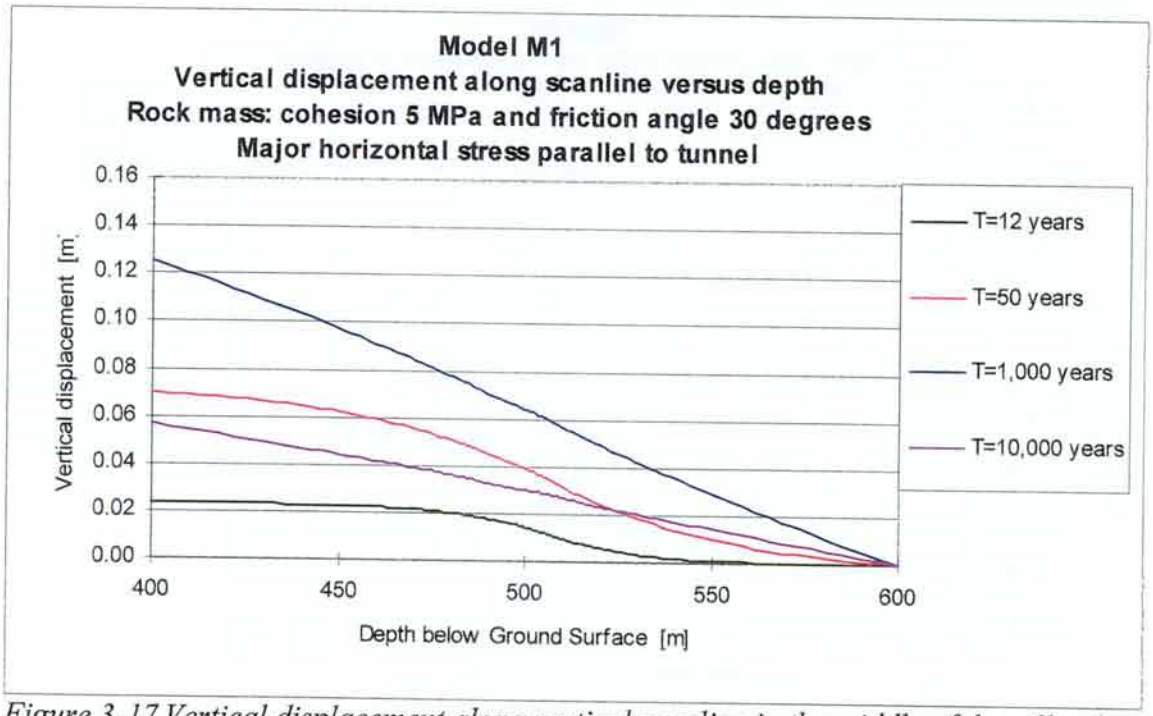

Figure 3-17 Vertical displacement along vertical scanline in the middle of the pillar for model M1. The curves correspond to different times after deposition (see legend). The repository is located at 500-m depth.

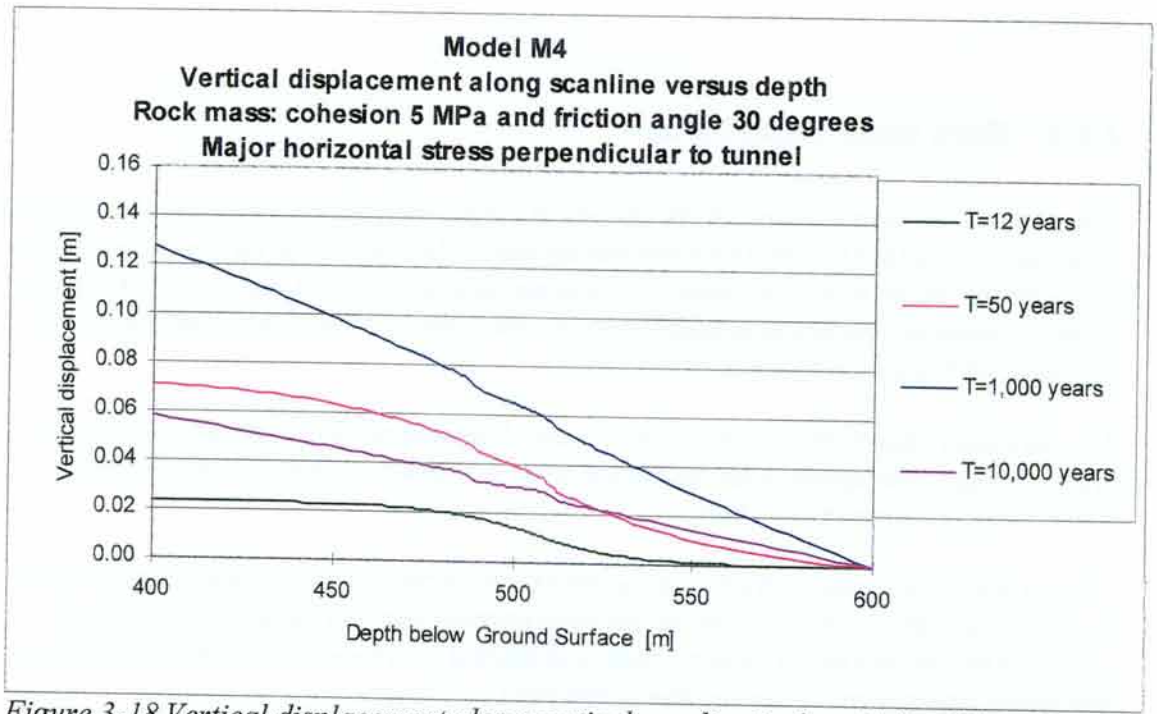

Figure 3-18 Vertical displacement along vertical scanline in the middle of the pillar for model M4. The curves correspond to different times after deposition (see legend). The repository is located at 500-m depth.

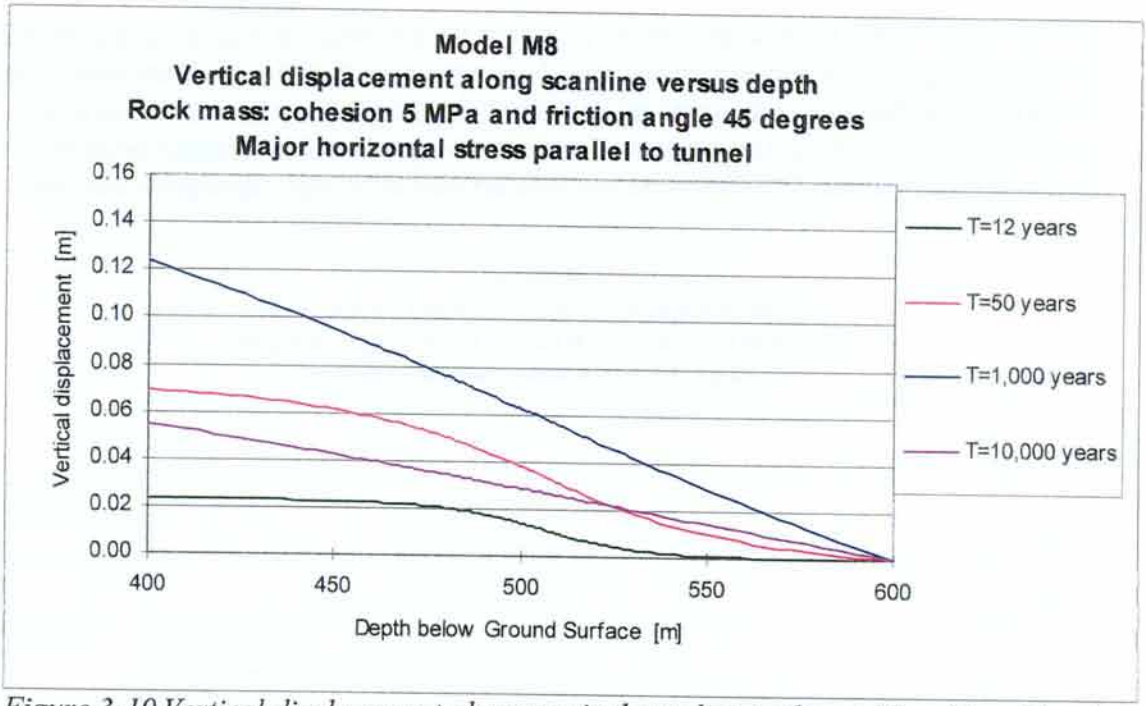

Figure 3-19 Vertical displacement along vertical scanline in the middle of the pillar for model M8. The curves correspond to different times after deposition (see legend). The repository is located at 500-m depth.

3.3.4 Convergence

In addition to the vertical uplifting of the repository the rock mass around the excavations will also move inwards towards the openings. The calculated convergence at four points in the model (see Figure 3-20) are presented in diagrams for model M1, M4 and M8 in Figures 3-21, 3-22 and 3-23.

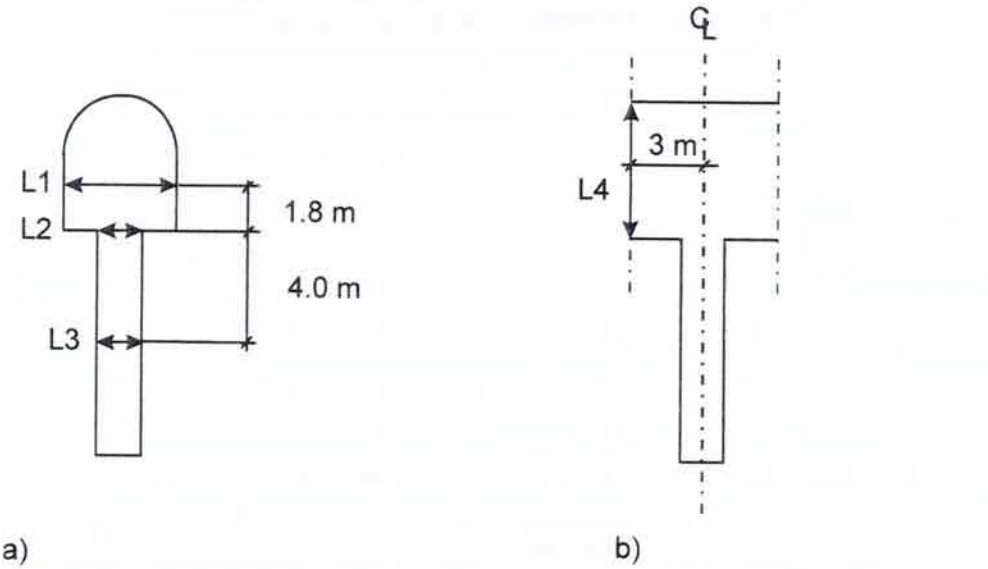

Figure 3-20 Selected convergence lines in repository tunnel and deposition hole.

One must here bear in mind that the effect of buffer and backfill was not considered in the modelling and the actual convergence development in future repository tunnels will probably be different. An accurate prediction of the detailed mechanical behaviour around the canister would requires detailed knowledge about the material properties of the buffer and the backfill, including possible influences of heat, saturation and time.

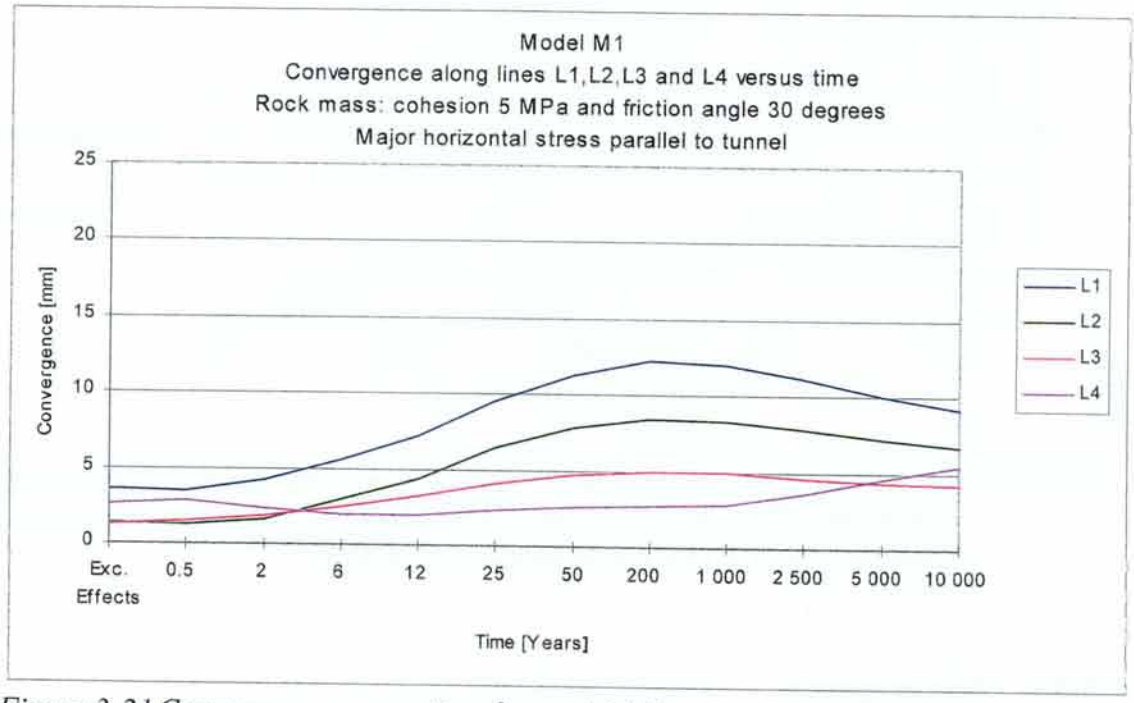

Figure 3-21 Convergence versus time for model M1.

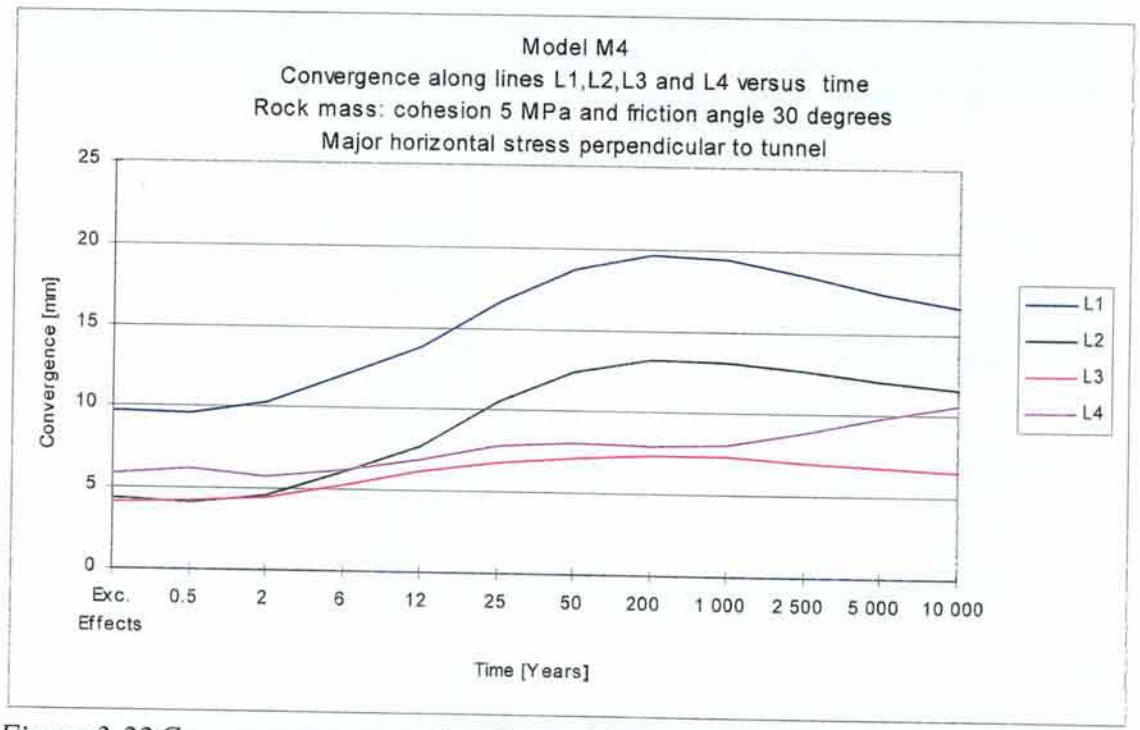

Figure 3-22 Convergence versus time for model M4.

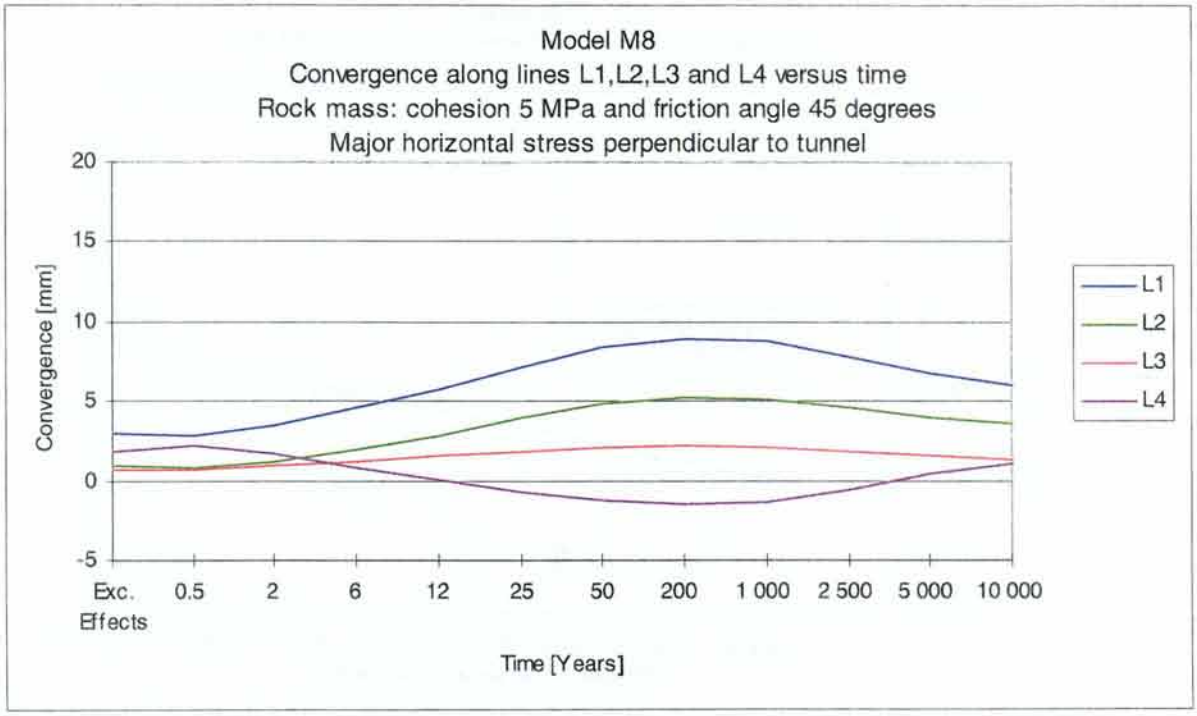

Figure 3-23 Convergence versus time for model M8.

3.3.5 Thermally induced stress paths

To further illustrate what happens in the model during the simulation, the stress paths for two zones were constructed. Figure 3-24 shows the result for model M1, where the rock strength is low and Figure 3-25 shows the result for the model M8 where the rock strength is high. The location of the two zones #1 and #2 is given in Figure 3-13. The stress path begins at the state after excavation and each point corresponds to the elapsed times 0, 0.5, 2, 6, 12, 25, 50, 200, 1 000, 2 500, 5 000 and 10 000 years.

The stress path of zone #1 differs from that of zone #2 in terms of the direction of minor stress change. This is a consequence of the different locations. Zone #1 is close to the heat source and will therefore at an early stage have an increase of both minor and major stress. Zone #2 is located at the pillar centre 5 m below the tunnel floor and, as can be seen also in Figure 3-14 the minor stress will initially decrease. The main change in stress for the whole area is the increase in major stress until the temperature reaches a maximum. During the cooling phase the stress state recovers towards the initial. (Note that the scales are different for the major and minor stress in the figures.)

It can also be noted that for model M1 (Fig. 3-24) both stress paths reach the yield envelope and the curves are kept on or below the envelope. In model M8 the stresses in the two points are far from yield (failure) during the whole thermal loading sequence. The stress paths at different points in the surrounding rock mass thus depend on their location and on the strength properties of the rock mass.

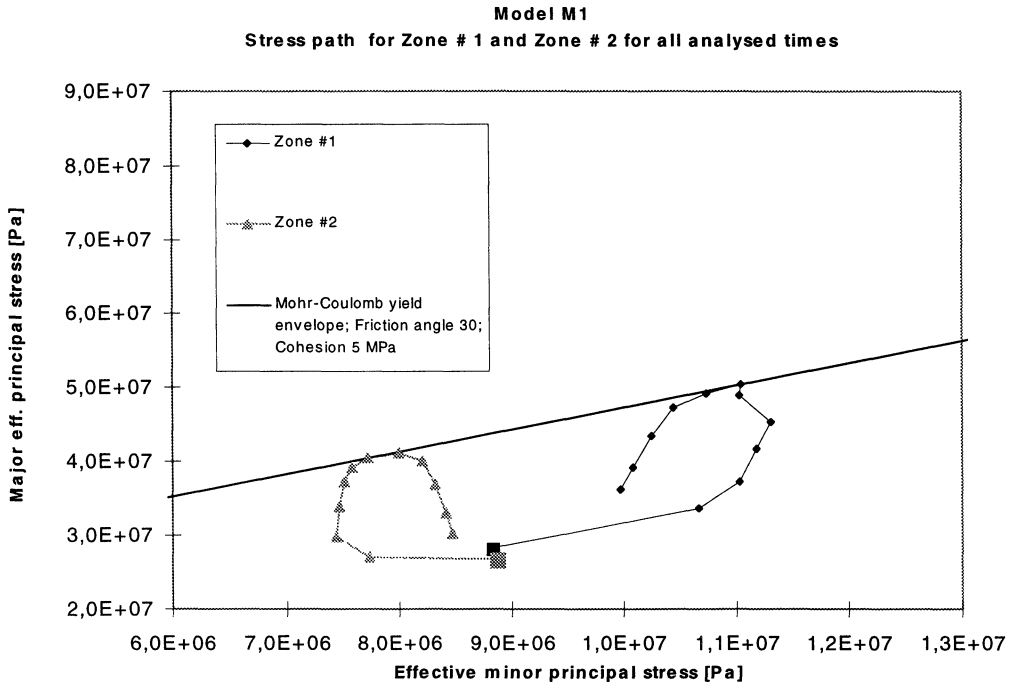

Figure 3-24 Stress path of zones 1# and #2 Figure 3-13 shows the location in model M1. The loading path starts at the filled square. The starting point is the state before thermal loading starts and each point corresponds to a thermal time step analysed.

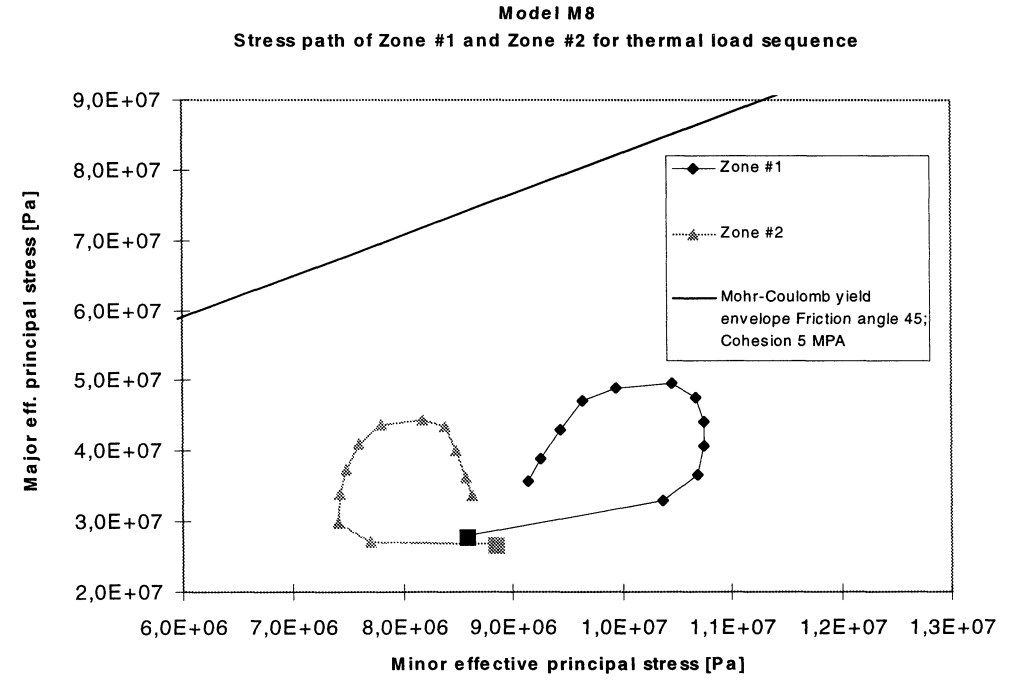

Figure 3-25 Stress path of zones 1# and #2 Figure 3-13 shows the location in model M8. The loading path starts at the filled square. The starting point is the state before thermal loading starts and each point corresponds to a thermal time step analysed.

3.3.6 Total stress analysis

The expression "total stress analysis" is used in referring to the model M7. In this model the water pressure was assumed to be zero at all times, such that the total stress equals the effective stress. This model is similar to model M1 except that in M1 a water pressure was initiated and "effective stress analysis" performed.

The plasticity states for model M7 for the thermal load time intervals are shown in Appendix G, as for the other models. As expected the area of yielded zones is smaller than for the corresponding effective stress analysis M1.

The performed total stress analysis allows for a direct comparison with the results in the previously performed global study (Hakami, et al., 1998). In the global study the three-dimensional distinct element code 3DEC was used and no water pressure was initiated. Both studies show similar results for the stress levels reached in the repository.

4 Discussion

4.1 Model geometry assumption

In this study the quarter-symmetry problem geometry means that heat can be conducted out from the repository only in the vertical direction. In the actual repository, with a limited horizontal extent, heat will also spread horizontally to the rock around the repository. It is therefore interesting to compare the results from temperature calculations in this study with the results from analytical calculations performed by Claesson and Probert (1996). They also calculated the temperature development around a repository (1000 m x 1000 m) with a similar power decay function as in this study.

Figures 4-1 and 4-2 show the results from (Claesson and Probert, 1996) at 100 years and 1 000 years after deposition. It can be noted that the temperature front is almost parallel to the repository boundaries during the first few hundred years and that after 1 000 years the front is more spherical in shape. For long time intervals the model presented in this report will thus give an overestimation (i.e., conservative estimation) of the temperatures and an extended cooling phase. However, since the major thermo-mechanical effects occur during the earlier stages of deposition the quarter-symmetric FLAC^{3D} model is considered to be an acceptable approximation.

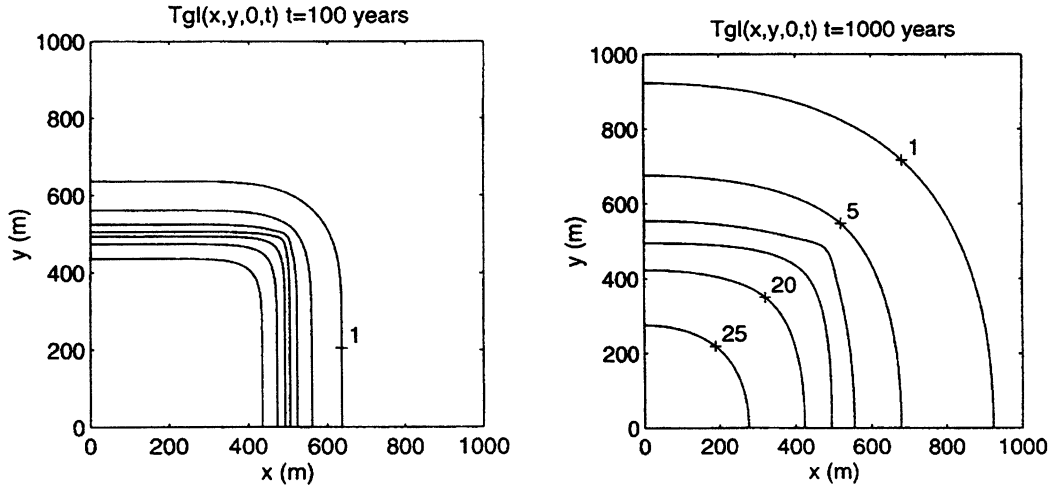

Figure 4-1 Global temperature isocurves (increase from initial) in a horizontal plane through the repository for 100 and 1 000 years. The isotherms are (counted from right to left) 1, 5, 10, 15, 20, 25 and 30 °C (Claesson and Probert, 1996). (The temperature values can not be compared with results of this study because the initial heat effect here is 1 000 W/canister.)

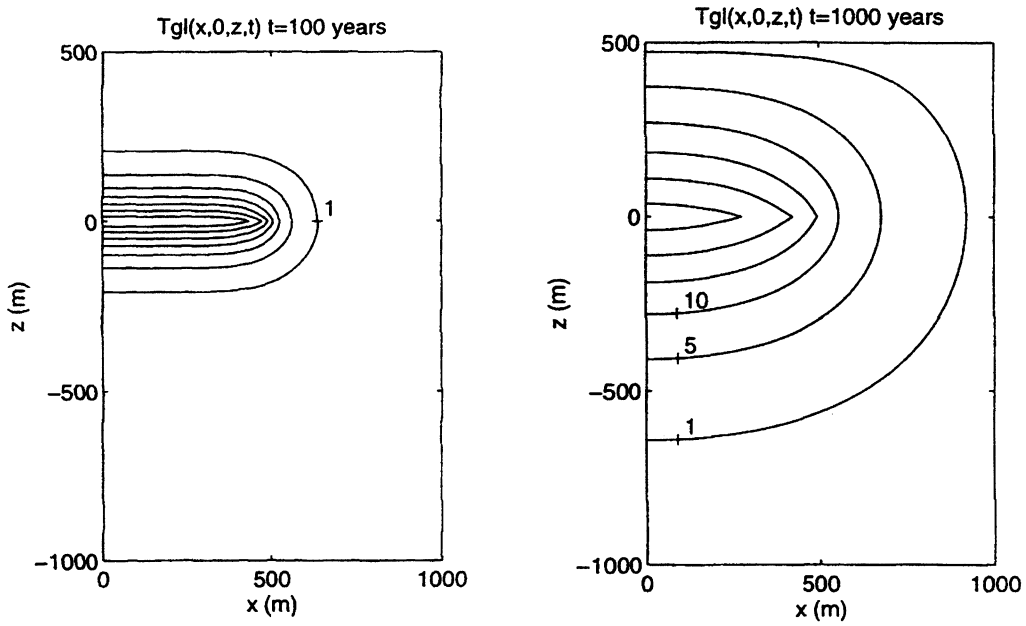

Figure 4-2 Global temperature isocurves in a vertical cross-section of a repository for 100 and 1 000 years. (Claesson and Probert, 1996). (The absolute values on the temperature can not be compared with results of this study because the initial heat effect here is 1 000 W/canister.)

The reliability of the predicted temperatures will further depend on the uncertainty in assumed heat conductivity and thermal boundary conditions. Another main factor controlling the expected temperature field is the initial area heat, in this case 10 W/m^2. A heat effect of somewhat lower value is currently considered a more realistic value for the future repository. The high value 10 W/m^2 was used in this study, and in the previous global study (Hakami et al., 1998), as being the possible upper limit for the initial area heat intensity.

4.2 Rock mass mechanical properties

The results from the analyses in this study, and in other similar studies, shows that the rock deformation properties and the rock mass strength criteria adopted are critical to the outcome. For the large rock masses involved in the problem is, however, difficult to determine what are the most appropriate material behaviour models (i.e., constitutive relations) and parameters. The difficulty comes from the inability to test rock masses at an appropriate scale. In most cases, and in this study, rock masses are idealised as elastic, perfectly plastic materials. Two slightly different yield (or failure) criteria are used. The most common is the Mohr-Coulomb yield criterion which has a linear failure envelope (i.e., the failure surface is not a function of confining stress). However, real rock masses can be expected to have different yield surfaces depending on the confining stress. The yield criterion suggested by Hoek and Brown (1982) has a curvilinear failure

envelope, which is a function of confining stress. The parameters used to describe the yield surface have been empirically derived, but are not universally accepted. In this study the Mohr-Coulomb criterion was selected because it is a simple criterion, already implemented in the code used, and well known by the rock mechanics community.

The internal friction angle chosen for the rock mass becomes particularly important in this application because the repository lies at great depth and the stress levels, together with the thermally induced stresses, become very high. The predicted strength from the Mohr-Coulomb criterion thus will be sensitive to the internal friction angle (cf. Figures 3-24 and 3-25). In the start of the thermo-mechanical study 30 degrees internal friction angle was chosen as an expected lower limit for the rock mass. During the course of the study it was discussed whether this is a realistic value for the expected rock mass around a future repository, and the model M8 with higher internal friction angle was analysed.

It may therefore be interesting to refer to a scheme proposed by Hoek and Brown (1997) shown in Figures 4-3 and 4-4. The scheme relates the parameters cohesion and (internal) friction angle to the structure of the rock mass, the fracture surface conditions and the uniaxial strength of the intact rock.

For a typical Swedish crystalline rock of "good" quality, expected for the repository area, the GSI value would be at least 50 based on the chart in Figure 4-3. A typical m_i value for granite and gneiss is 33 (Hoek and Brown, 1997), and this gives a minimum friction angle of 43°, according to Figure 4-4a. If the uniaxial strength of the intact rock is assumed to be minimum 150 MPa the expected cohesion strength would be at least 8 MPa (see Fig. 4-4b). Thus the scheme proposed by Hoek and Brown (1997) suggests that the strength parameters used in model M8 of this study (see Table 2-4) are probably the most appropriate for predicting the rock mass response to a deep geological repository.

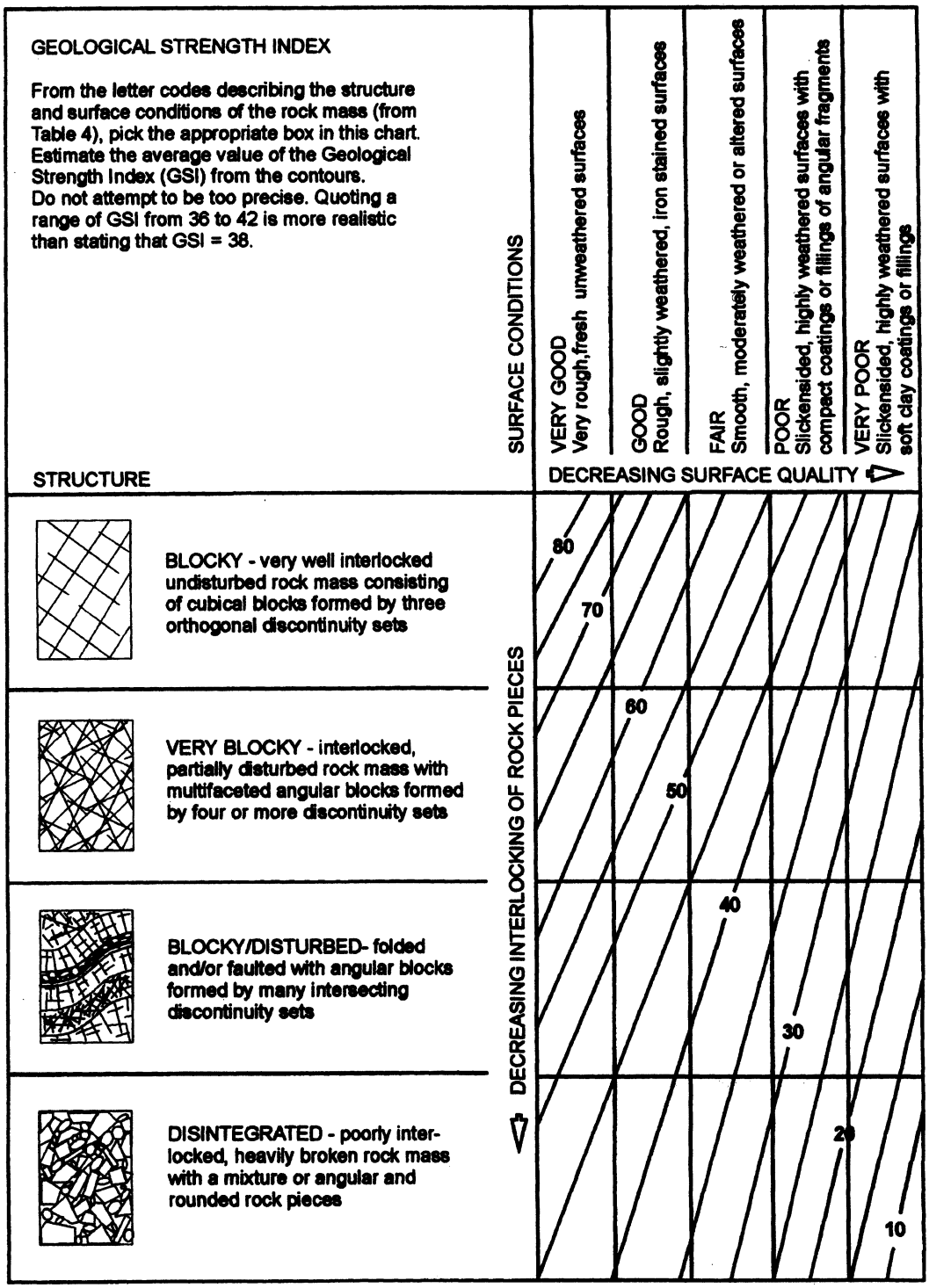

Figure 4-3 Estimate of Geological Strength Index, GSI, based on geological description. From (Hoek and Brown, 1997).

a)

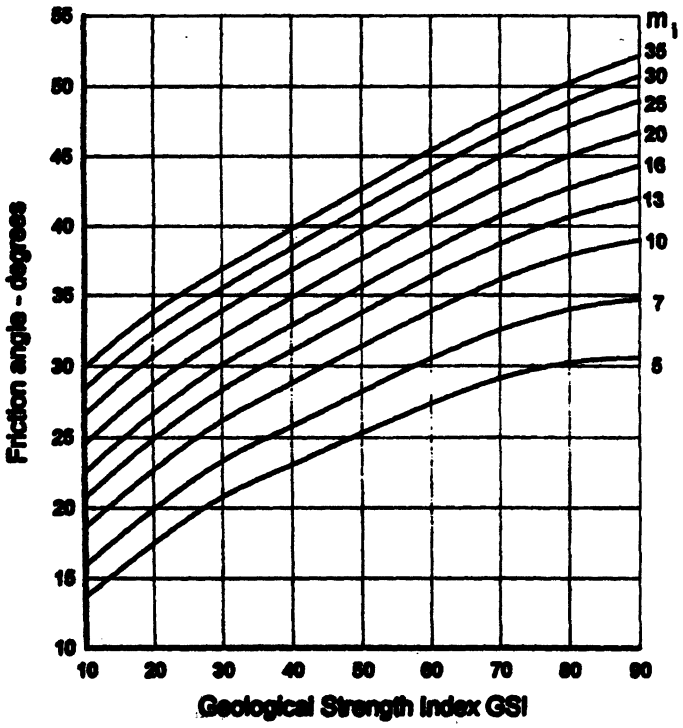

b)

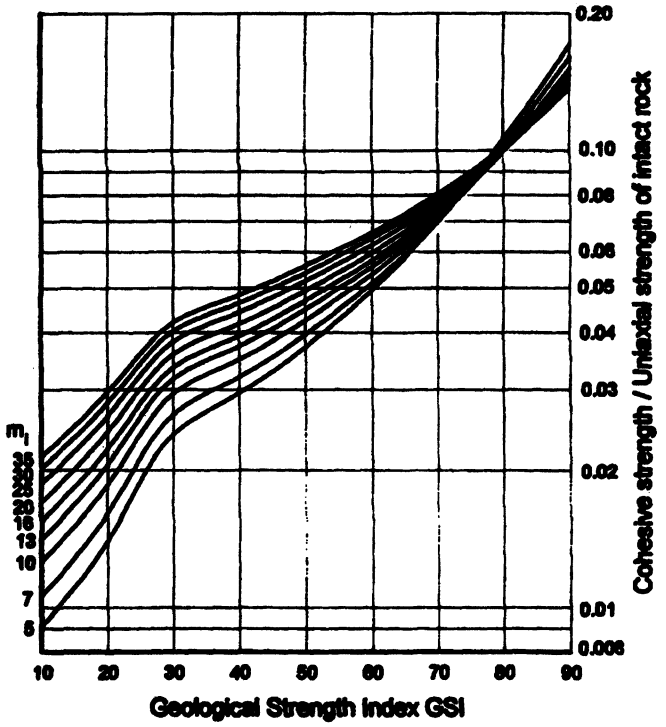

Figure 4-4 Estimate of a) friction angle and b) cohesion for different GSI and m_i values. From (Hoek and Brown, 1997).

4.3 Conservative Assumptions

The presented analysis includes simplifications and idealisations, necessary due to the complex nature of the problem. Further, the parameters to be used in the applied models can not be determined without uncertainty. The approach taken for this analysis has been to choose the most unfavourable parameter (or condition) with respect to rock mass stability. If the analysis shows acceptable conditions for these unfavourable assumptions, so called conservative assumptions, it may be concluded that conditions would be acceptable also for more favourable assumptions.

However, if many conservative assumptions are made in the same modelling, the results may show rock behaviour that is not acceptable. In such cases the assumptions and parameter choices should, if possible, be revaluated, with the aim to make the analysis more close to expected real conditions. The modelling work in this project illustrates such investigation steps. The models M1 to M6 of this report, and in particular models M3 and M6, resulted in failure of large rock volumes. The strength parameters were in this case assumed too low and this caused, together with other conservative assumptions, rock stress conditions exceeding the yield limit. In model M8 the strength parameters were therefore revaluated and as a consequence the predicted rock conditions in the repository improved.

Conservative assumptions have been made in this modelling not only with respect to rock strength but also in terms of geometry and thermal conditions, as described in Sections 2.3 –2.5 and discussed in section 4.1 and 4.2. Apart from mechanical properties and stress directions the assumption were kept the same in all models (see Table 2-4). The various conservative assumptions made in the modelling, of different importance to the results, are listed in the following:

- All waste is deposited at exactly the same time.
- Distance between tunnels is 25 m.
- Heat can only be conducted vertically.
- Heat transfer in filling material is zero. Heat applied on walls of deposition hole.
- Total heat effect is 10 W/m^2.
- Rock mass cohesion is low, $\leq$ 5 MPa.
- Full ground water pressure is modelled instantaneously in the model.
- No reinforcement or confinement from buffer and backfill are simulated.
- Tensile strength of the rock mass is zero.
- For models M1-M7, the internal friction angle of the rock mass is low, 30°.

5 Summary and Conclusions

The thermal load applied (1500 W/canister) gives rise to a maximum temperature of about 85 °C, at the deposition hole boundary, 44 years after deposition. In the pillar between the repository tunnels the temperature reaches a maximum of about 70 °C after 55 years. The initial area heat intensity was assumed to be 10 W/m².

The thermo-mechanical effects reach a maximum at about 200 years after deposition. The extension of yield (or failure) volume depends on the quality of the rock mass and the orientation of the in-situ stress field. For relatively "poor" quality rock (internal friction angle 30°) shear failure initiates at the boundary of the tunnels and extend upwards and downwards at about a 45° angle from the horizontal. The shear failure bands reach the symmetry plane between the tunnels suggesting that the pillar between the tunnels may collapse if not reinforced. For "good" rock (internal friction angle 45°) the yield is limited in depth to a maximum of 1.5 m. A typical Swedish crystalline bedrock is expected to have a generally high strength, corresponding to an internal friction angle of about 45° for the rock mass as a whole.

The largest thermo-mechanical effects are found in the tunnel floor at the upper part of the deposition holes, i.e. the largest displacements occur in this area. In the walls of the tunnel tension failure is expected to develop to a limited depth. Tension and shear failure in the immediate surrounding of the excavations will occur already due to the rock excavation. The depth extension of failure is depending on the magnitude and orientation of the in-situ stresses, as well as rock mass quality. All modelling results show some rock failure around the excavations suggesting that, to ensure stability, reinforcement of the tunnels may be required.

The maximum convergence between the wall of the repository tunnels was calculated to be about 9 mm, assuming a rock mass with 5 MPa cohesion and internal friction angle of 45°. Both displacements and yielded areas are less when the major principal stress is oriented parallel with the deposition tunnels, compared to the case when major principal stress is perpendicular to the tunnels. Possible confining effects from the buffer and backfill material was neglected in this study.

The rock mass was simulated as a Mohr-Coulomb material with a yield envelope defined by cohesion and internal friction angle, and a zero tensile strength was assumed. Further, effective stress analysis was used in the numerical modelling. At repository depth, the water pressure is expected to be high (5 MPa) and the use of effective stress makes a considerable difference in the prediction of yielded areas. When performing an analysis assuming poor rock and no water pressure, the yielded areas reach only a few metres into the pillar while they extend throughout the pillar in the corresponding analysis with water pressure.

In conclusion, the results from this study indicate that the central part of the rock pillar between repository tunnels will remain stable and keep its initial properties, on the assumption that the overall quality of the rock mass is good and the thermal load from the radioactive waste is limited (initial area heat intensity not higher than 10 W/m²).

In the rock close to the excavations (< 1 m) the stiffness and strength should be expected to reduce to some extent, i.e. the hydraulic conductivity and porosity may increase and the stiffness and strength decrease, compared to initial properties. This reduction in stiffness and strength results from "damage" to the rock, brought about by rock failure or rock fracture movements, and is often referred to as strain softening. Strain softening was not explicitly considered.

This study concerns the behaviour of a fairly homogeneous fractured crystalline rock mass exposed to stable stress conditions. The possible deformation around the repository tunnel and deposition holes in cases where major discontinuities intersect the repository area, or major changes in tectonic stresses take place, have not been investigated. Creep of the heated rock mass, which has not been considered in this study, may also play an important role.

References

Claesson, J., Probert, T., 1996. Temperature field due to time-dependent heat sources in a large rectangular grid - Derivation of analytical solution. SKB, Technical Report TR 96-12, Stockholm, Sweden.

Hakami, E., Olofsson, S-O., 1998. Global thermo-mechanical effects from a KBS-3 type repository – Summary report, SKB, Technical Report, TR 98-01, Stockholm, Sweden.

Hoek, E., Brown, E.T., 1997. Practical estimates of rock mass strength. Int. J of Rock Mech & Geomech Sci., Vol. 34, pp 1165-1186.

Hoek, E., Brown, E.T., 1982. Underground excavations in rock. The Institute of Mining and Metallurgy, London, England.

Håkansson, R., 1999. Beräkningar av nuklidinnehåll, resteffekt, aktivitet samt doshastighet för utbränt kärnbränsle. SKB, R-99- , Stockholm, Sweden. (In print)

Itasca Consulting Group Inc., 1997. *FLAC*^{3D} –User's Manual," Minneapolis, Minnesota.

Thunvik, R., Braester, C., 1991. Heat propagation from a radioactive waste repository. SKB 91 reference canister. SKB, Technical Report TR 91-61, Stockholm, Sweden.

Pusch, R., Touret, O., 1988. Heat effects on soft Na bentonite gels. Geologiska Föreningens i Stockholm Förhandlingar. Vol. 110 (2), p 183-190.

Pusch, R., Börgesson, L., 1992. PASS – Project on alternative systems study. Performance assessment of bentonite clay barrier in three repository concepts. SKB, Technical Report TR 92-40, Stockholm, Sweden.

SKB, 1992. Project on alternative systems study (PASS) – Final Report, SKB, Technical Report TR 93-04, Stockholm, Sweden.

Acknowledgements

The participation in the project reference group by Prof. Ove Stephansson and Dr. Jing Lanru (Royal Institute of Technology, Stockholm) and the contributions they made are acknowledged. The acknowledgement is also extended to Dr. Loren Lorig (Itasca S.A.) for his review of the report.

Appendix A: PLASTICITY STATE OF THE ZONES AFTER EXCAVATION OF REPOSITORY TUNNEL AND DEPOSITION HOLE (M1-M6, M8)

In the subsequent figures, plasticity states of zones are identified by different colours with the following meaning:

None elastic,

Shear-n at shear yield now,

Shear-p elastic, but previously at shear yield,

Tension-n at tensile yield now,

Tension-p elastic, but previously at tensile yield.

These states can be combined and the combination will have its own colour (e.g. shear-p combined with tension-p).

List of thermo-mechanical models

Model	Direction of major horizontal stress relative to repository tunnel axis	Rock mass cohesion [MPa]	Rock mass friction angle [°]	Effective or total stress analysis
M1	Parallel	5	30	Effective
M2	Parallel	3	30	Effective
M3	Parallel	1	30	Effective
M4	Perpendicular	5	30	Effective
M5	Perpendicular	3	30	Effective
M6	Perpendicular	1	30	Effective
M7	Parallel	5	30	Total
M8	Parallel	5	45	Effective

Model M1

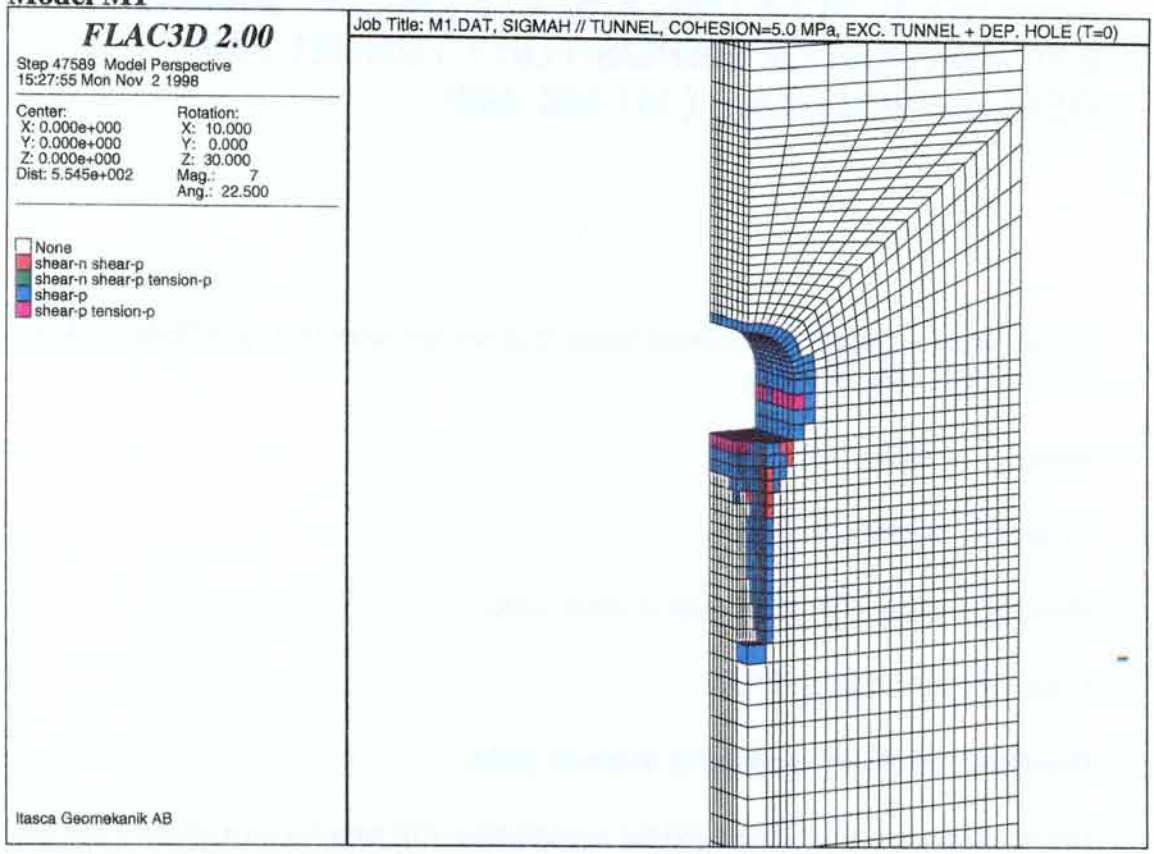

Model M2

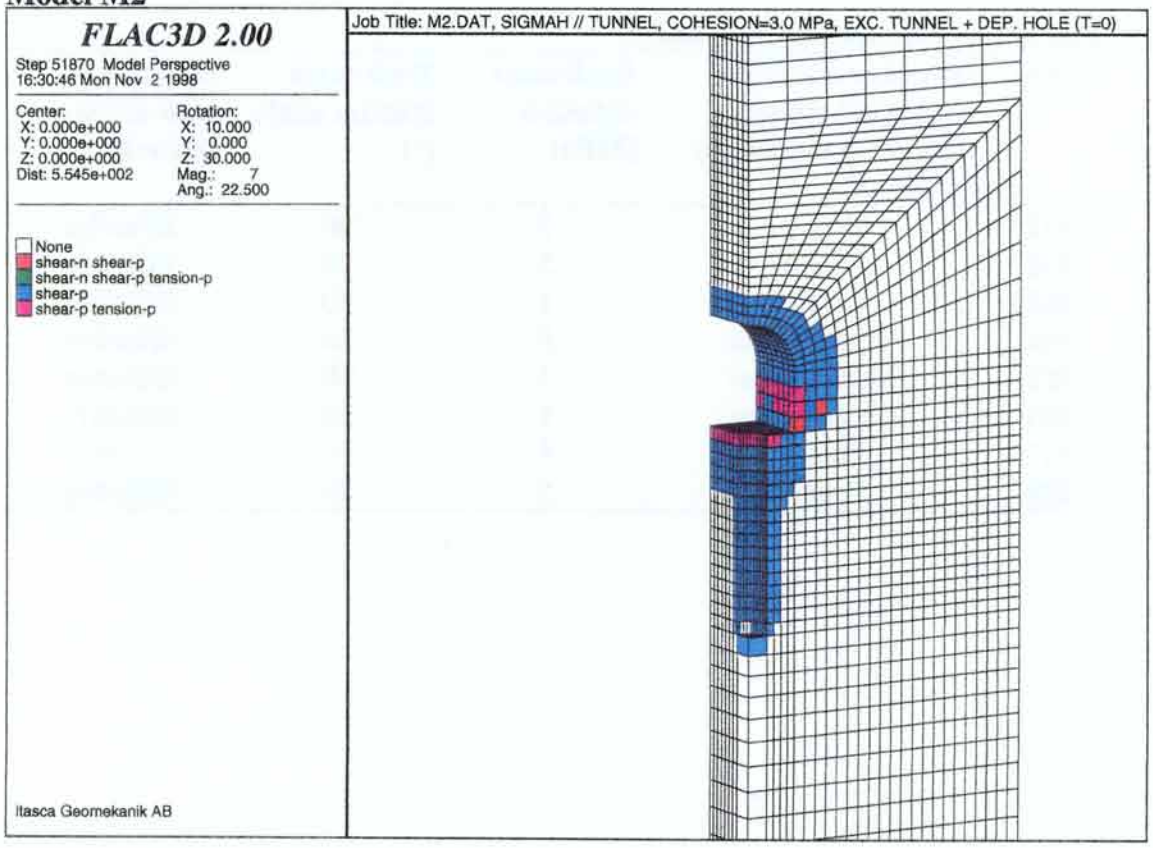

Model M3

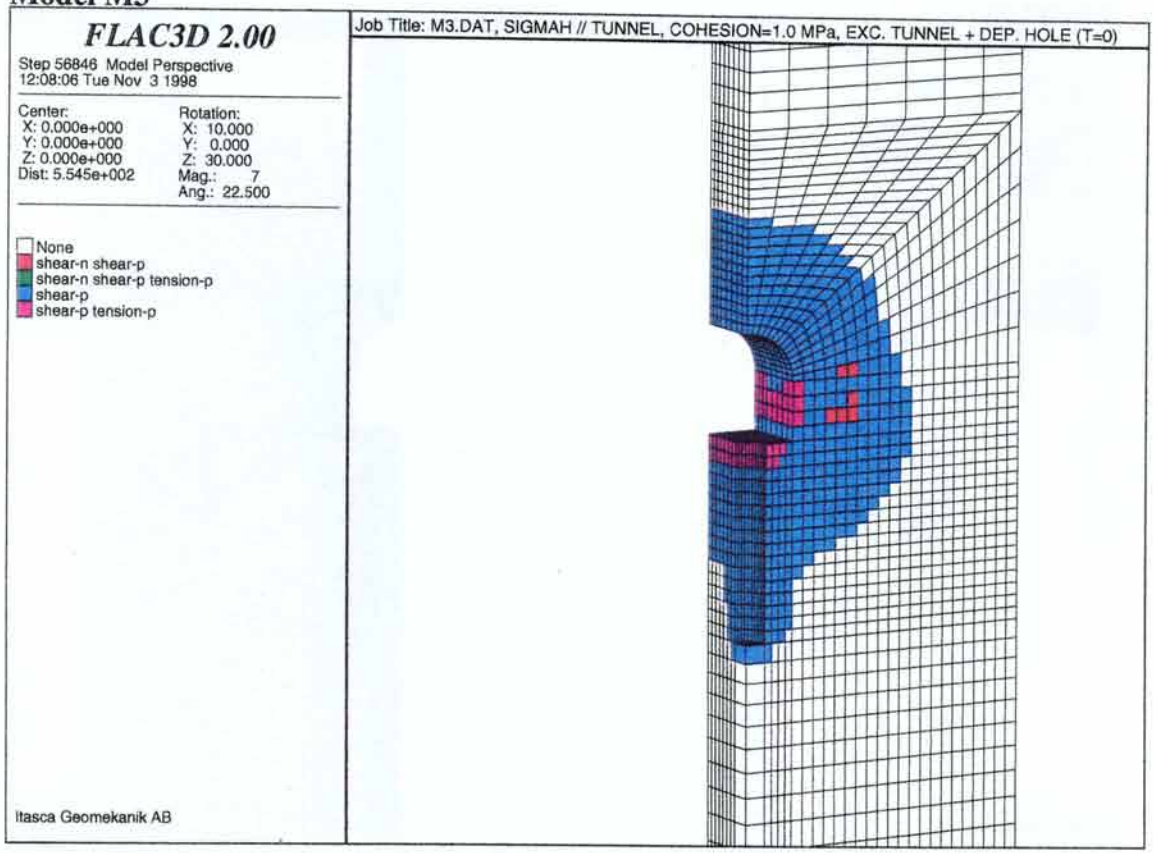

Model M4

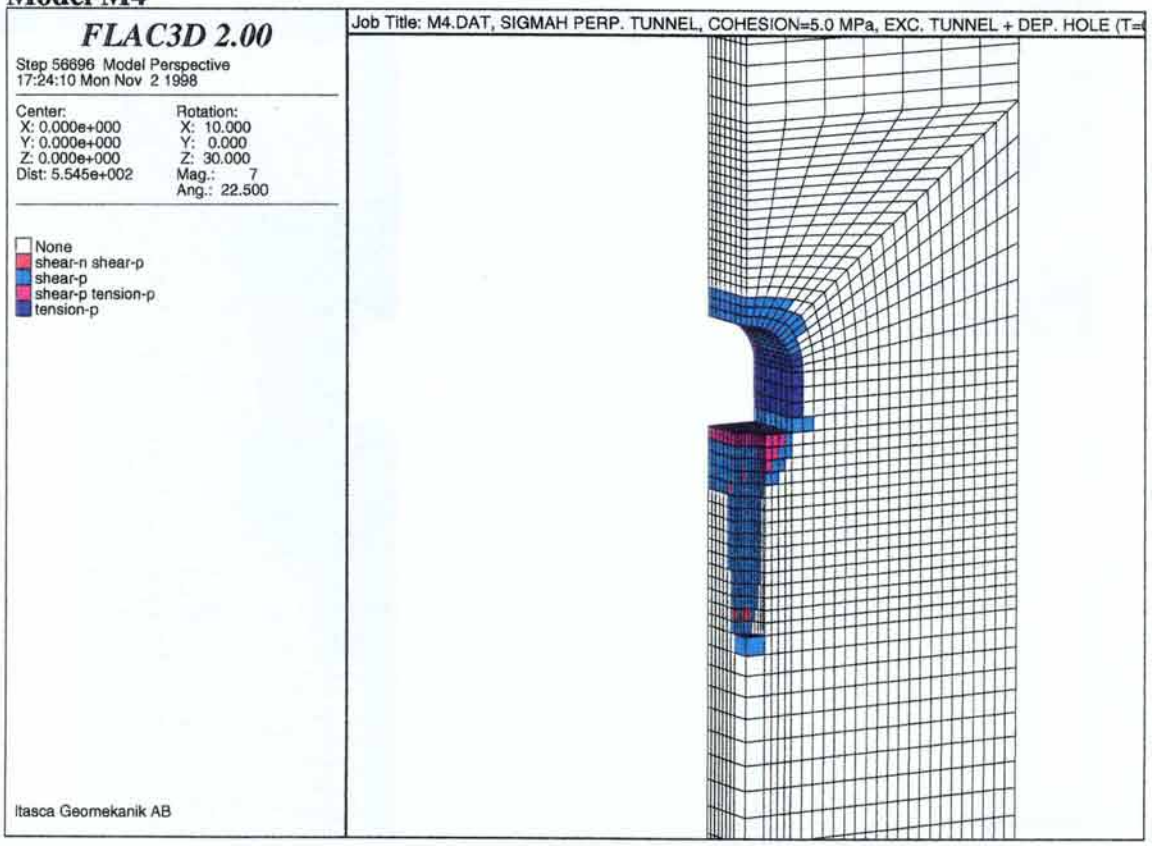

Model M5

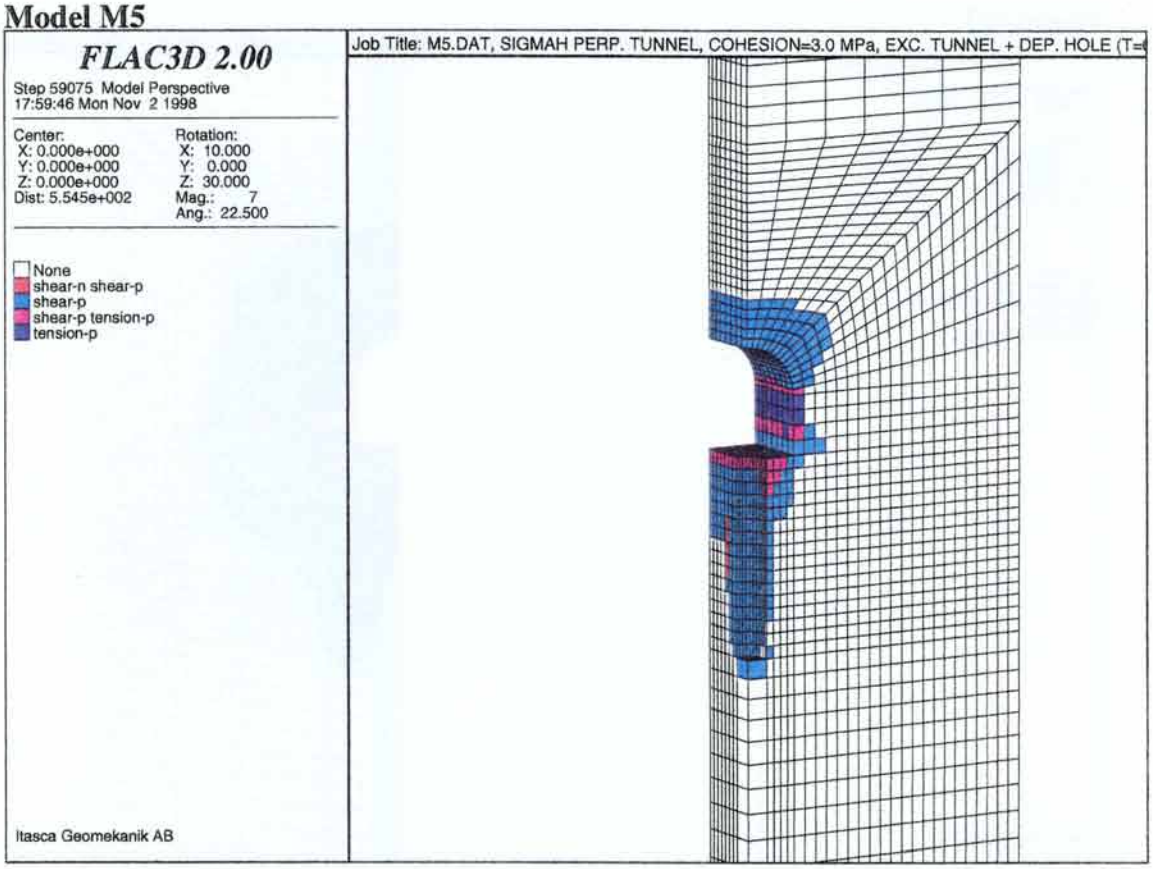

Model M6

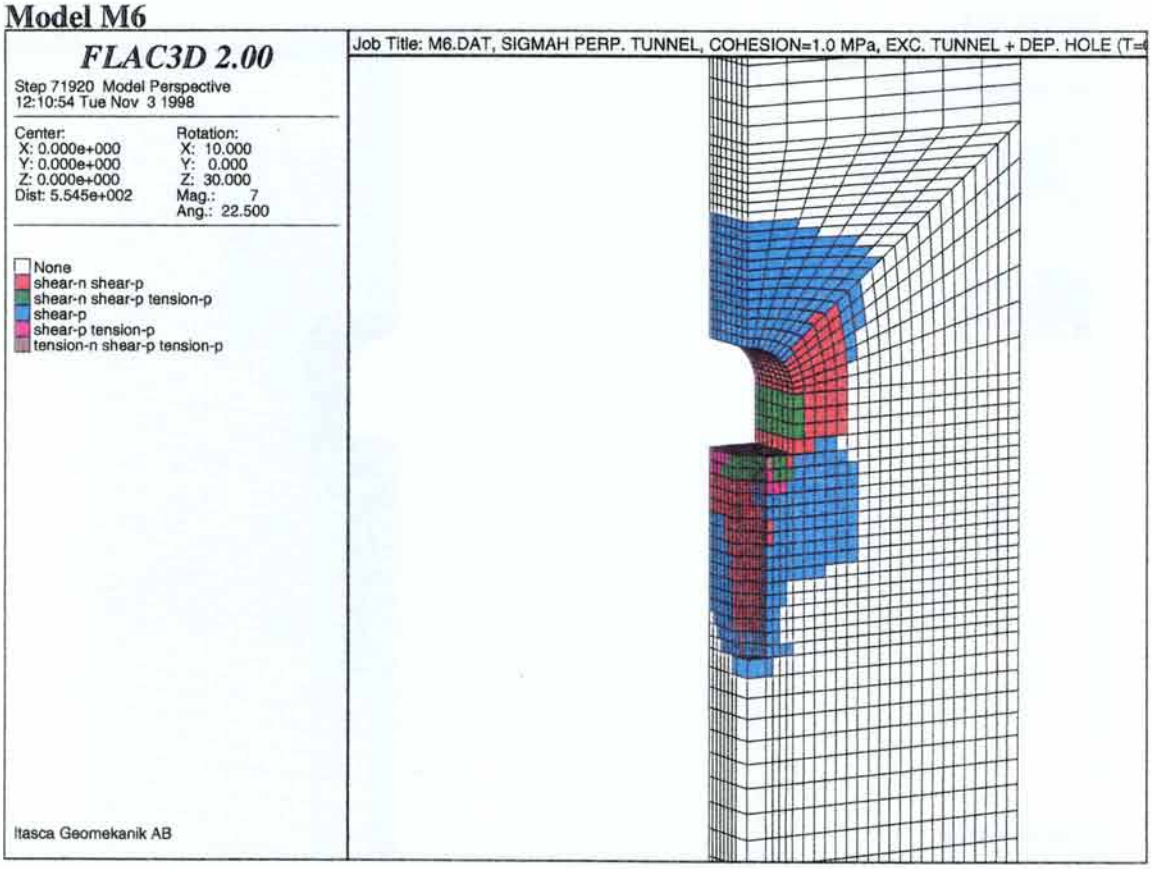

Model M8

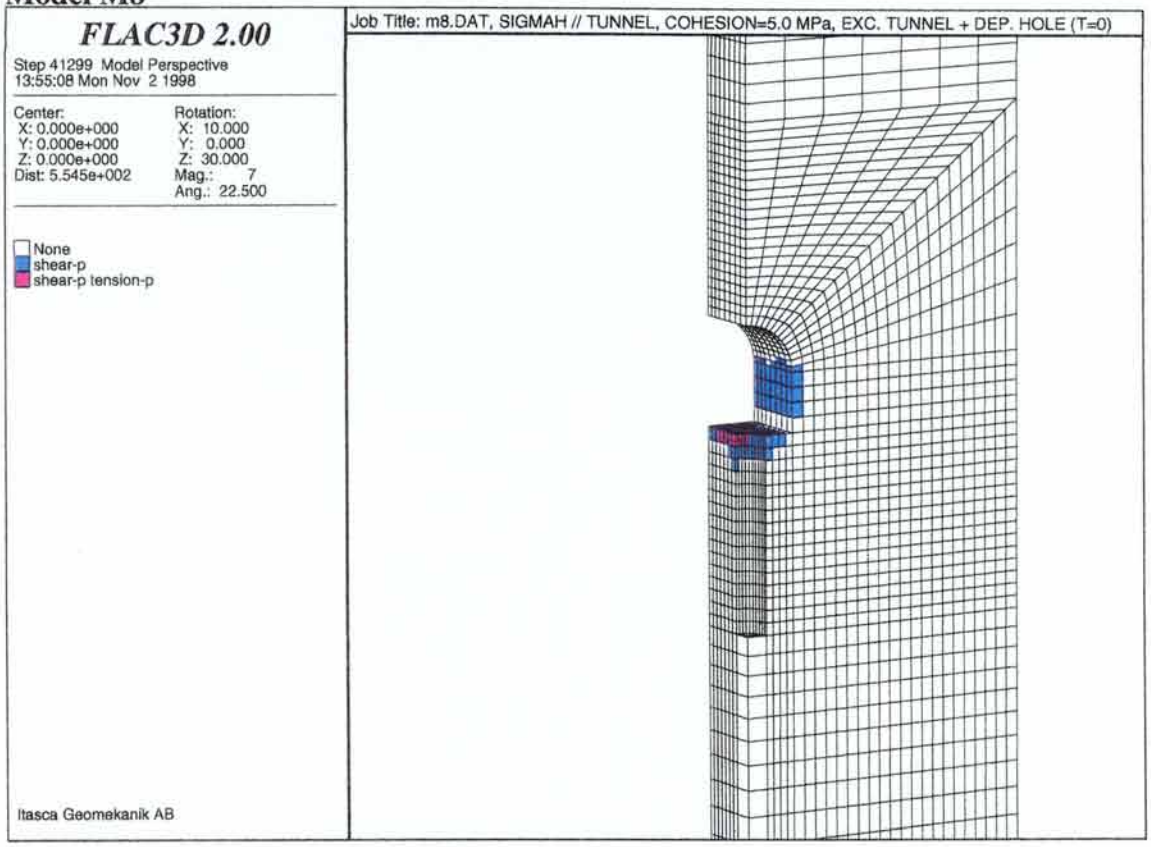
FLAC3D 2.00
Step 41299 Model Perspective
13:55:08 Mon Nov 2 1998
Center:
X: 0.000e+000
Y: 0.000e+000
Z: 0.000e+000
Dist: 5.545e+002
Rotation:
X: 10.000
Y: 0.000
Z: 30.000
Mag.: 7
Ang.: 22.500
None
shear-p
shear-p tension-p
Itasca Geomekanik AB
Job Title: m8.DAT, SIGMAH // TUNNEL, COHESION=5.0 MPa, EXC. TUNNEL + DEP. HOLE (T=0)

Appendix B: PLASTICITY STATE OF THE ZONES FOR MODEL M1

Plasticity state indicators for the thermo-mechanical calculations shows which zones that have been activated for that particular time interval. Thus, a zone can have state yield at one time interval and state no yield at another time interval.

In the subsequent figures, plasticity states of zones are identified by different colours with the following meaning:

None elastic,

Shear-n at shear yield now,

Shear-p elastic, but previously at shear yield,

Tension-n at tensile yield now,

Tension-p elastic, but previously at tensile yield.

These states can be combined and the combination will have its own colour (e.g. shear-p combined with tension-p).

List of thermo-mechanical models

Model	**Direction of major horizontal stress relative to repository tunnel axis**	**Rock mass cohesion [MPa]**	**Rock mass friction angle** [°]	**Effective or total stress analysis**
M1	Parallel	5	30	Effective
M2	Parallel	3	30	Effective
M3	Parallel	1	30	Effective
M4	Perpendicular	5	30	Effective
M5	Perpendicular	3	30	Effective
M6	Perpendicular	1	30	Effective
M7	Parallel	5	30	Total
M8	Parallel	5	45	Effective

Model M1, Time 0 years (Groundwater pressure initiated)

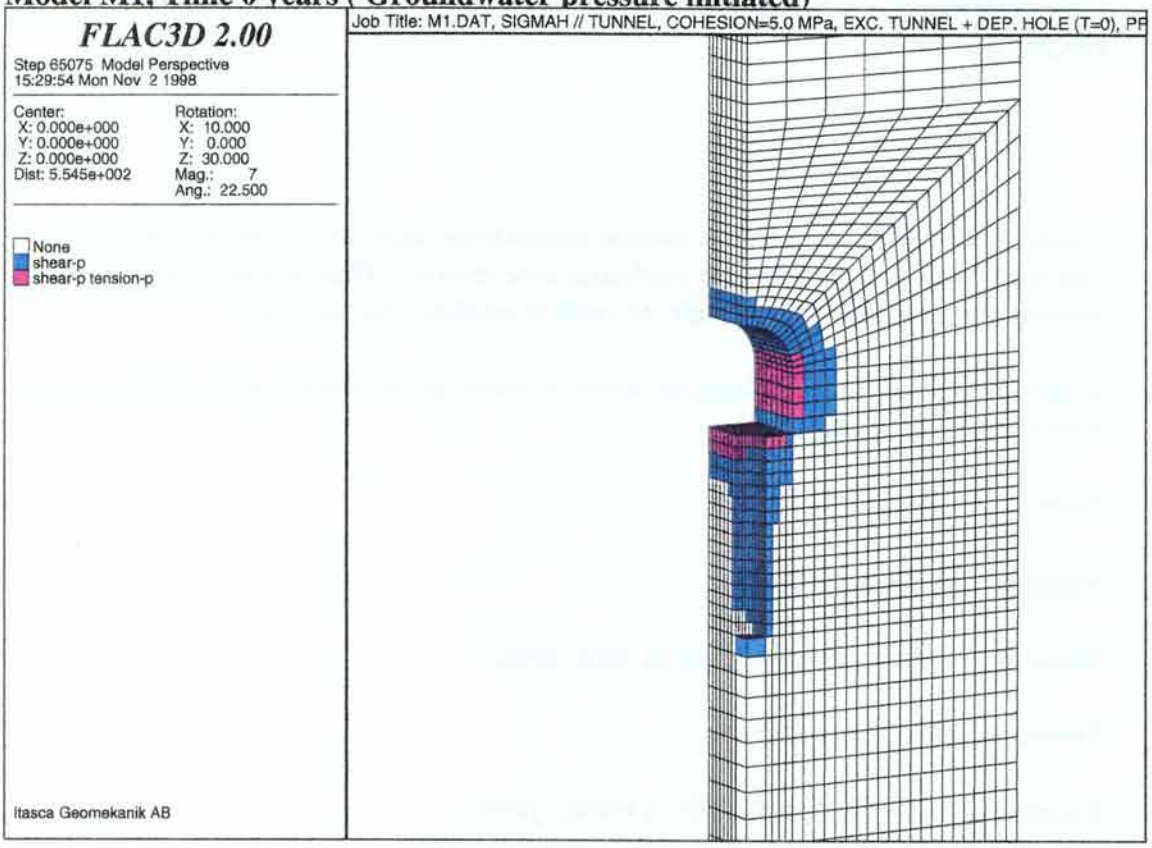

Model M1, Time interval 0 - 0.5 years

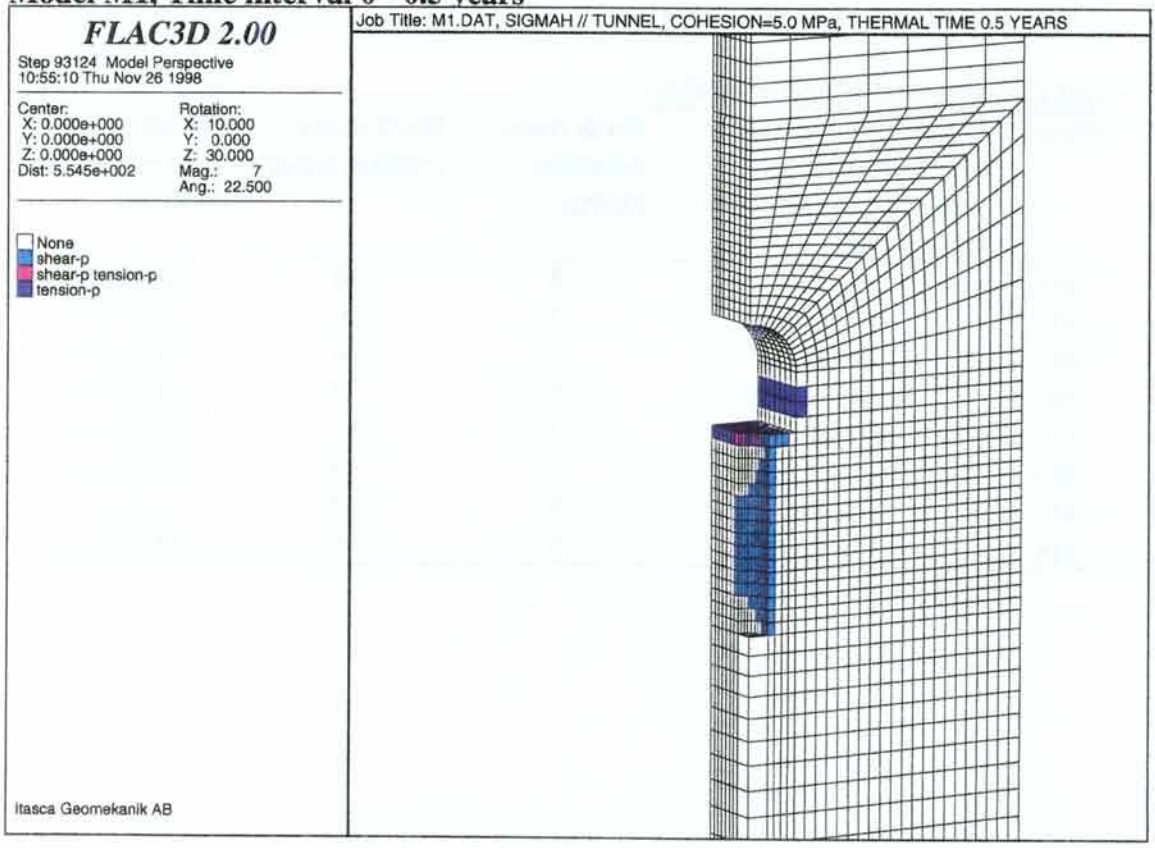

Model M1, Time interval 0.5 - 2 years

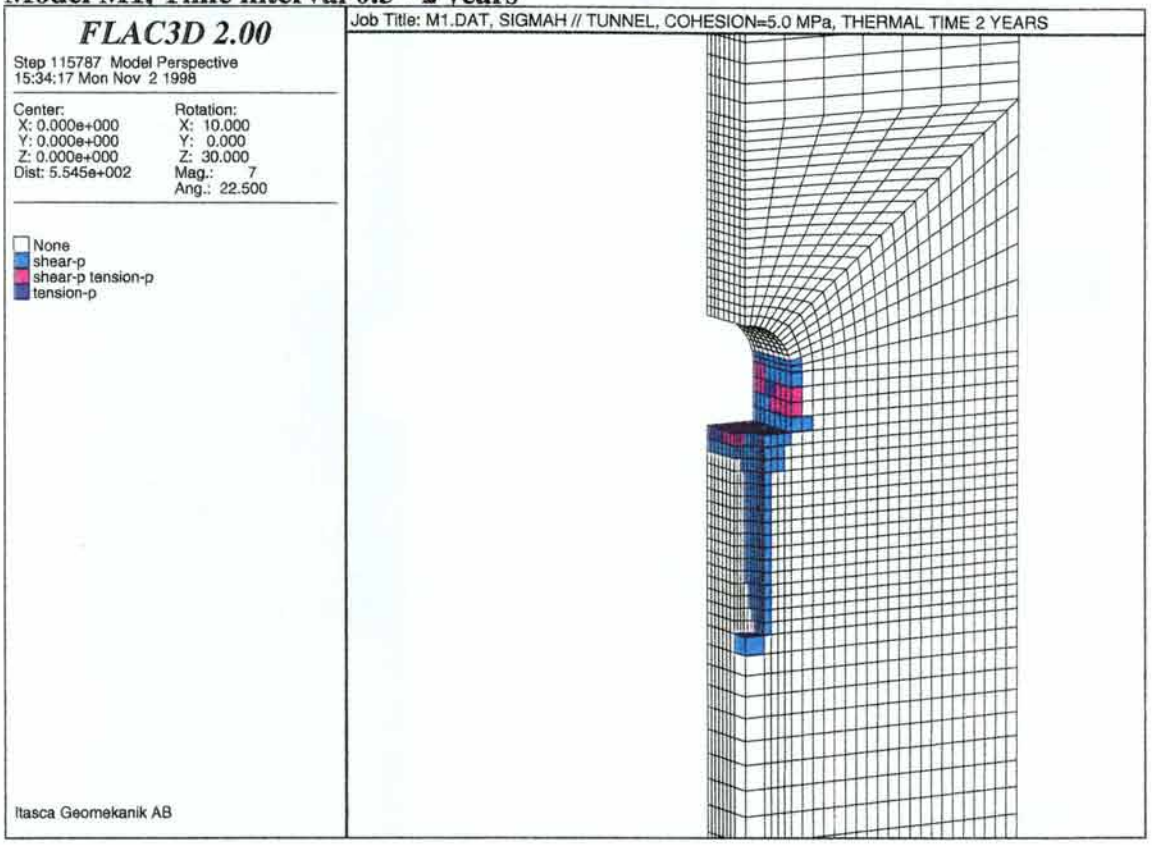

Model M1, Time interval 2 - 6 years

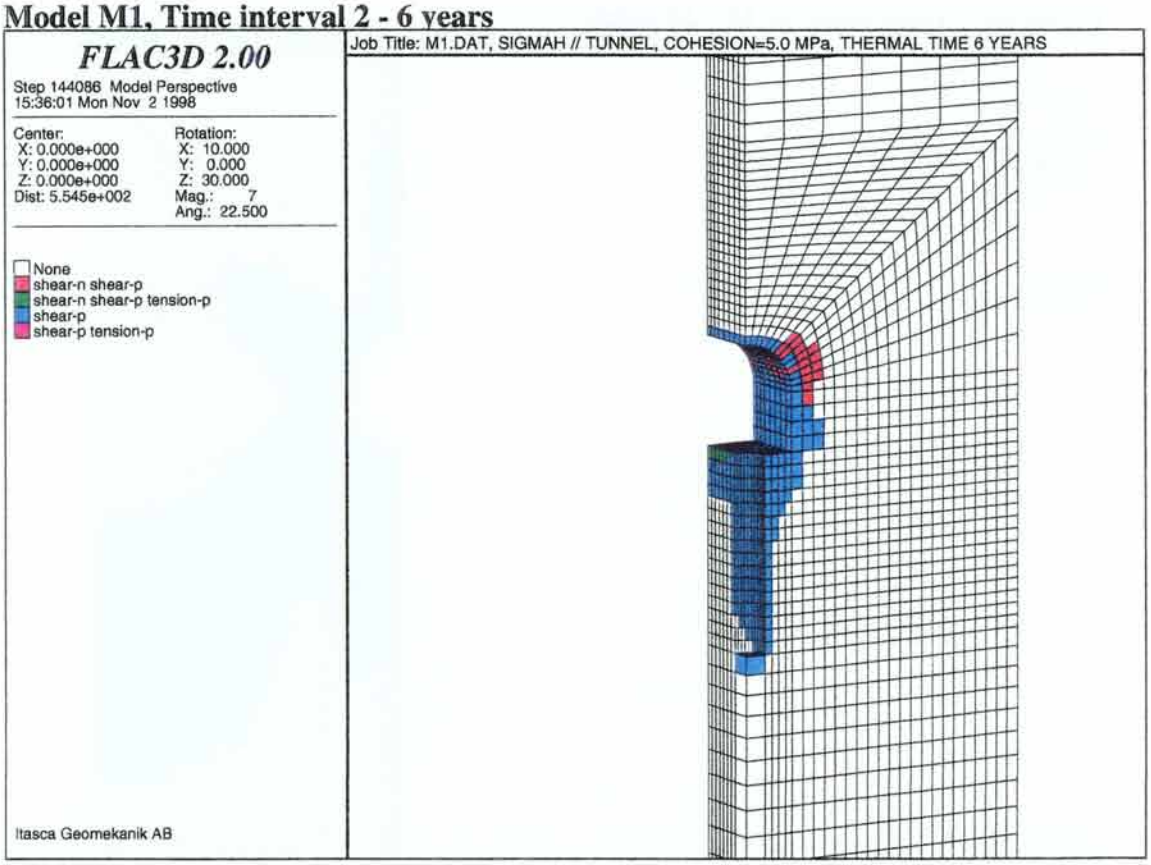

Model M1, Time interval 6 - 12 years

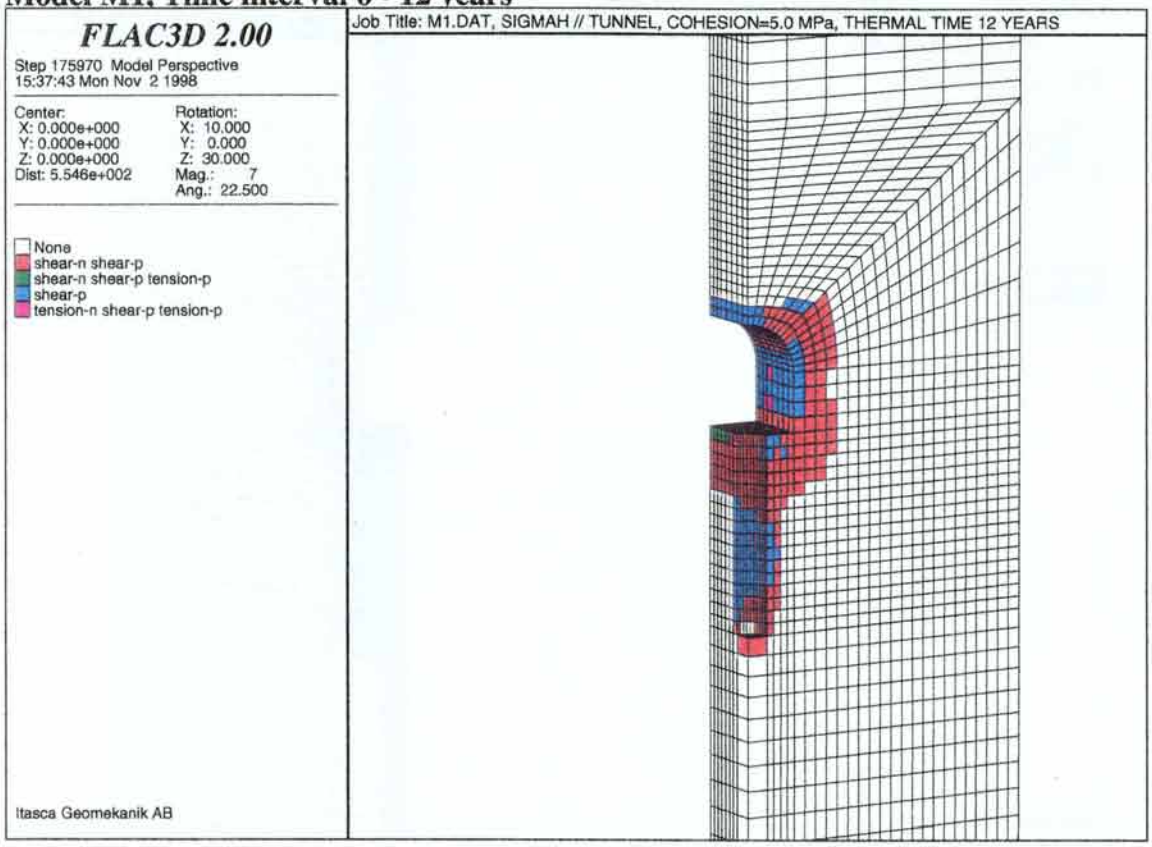

Model M1, Time interval 12 - 25 years

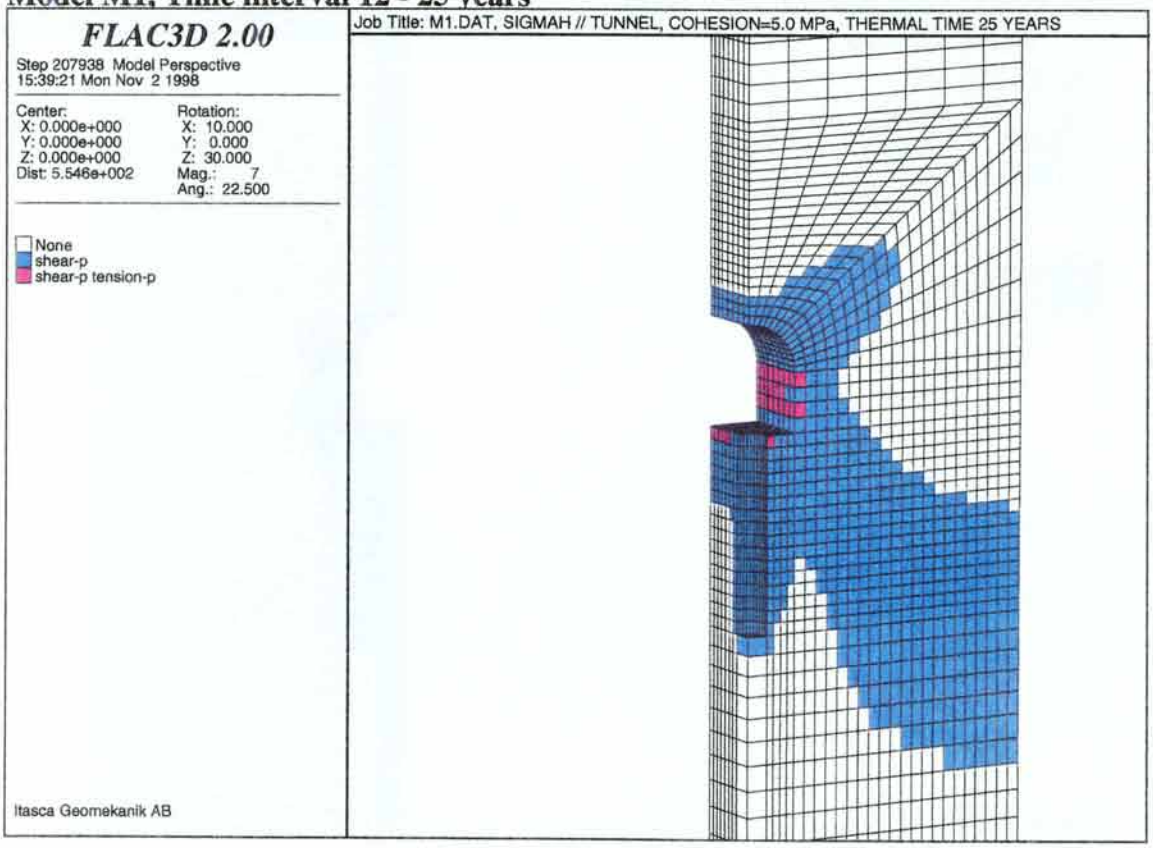

Model M1, Time interval 25 - 50 years

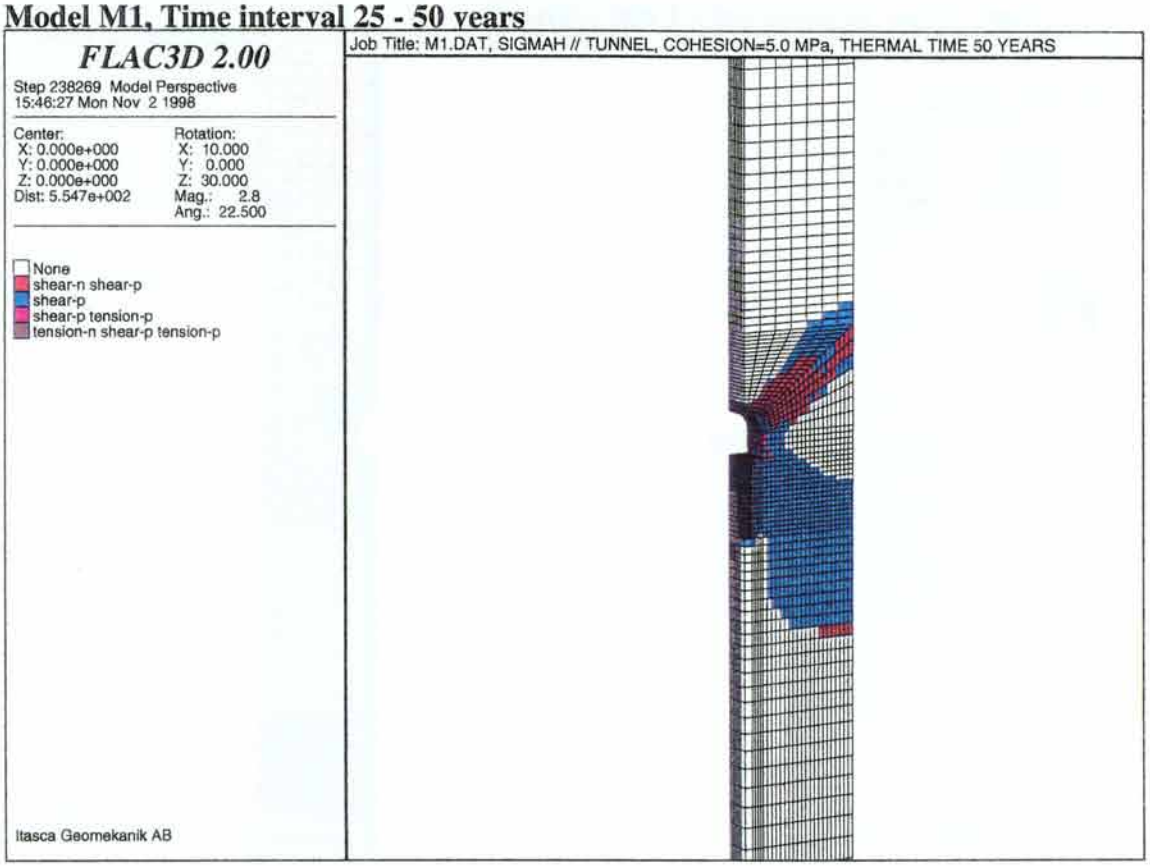

Model M1, Time interval 50 - 200 years

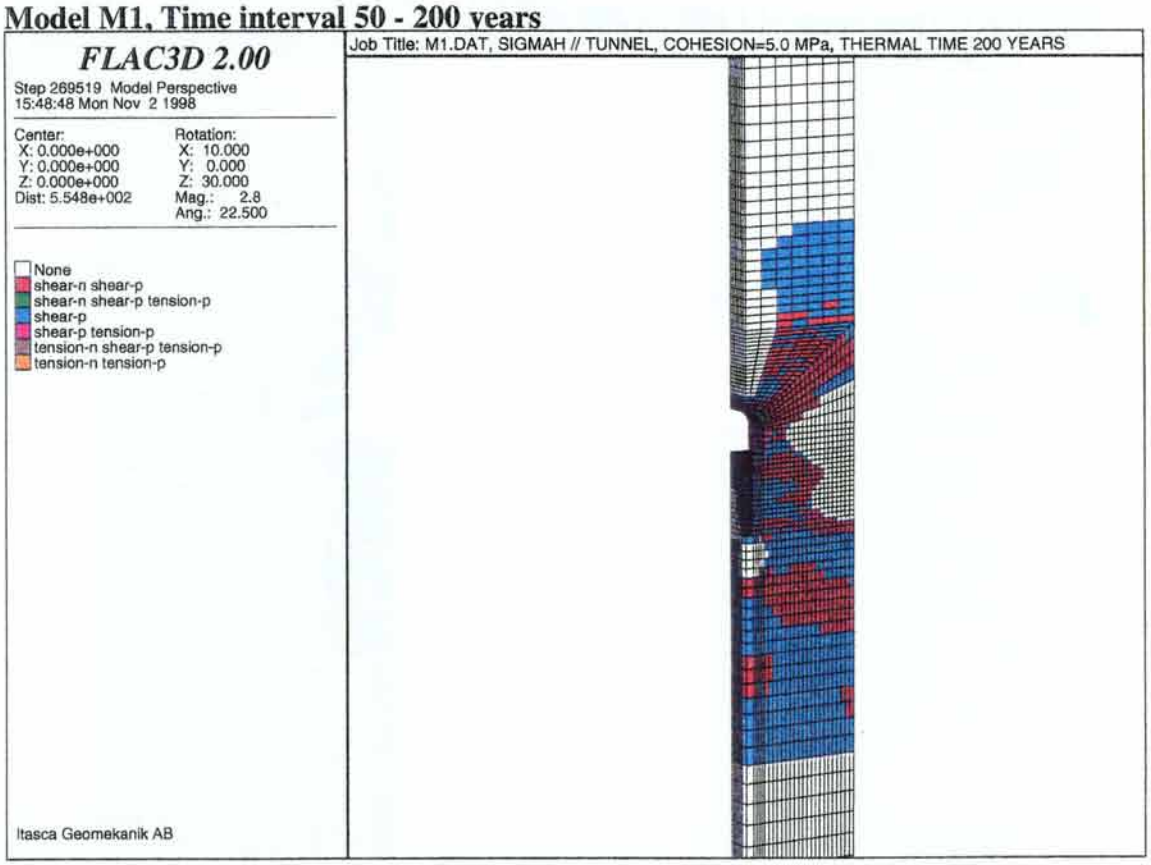

Model M1, Time interval 200 - 1 000 years

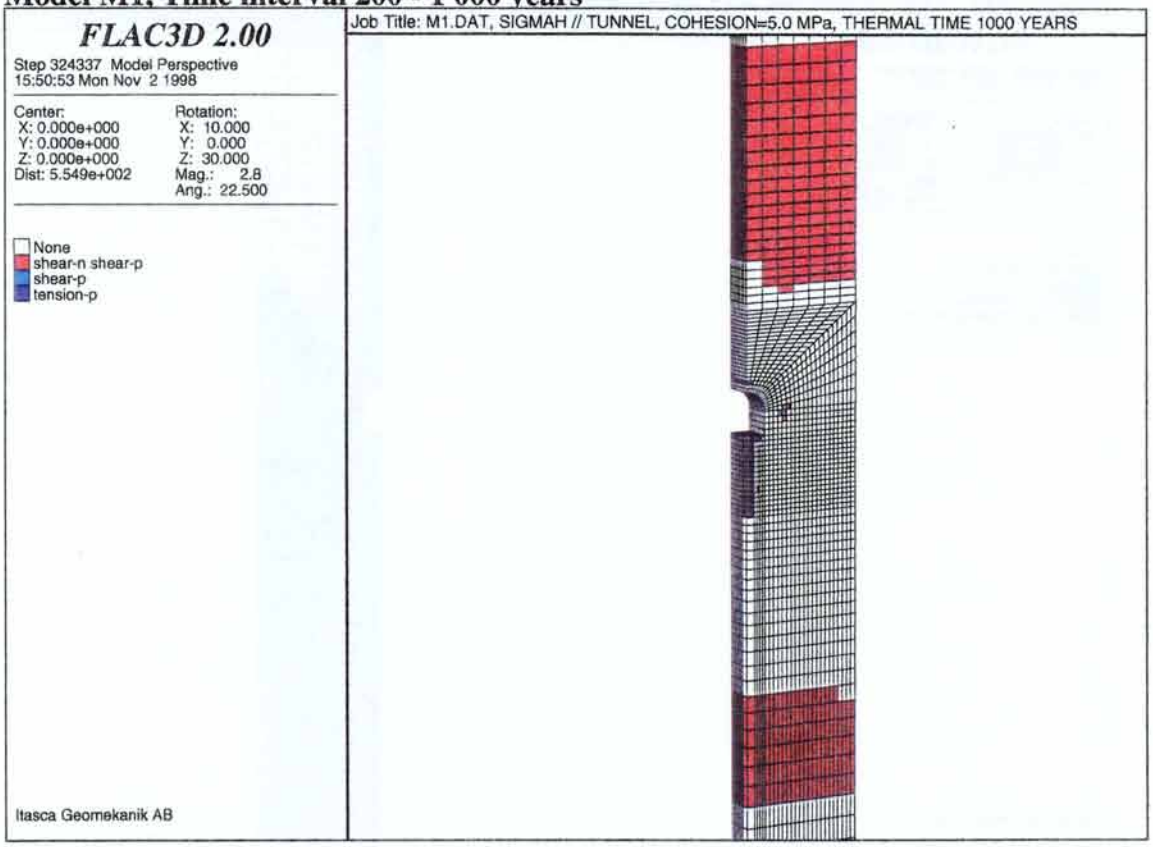

Model M1, Time interval 1 000 - 2 500 years

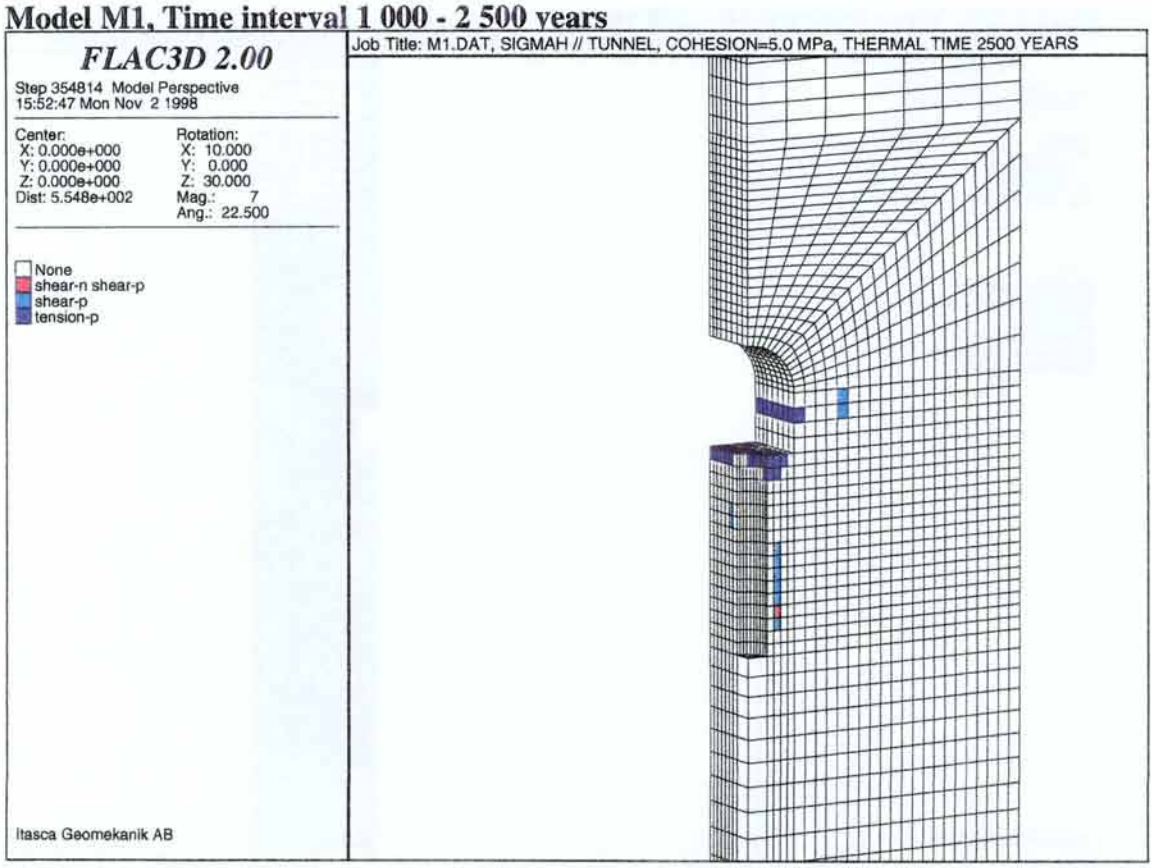

Model M1, Time interval 2 500 - 5 000 years

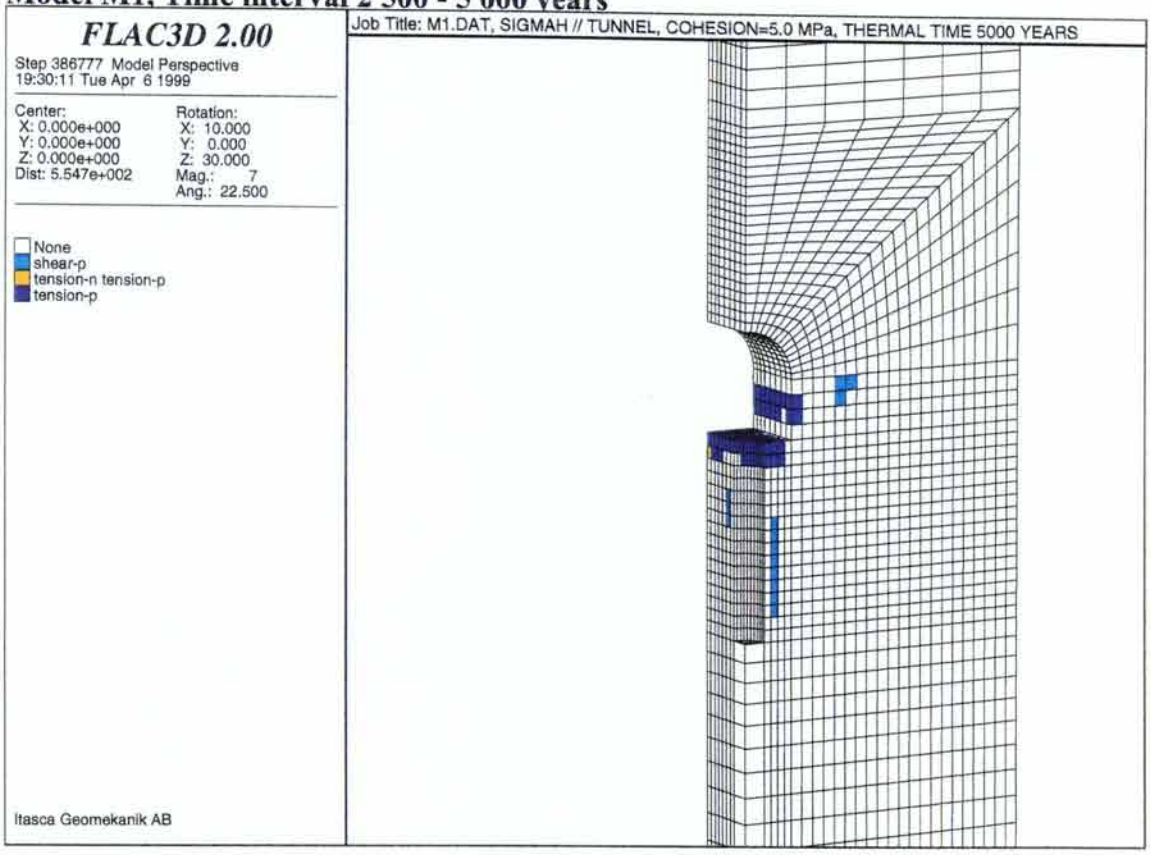

Model M1, Time interval 5 000 - 10 000 years

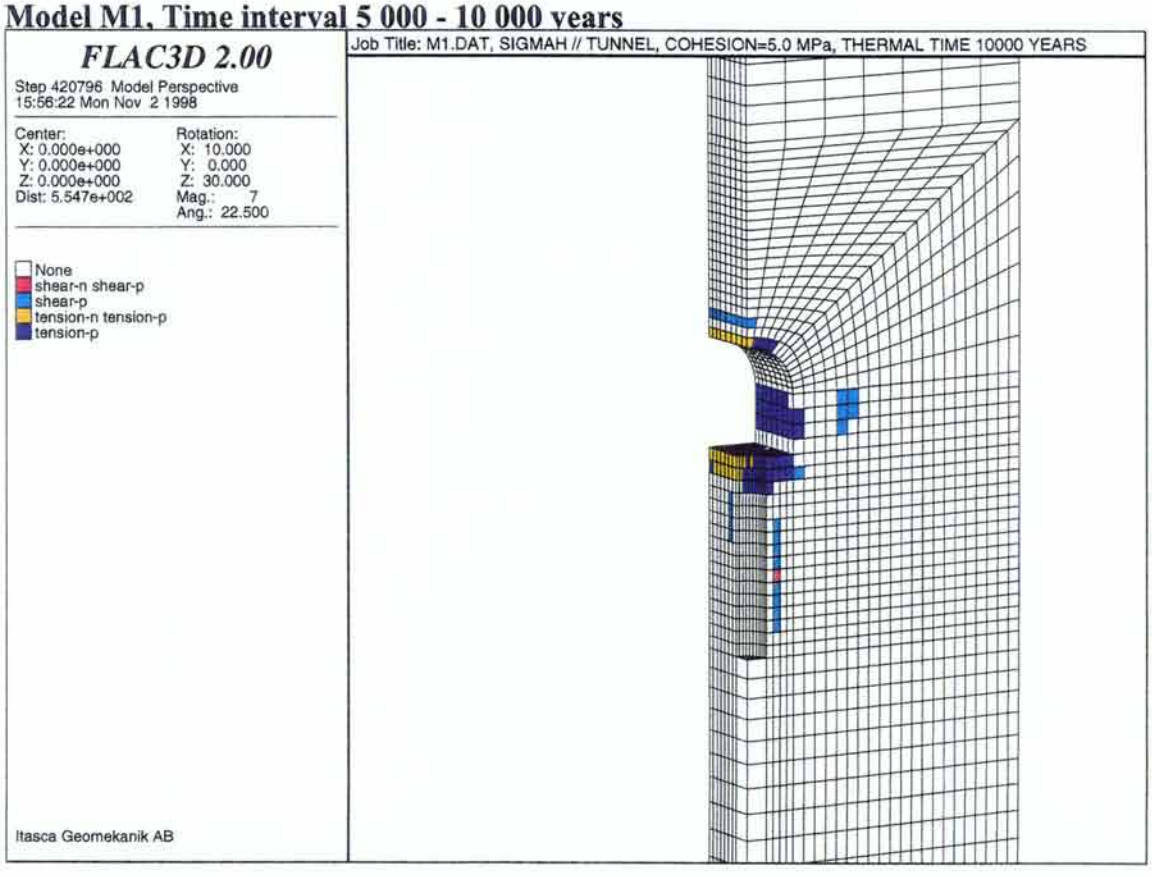

Appendix C: PLASTICITY STATE OF THE ZONES FOR MODEL M2

Plasticity state indicators for the thermo-mechanical calculations shows which zones that have been activated for that particular time interval. Thus, a zone can have state yield at one time interval and state no yield at another time interval.

In the subsequent figures, plasticity states of zones are identified by different colours with the following meaning:

None elastic,

Shear-n at shear yield now,

Shear-p elastic, but previously at shear yield,

Tension-n at tensile yield now,

Tension-p elastic, but previously at tensile yield.

These states can be combined and the combination will have its own colour (e.g. shear-p combined with tension-p).

List of thermo-mechanical models

Model	Direction of major horizontal stress relative to repository tunnel axis	Rock mass cohesion [MPa]	Rock mass friction angle [°]	Effective or total stress analysis
M1	Parallel	5	30	Effective
M2	Parallel	3	30	Effective
M3	Parallel	1	30	Effective
M4	Perpendicular	5	30	Effective
M5	Perpendicular	3	30	Effective
M6	Perpendicular	1	30	Effective
M7	Parallel	5	30	Total
M8	Parallel	5	45	Effective

Model M2, Time 0 years (Groundwater pressure initiated)

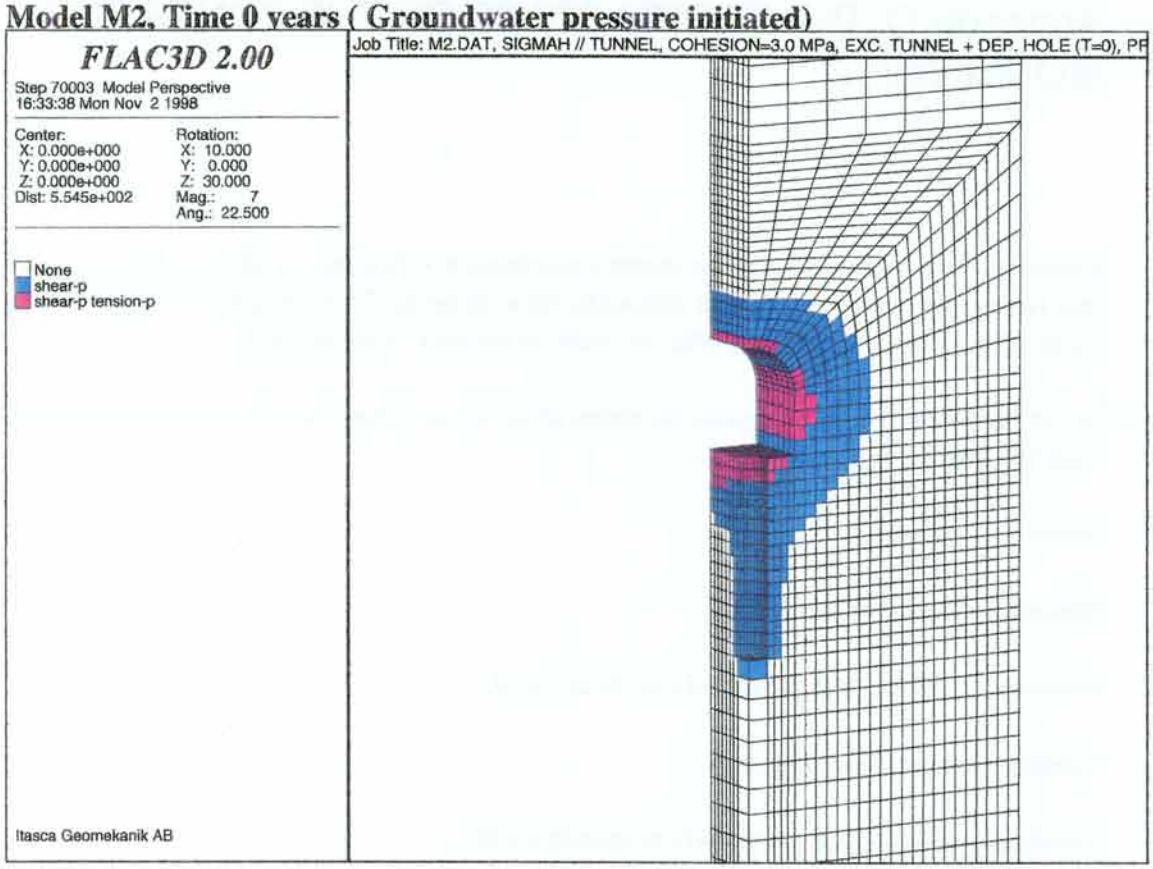

Model M2, Time interval 0 - 0.5 years

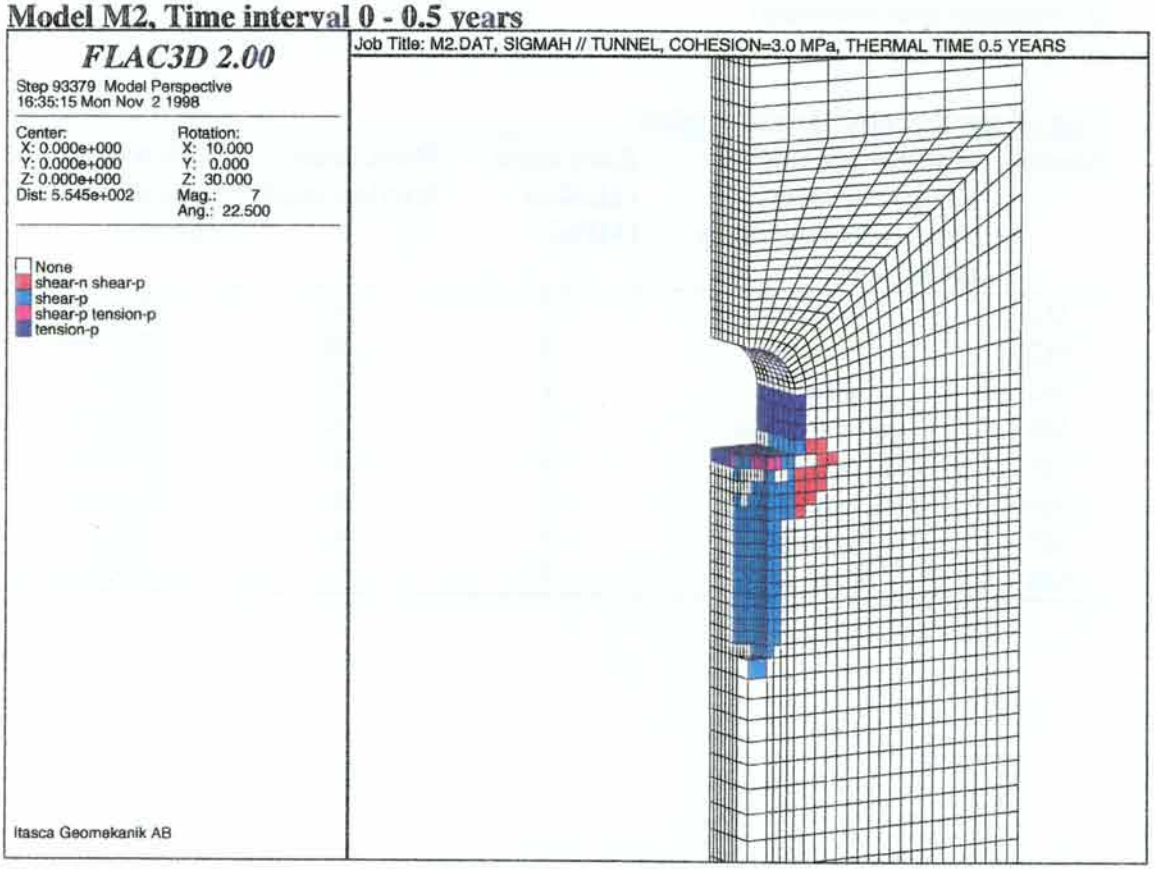

Model M2, Time interval 0.5 - 2 years

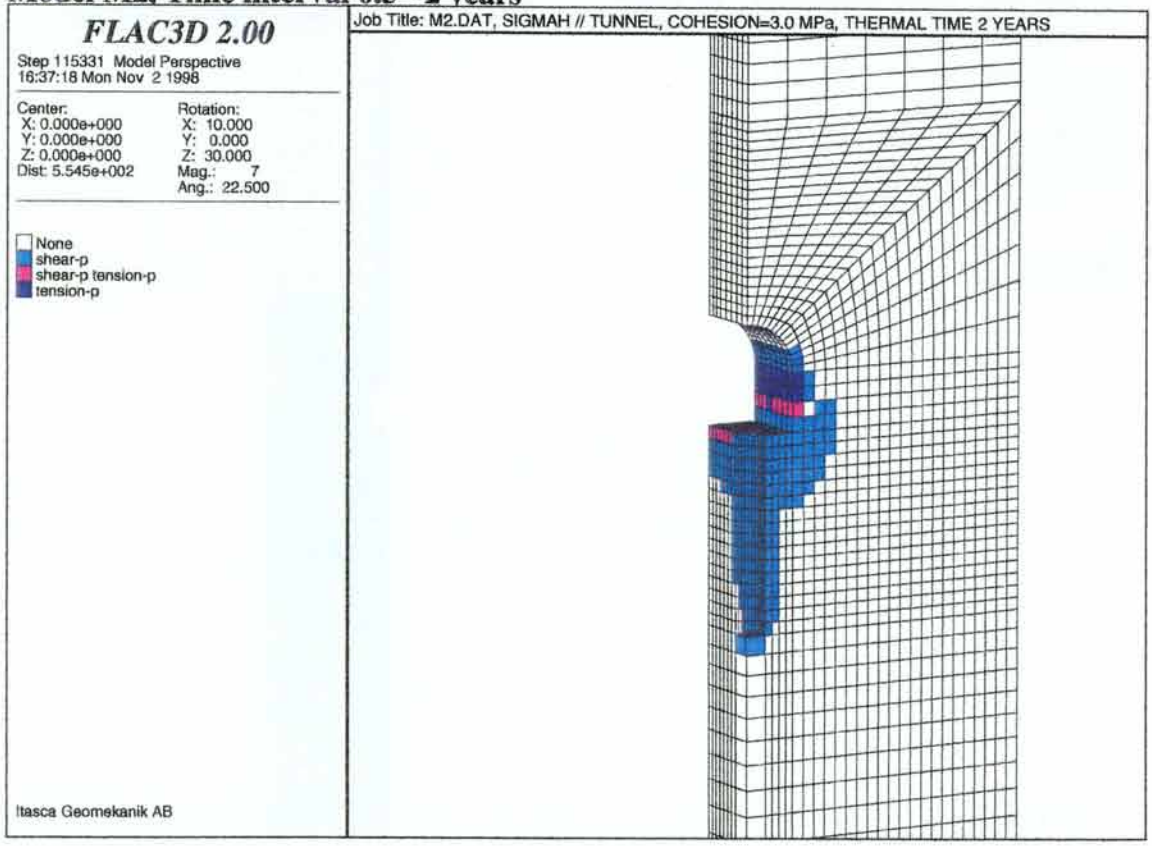

Model M2, Time interval 2 - 6 years

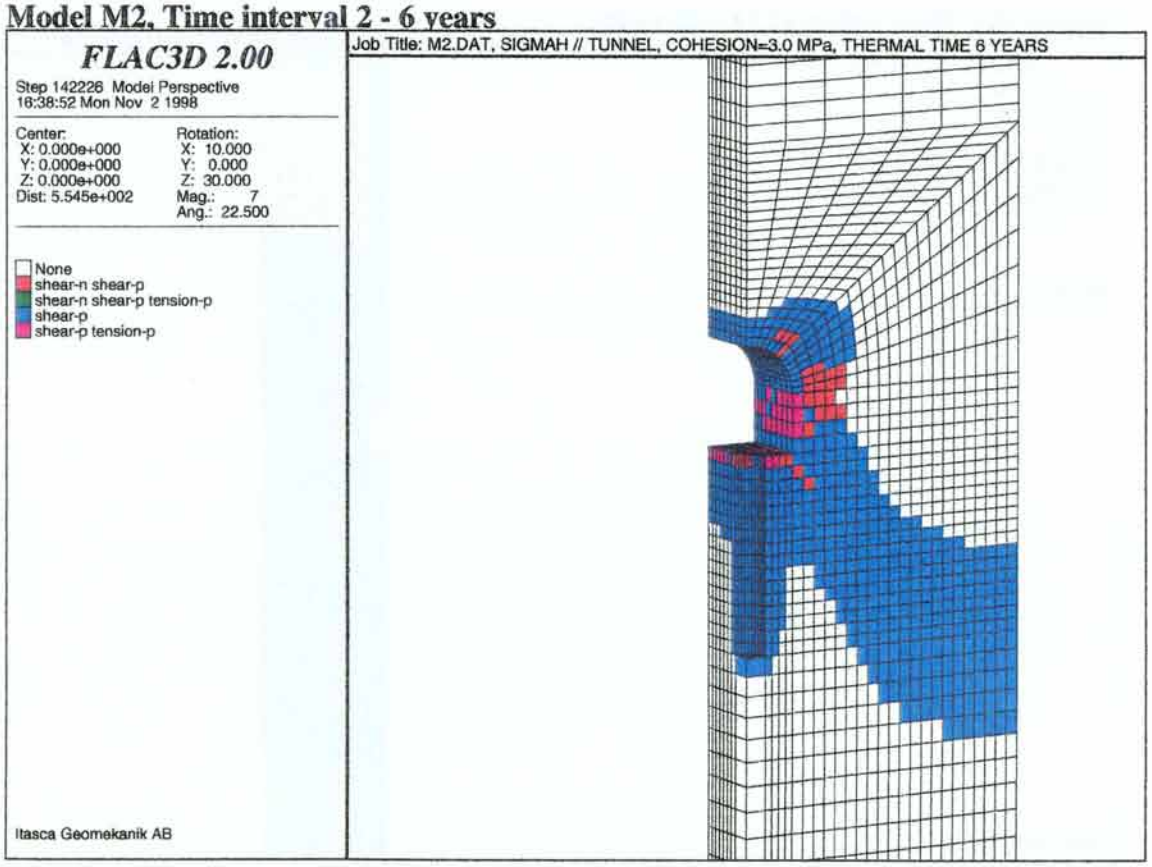

Model M2, Time interval 6 - 12 years

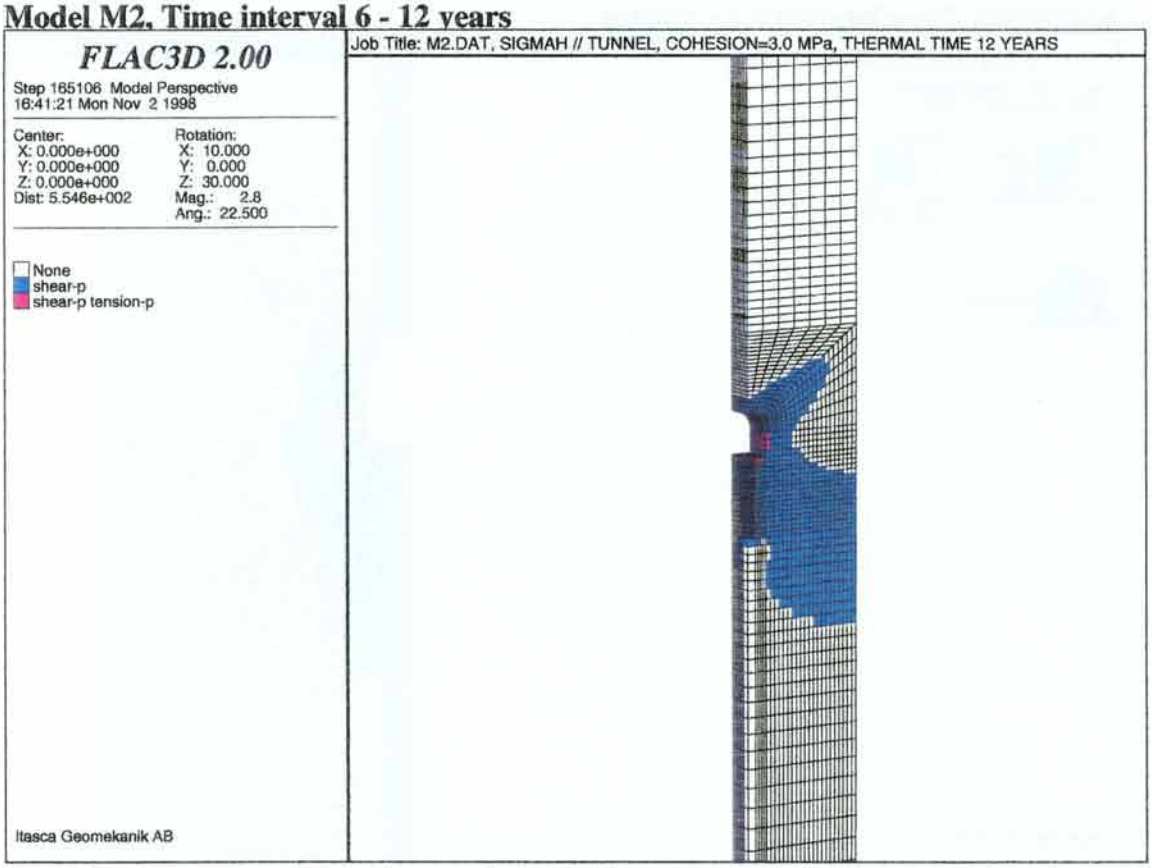

Model M2, Time interval 12 - 25 years

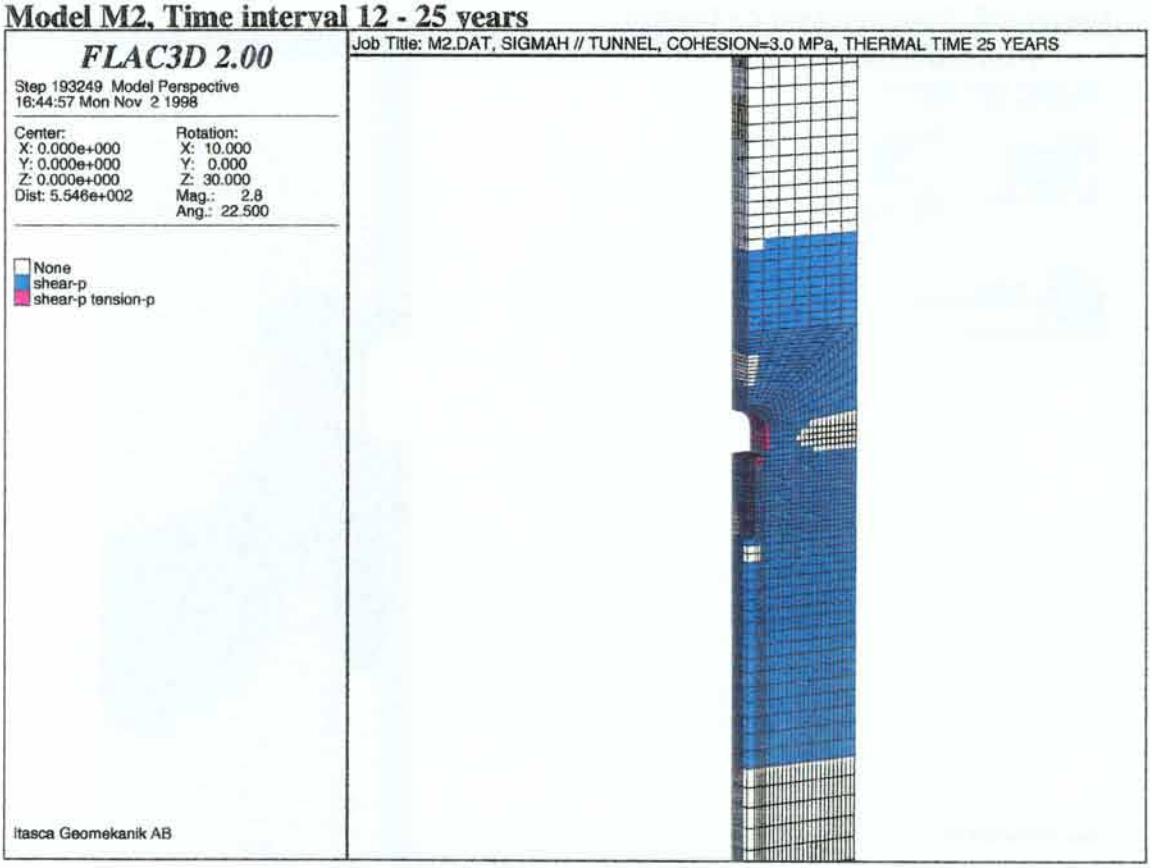

Model M2, Time interval 25 - 50 years

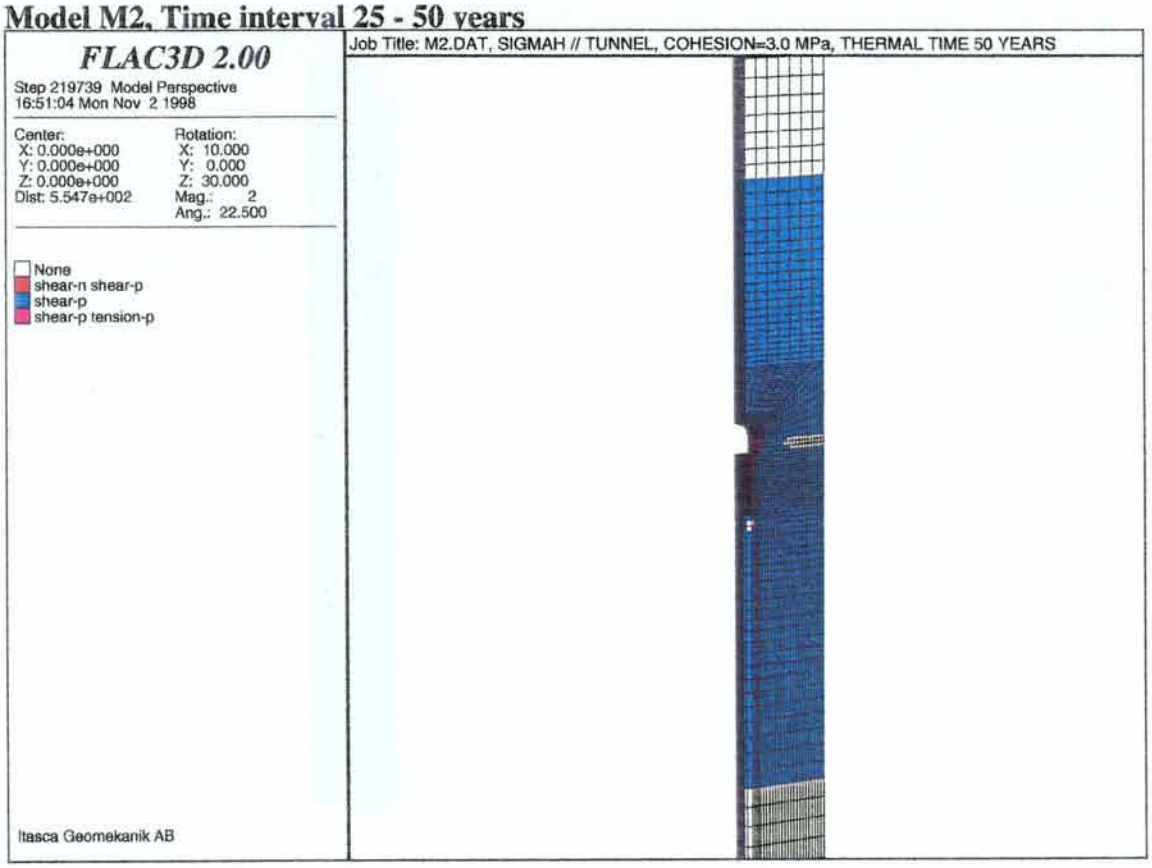

Model M2, Time interval 50 - 200 years (upper part of model)

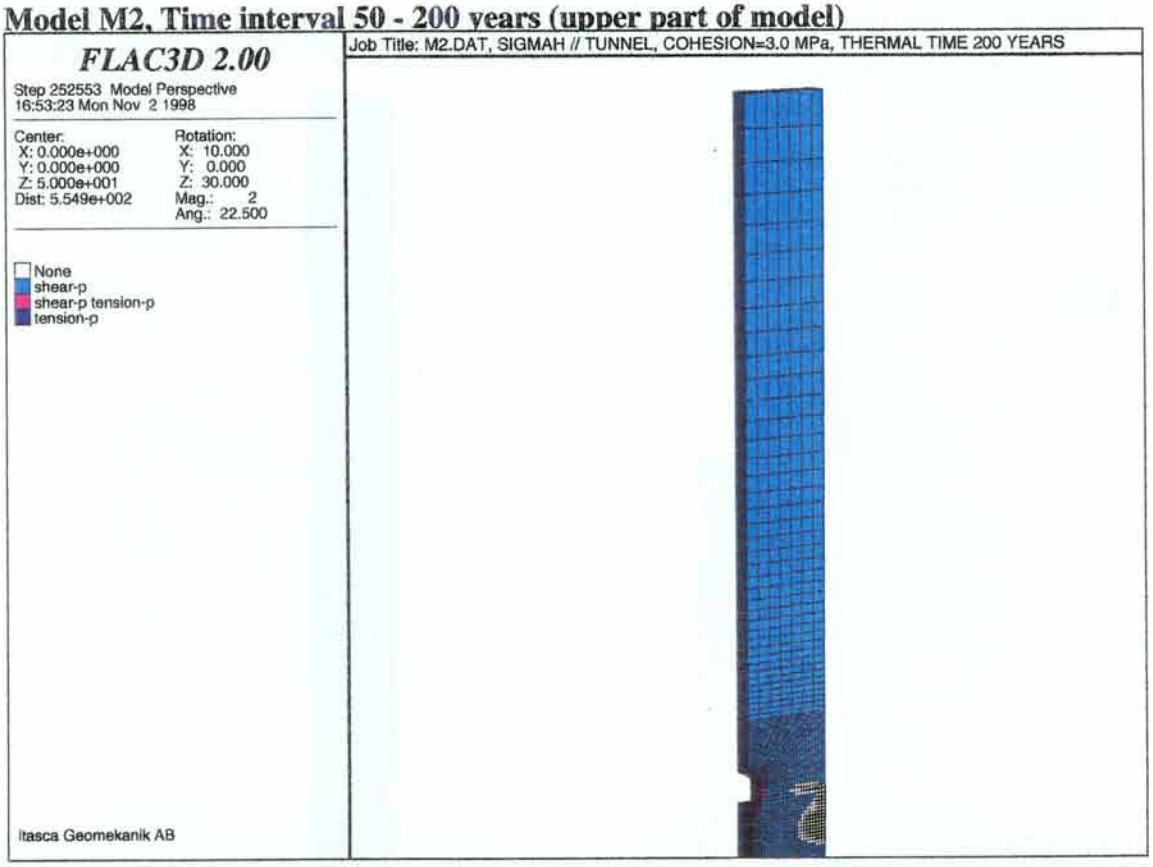

Model M2, Time interval 50 - 200 years (lower part of model)

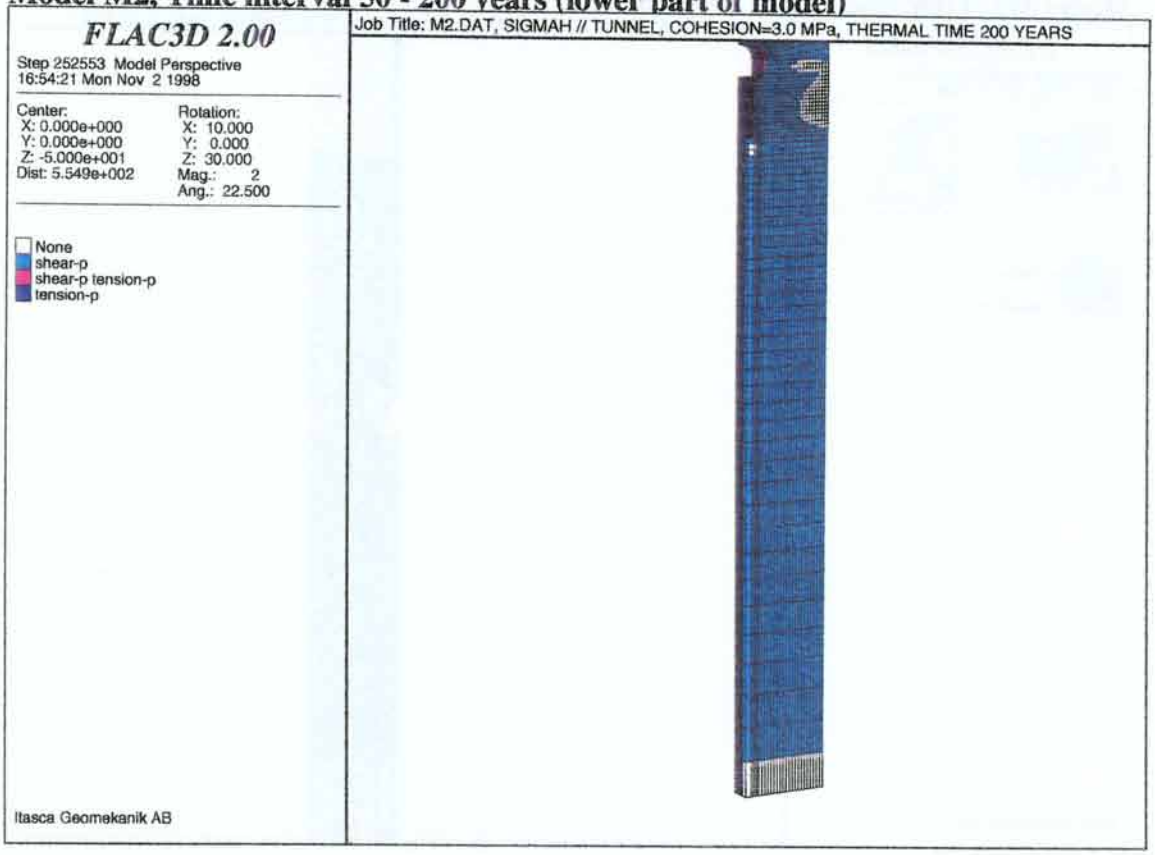

Model M2, Time interval 200 - 1 000 years (upper part of model)

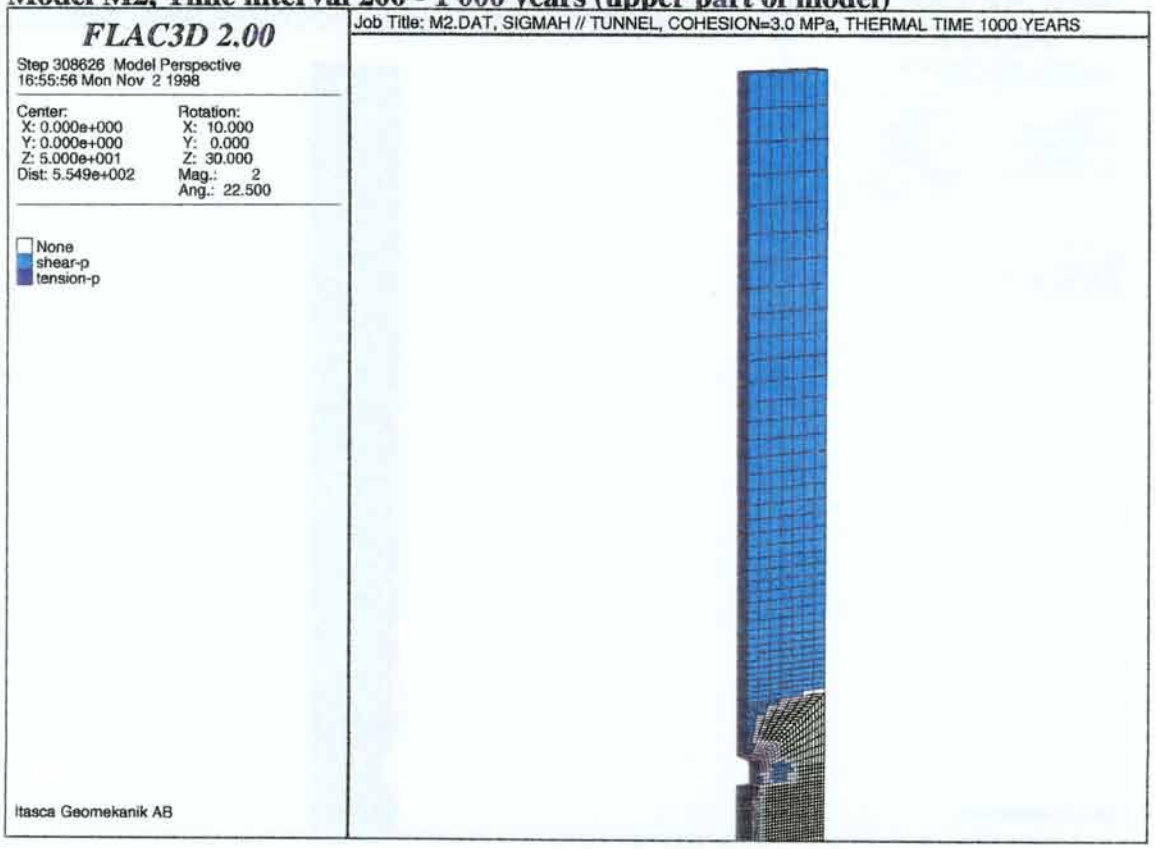

Model M2, Time interval 200 - 1 000 years (lower part of model)

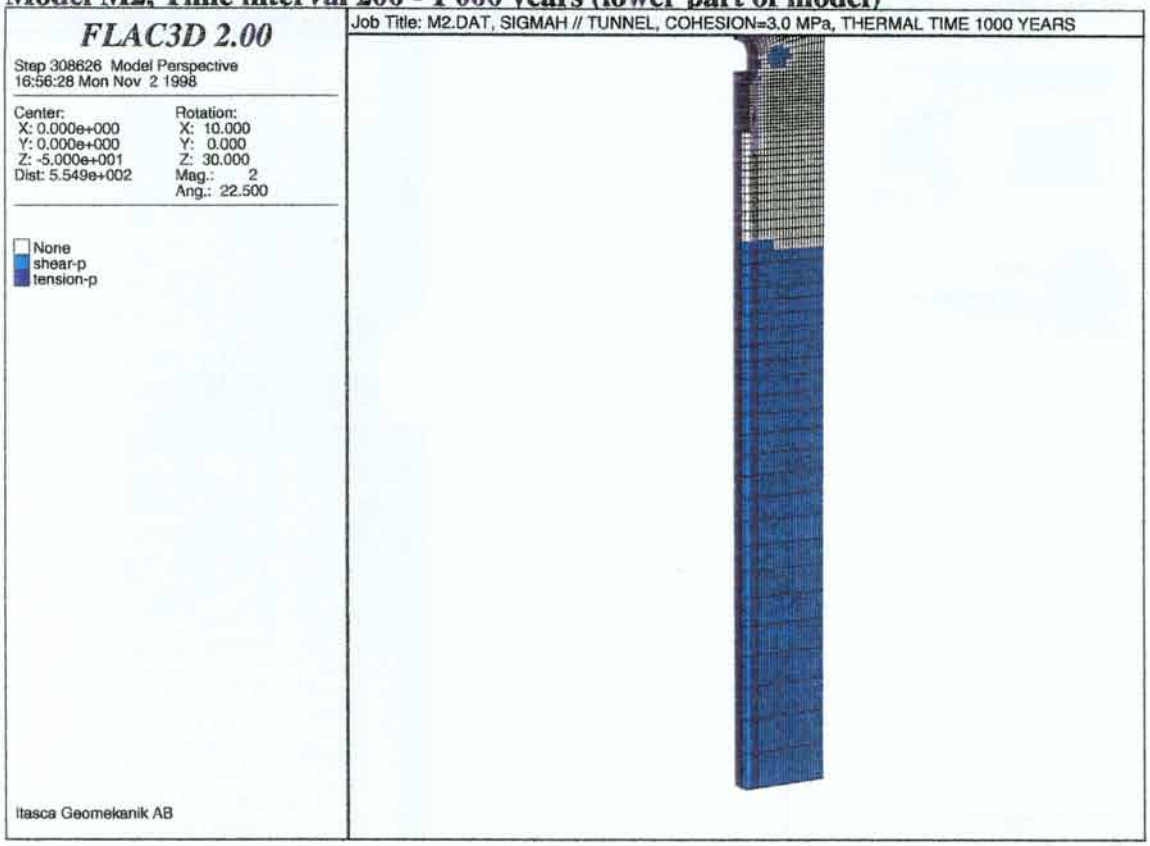

Model M2, Time interval 1 000 - 2 500 years

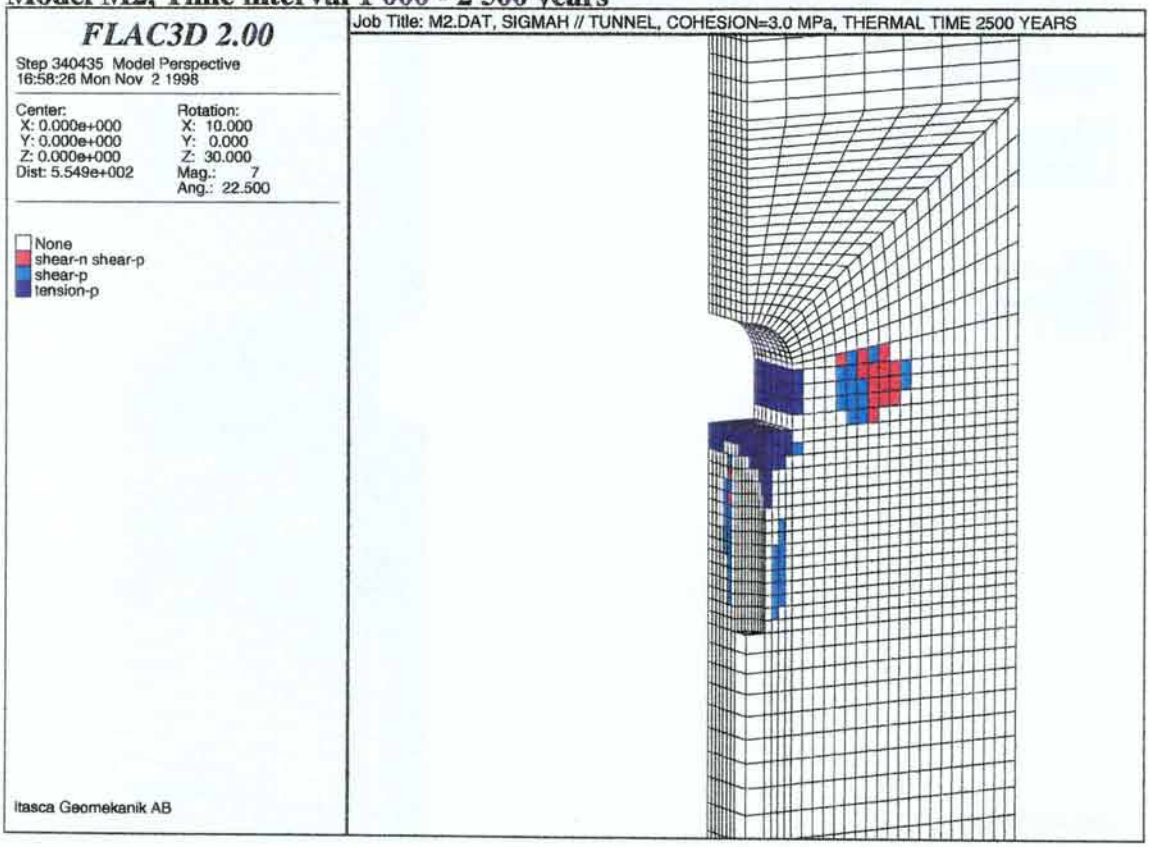

Model M2, Time interval 2 500 - 5 000 years

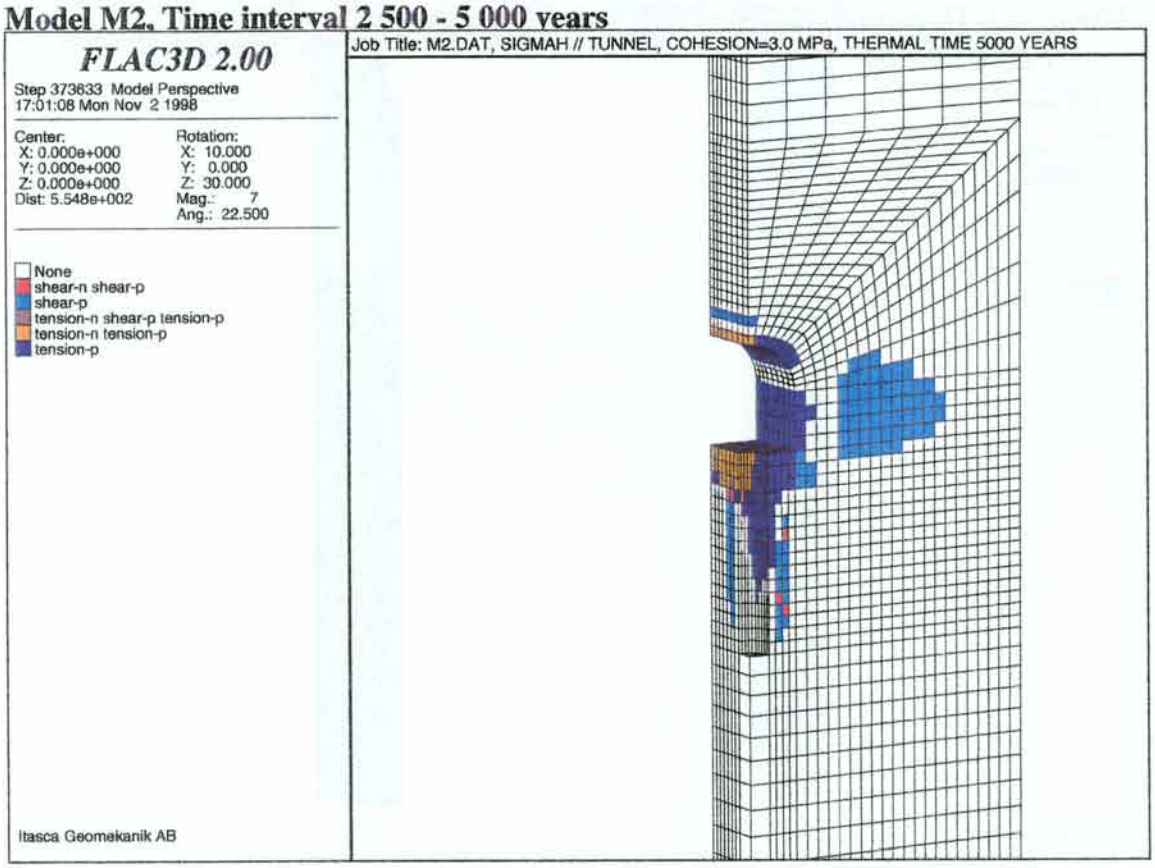

Model M2, Time interval 5 000 - 10 000 years

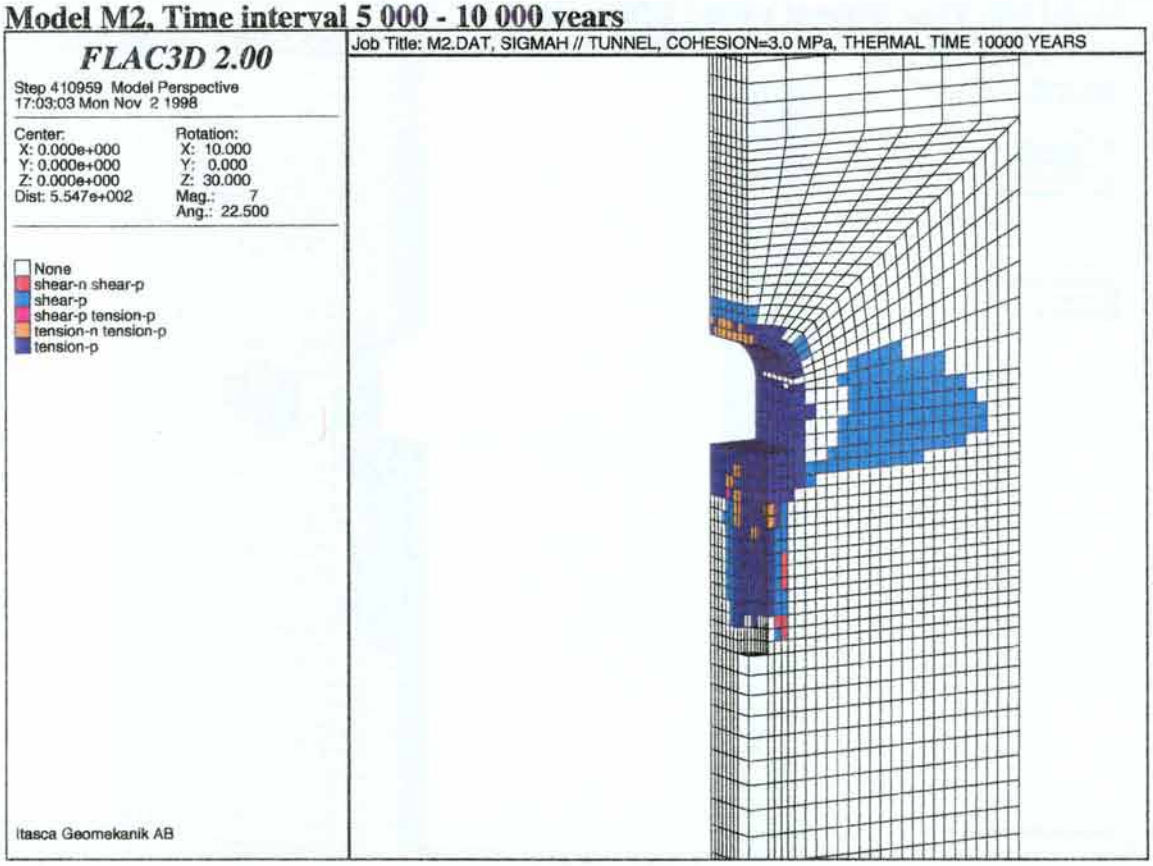

Appendix D: PLASTICITY STATE OF THE ZONES FOR MODEL M4

Plasticity state indicators for the thermo-mechanical calculations shows which zones that have been activated for that particular time interval. Thus, a zone can have state yield at one time interval and state no yield at another time interval.

In the subsequent figures, plasticity states of zones are identified by different colours with the following meaning:

None elastic,

Shear-n at shear yield now,

Shear-p elastic, but previously at shear yield,

Tension-n at tensile yield now,

Tension-p elastic, but previously at tensile yield.

These states can be combined and the combination will have its own colour (e.g. shear-p combined with tension-p).

List of thermo-mechanical models

Model	Direction of major horizontal stress relative to repository tunnel axis	Rock mass cohesion [MPa]	Rock mass friction angle [°]	Effective or total stress analysis
M1	Parallel	5	30	Effective
M2	Parallel	3	30	Effective
M3	Parallel	1	30	Effective
M4	Perpendicular	5	30	Effective
M5	Perpendicular	3	30	Effective
M6	Perpendicular	1	30	Effective
M7	Parallel	5	30	Total
M8	Parallel	5	45	Effective

Model M4, Time 0 years (Groundwater pressure initiated)

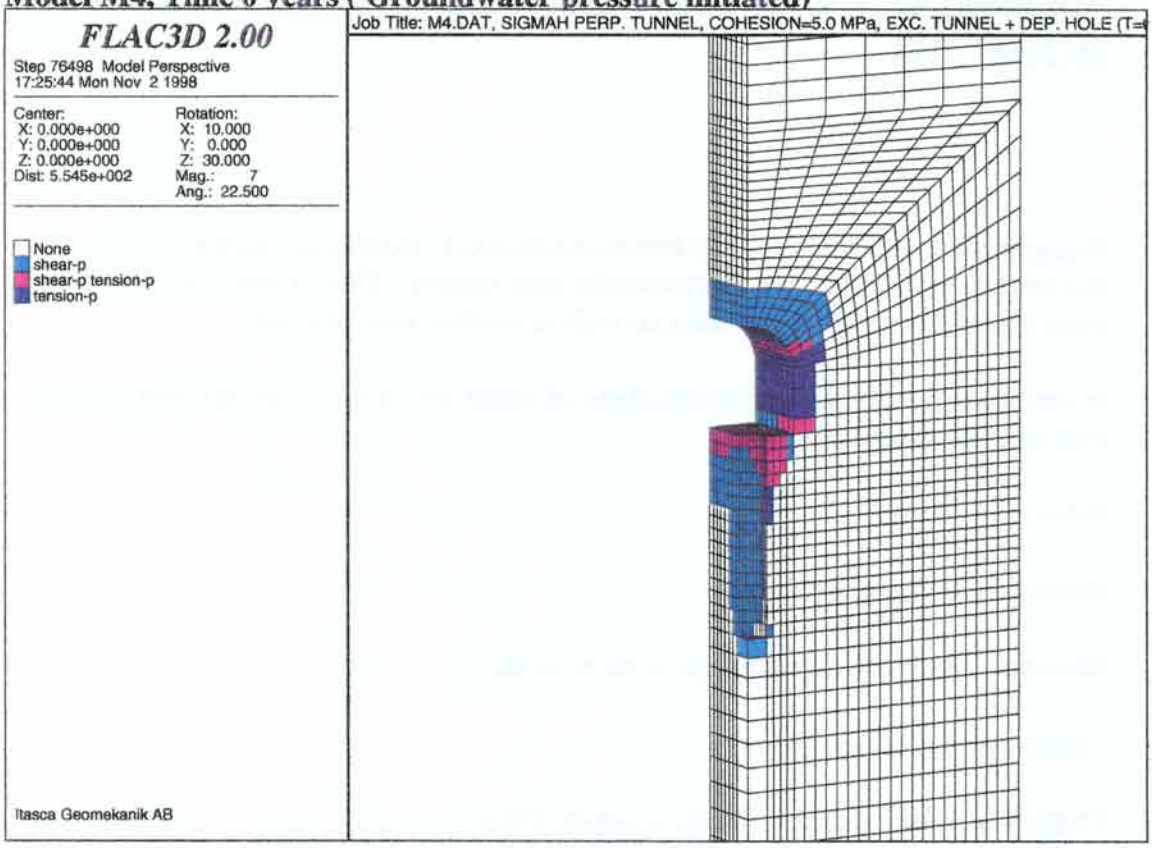

Model M4, Time interval 0 - 0.5 years

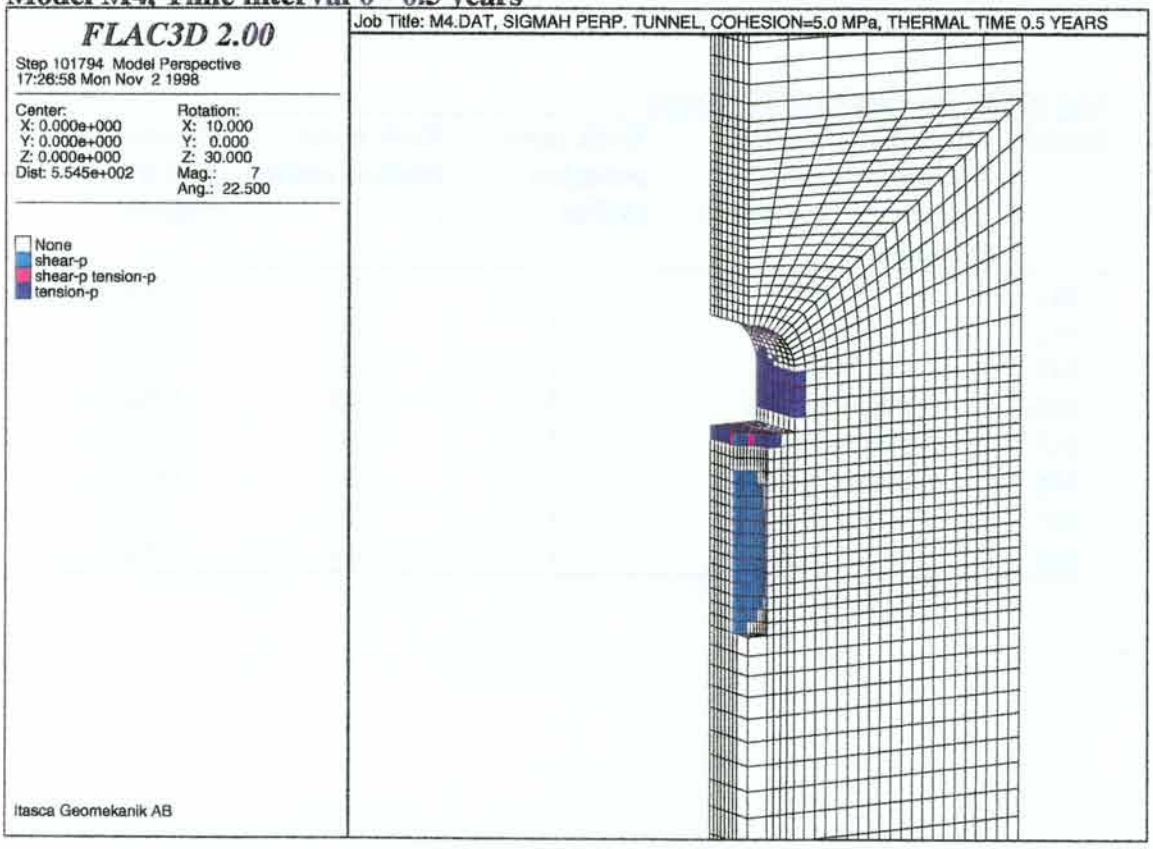

Model M4, Time interval 0.5 - 2 years

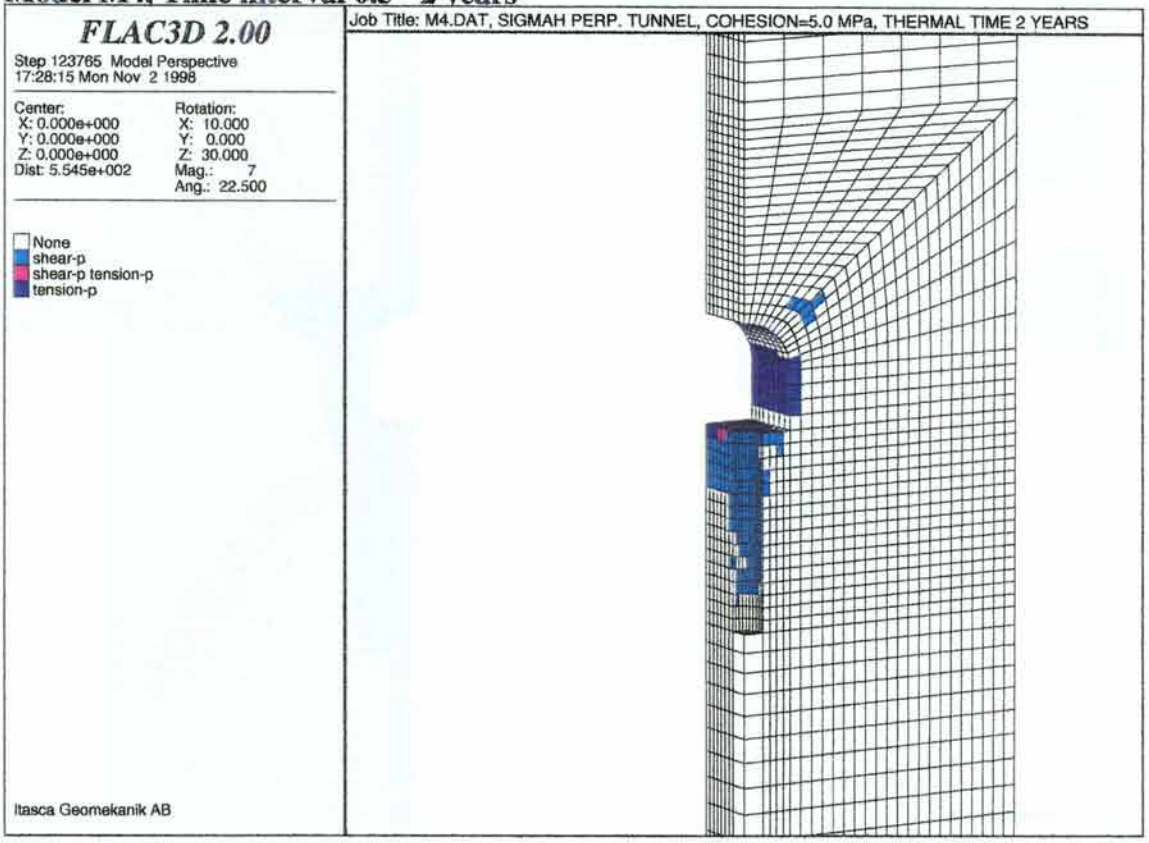

Model M4, Time interval 2 - 6 years

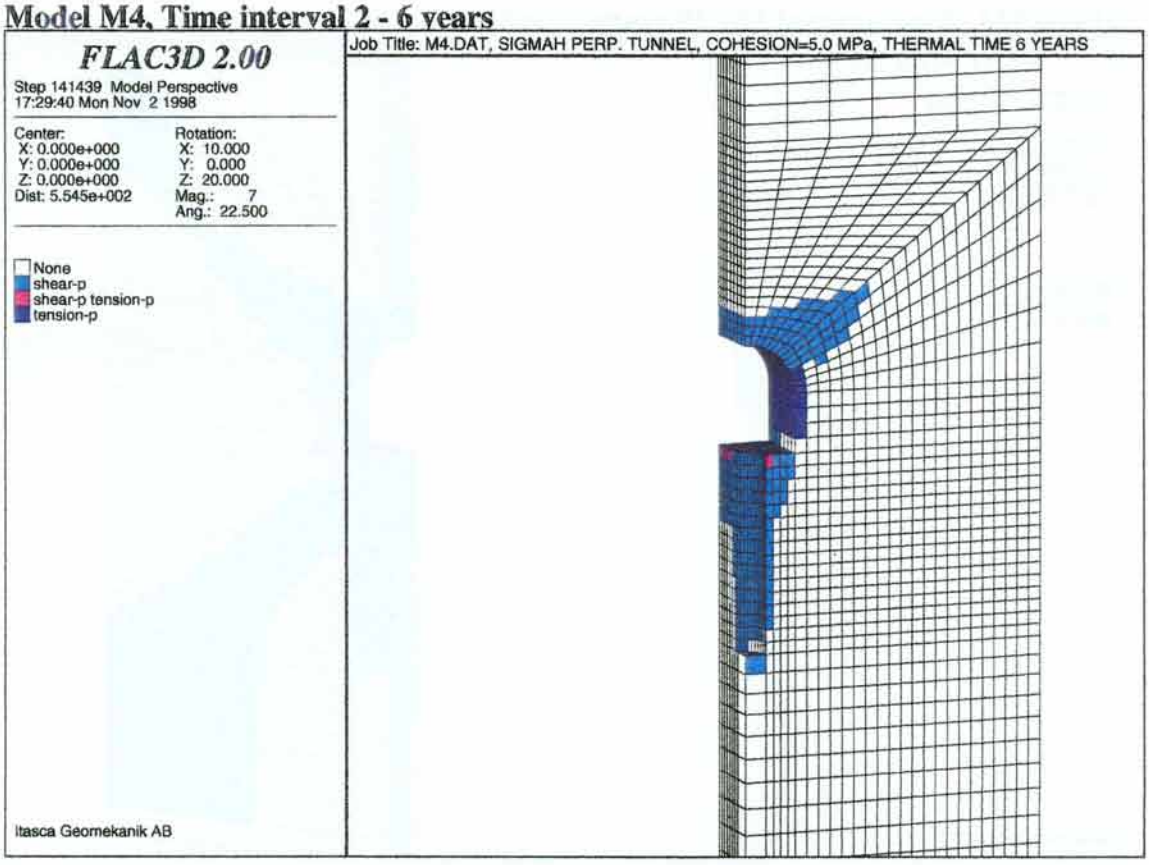

Model M4, Time interval 6 - 12 years

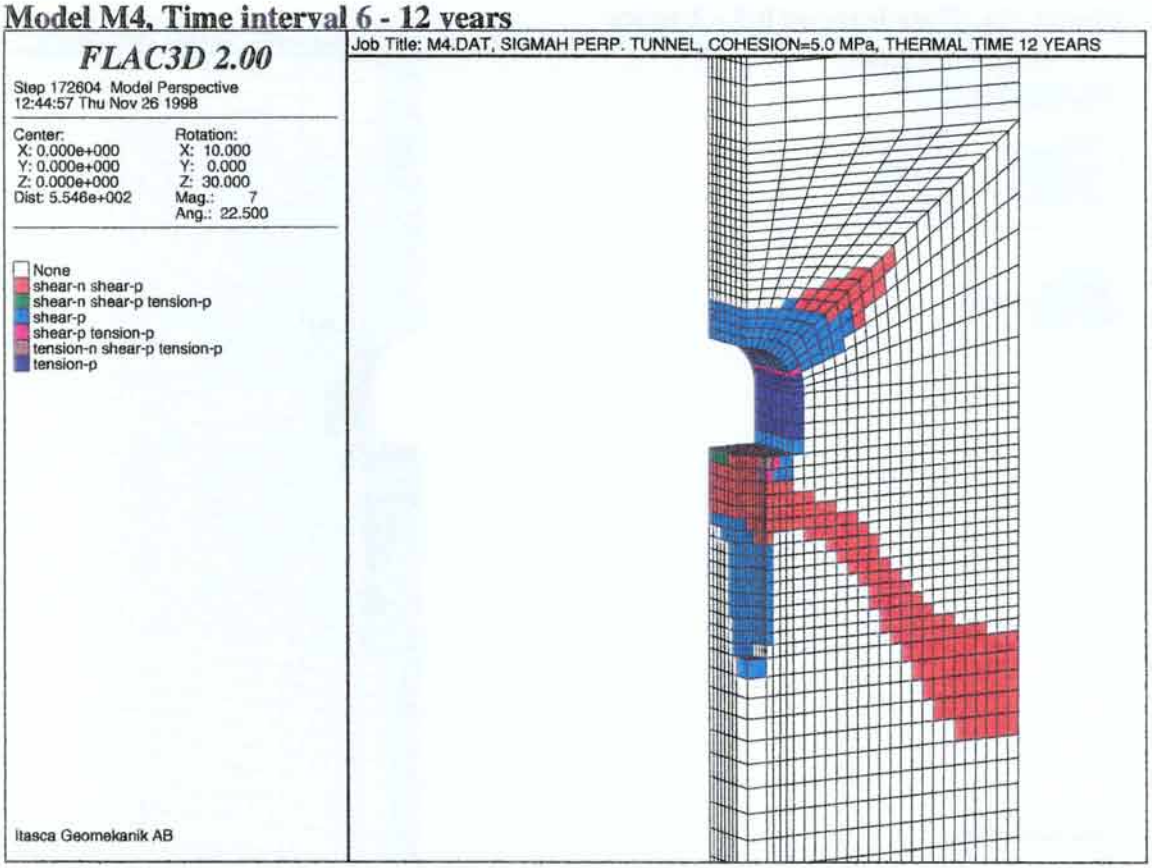

Model M4, Time interval 12 - 25 years

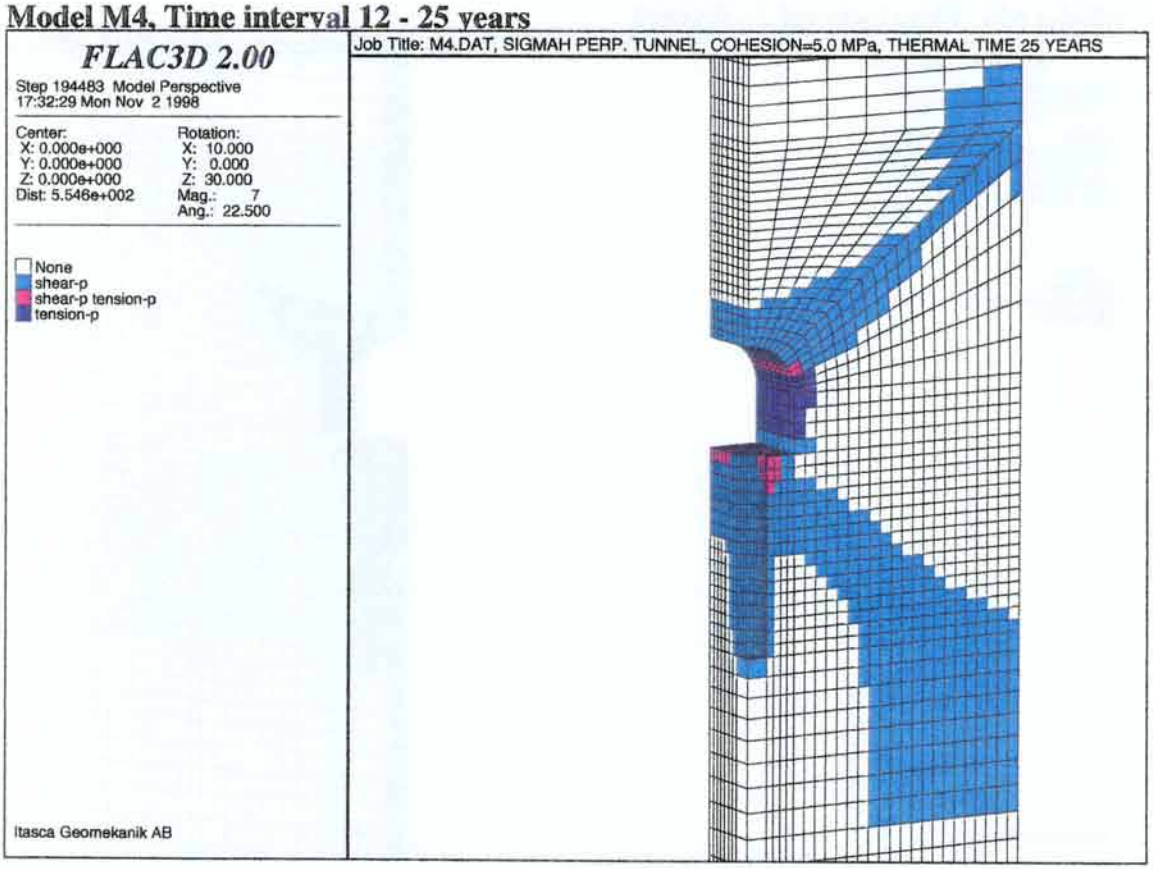

Model M4, Time interval 25 - 50 years

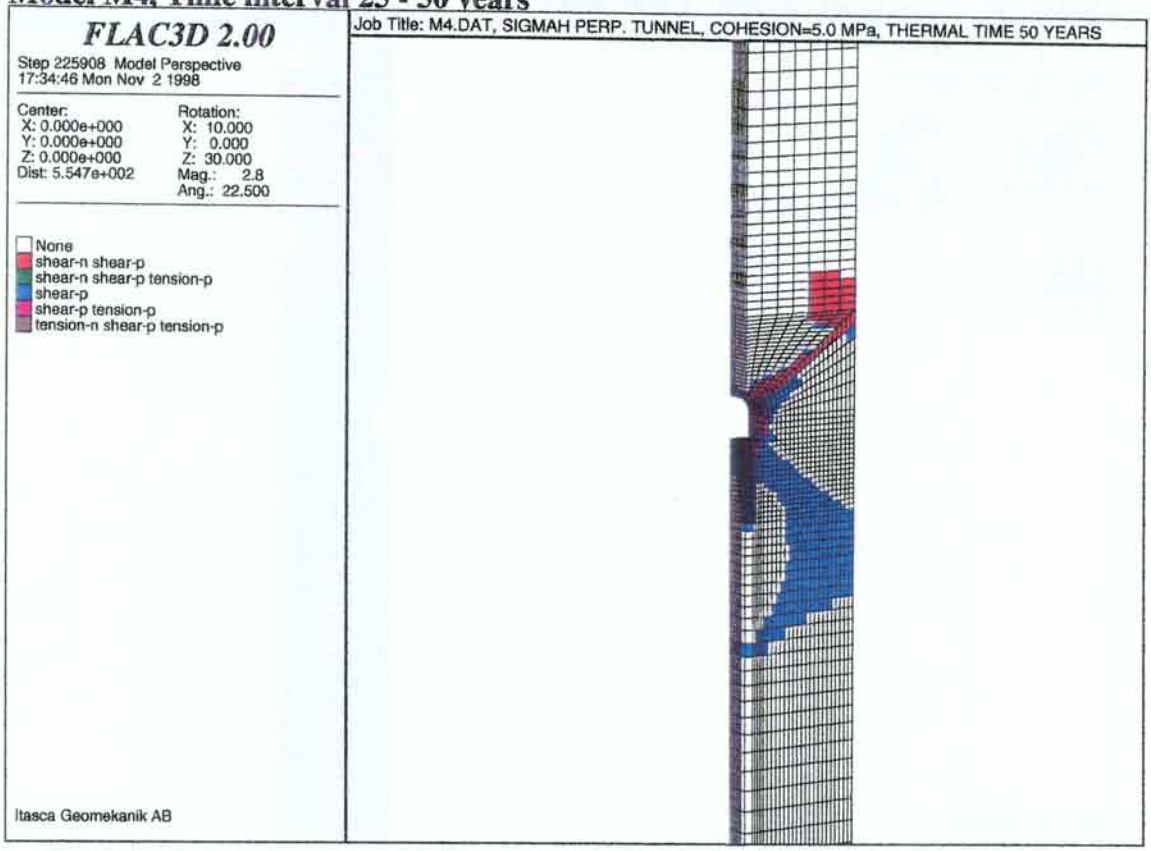

Model M4, Time interval 50 - 200 years

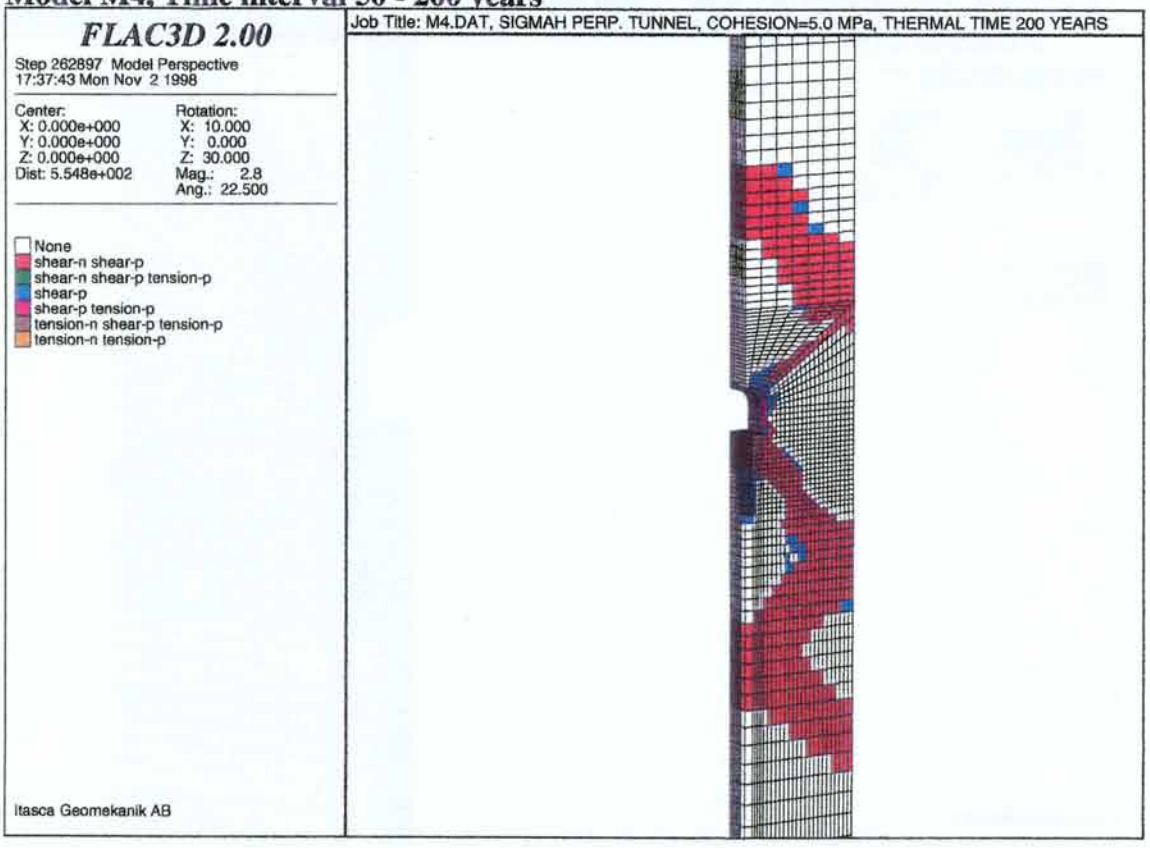

Model M4, Time interval 200 - 1 000 years

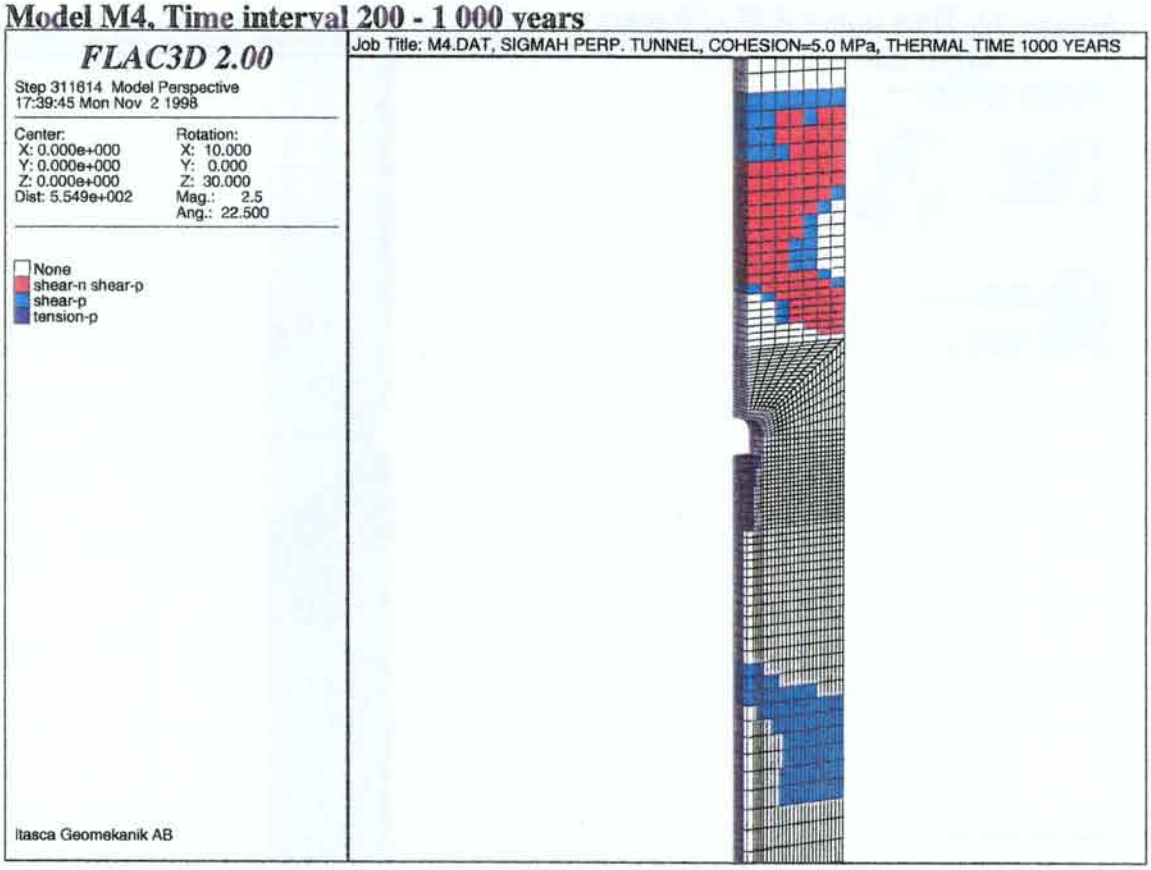

Model M4, Time interval 1 000 - 2 500 years

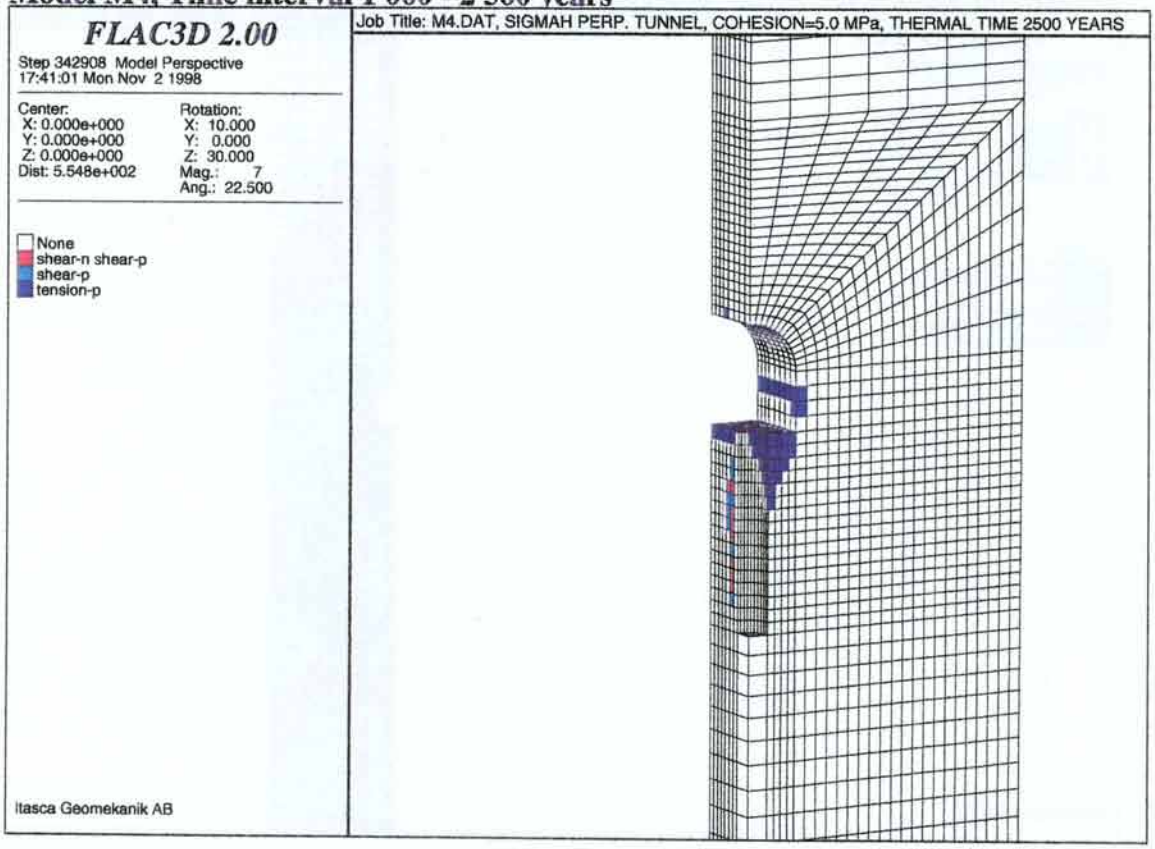

Model M4, Time interval 2 500 - 5 000 years

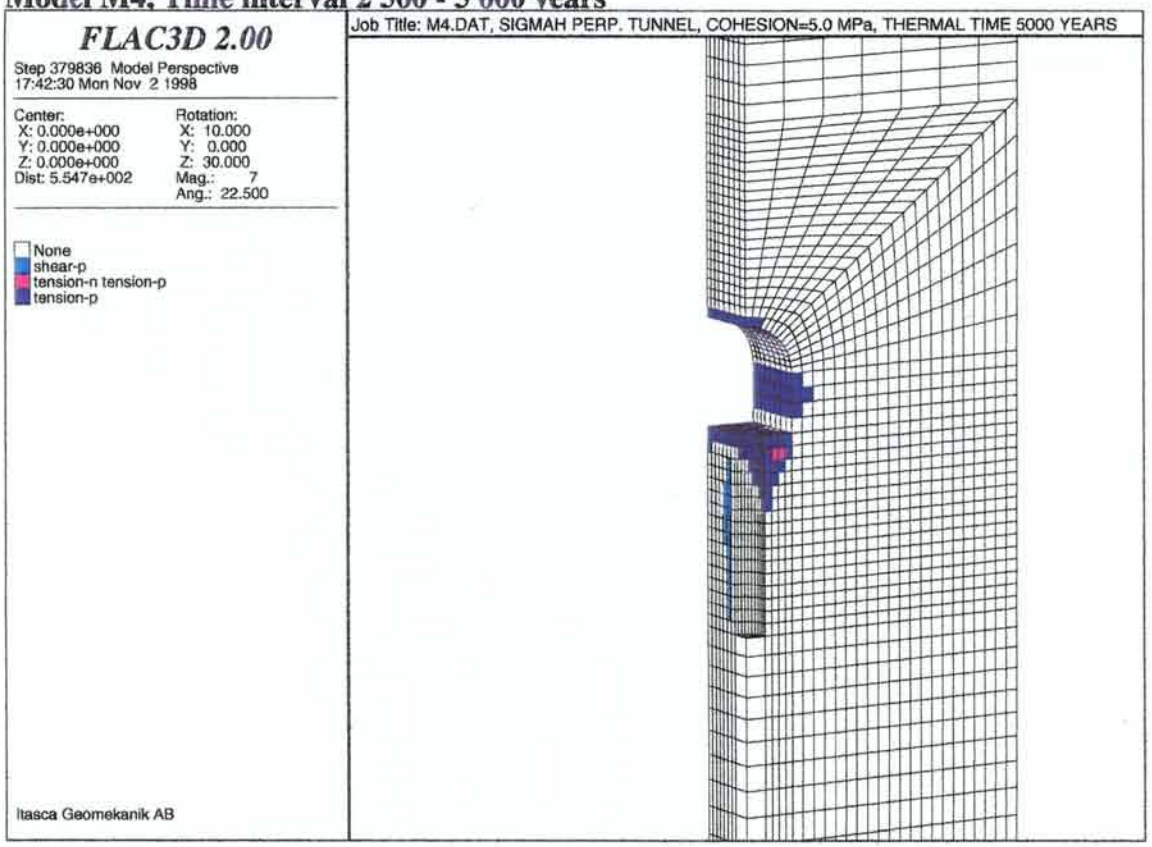

Model M4, Time interval 5 000 - 10 000 years

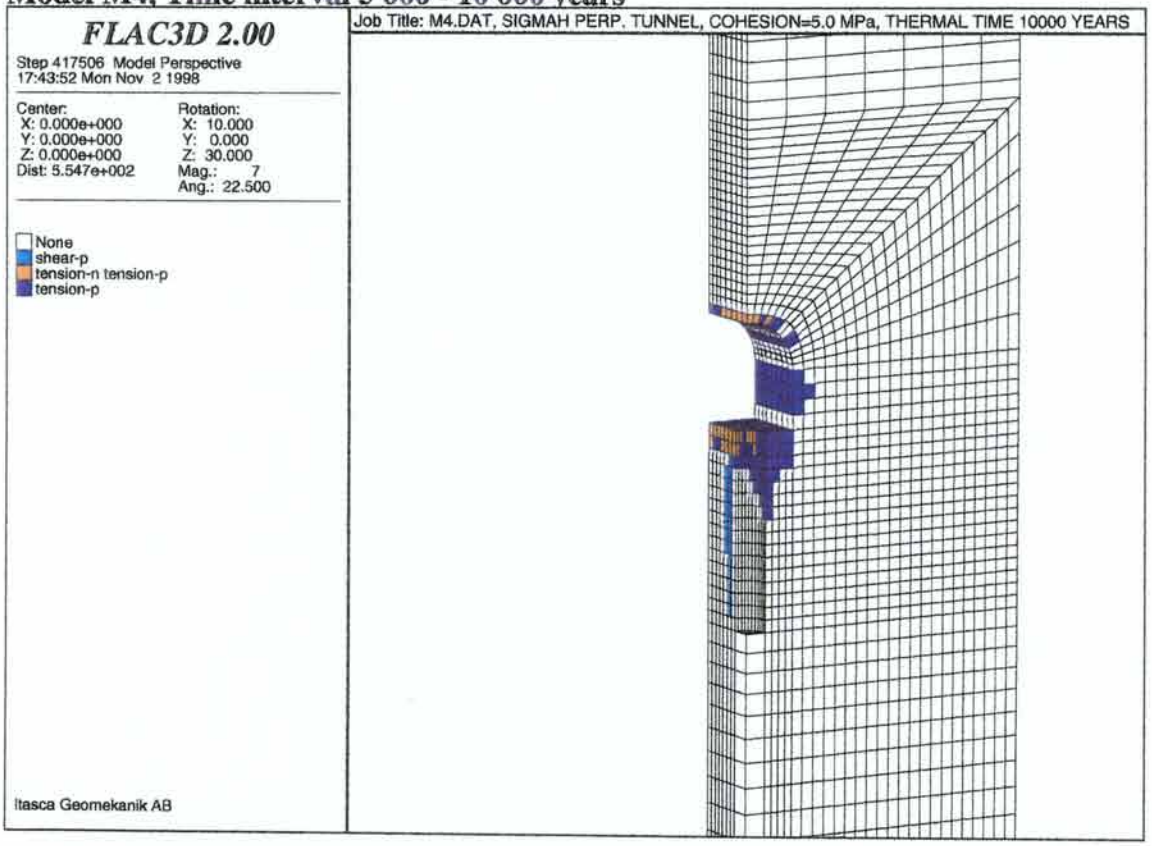

Appendix E: PLASTICITY STATE OF THE ZONES FOR MODEL M5

Plasticity state indicators for the thermo-mechanical calculations shows which zones that have been activated for that particular time interval. Thus, a zone can have state yield at one time interval and state no yield at another time interval.

In the subsequent figures, plasticity states of zones are identified by different colours with the following meaning:

None elastic,

Shear-n at shear yield now,

Shear-p elastic, but previously at shear yield,

Tension-n at tensile yield now,

Tension-p elastic, but previously at tensile yield.

These states can be combined and the combination will have its own colour (e.g. shear-p combined with tension-p).

List of thermo-mechanical models

Model	Direction of major horizontal stress relative to repository tunnel axis	Rock mass cohesion [MPa]	Rock mass friction angle [°]	Effective or total stress analysis
M1	Parallel	5	30	Effective
M2	Parallel	3	30	Effective
M3	Parallel	1	30	Effective
M4	Perpendicular	5	30	Effective
M5	Perpendicular	3	30	Effective
M6	Perpendicular	1	30	Effective
M7	Parallel	5	30	Total
M8	Parallel	5	45	Effective

Model M5, Time 0 years (Groundwater pressure initiated)

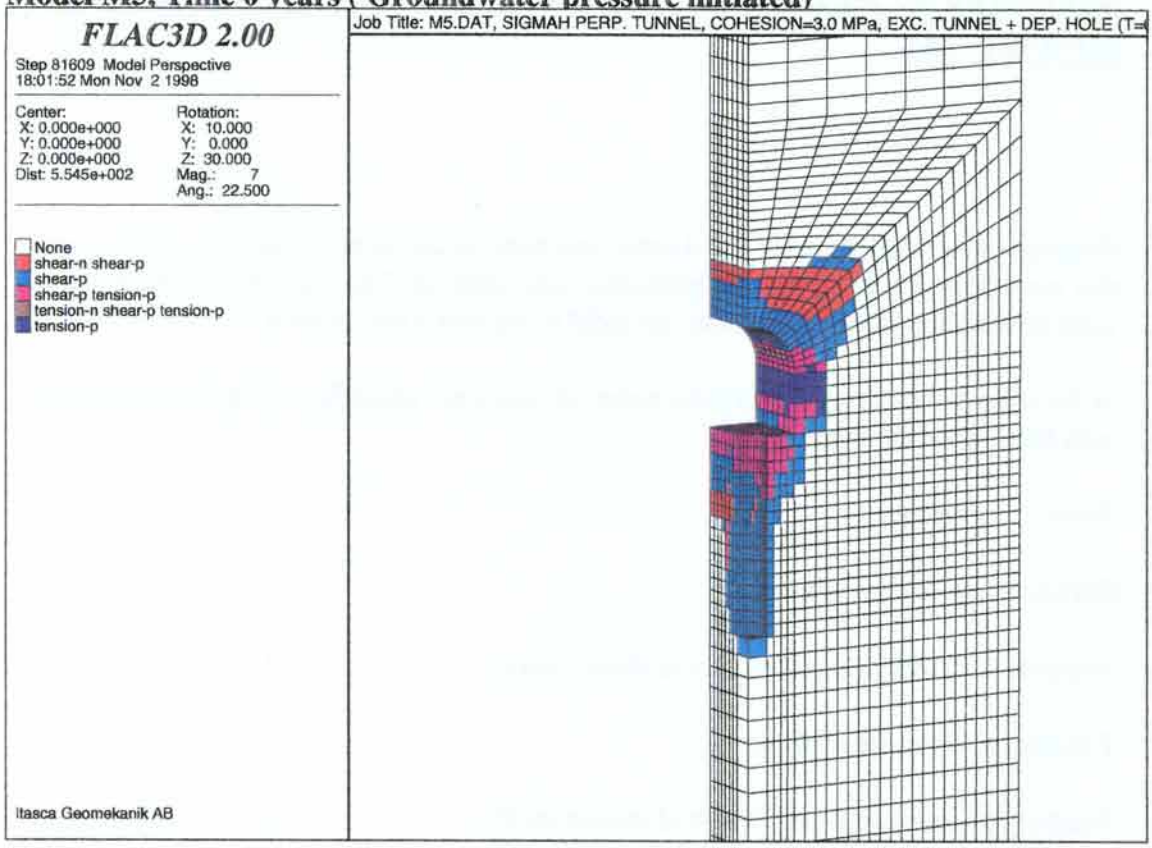

Model M5, Time interval 0 - 0.5 years

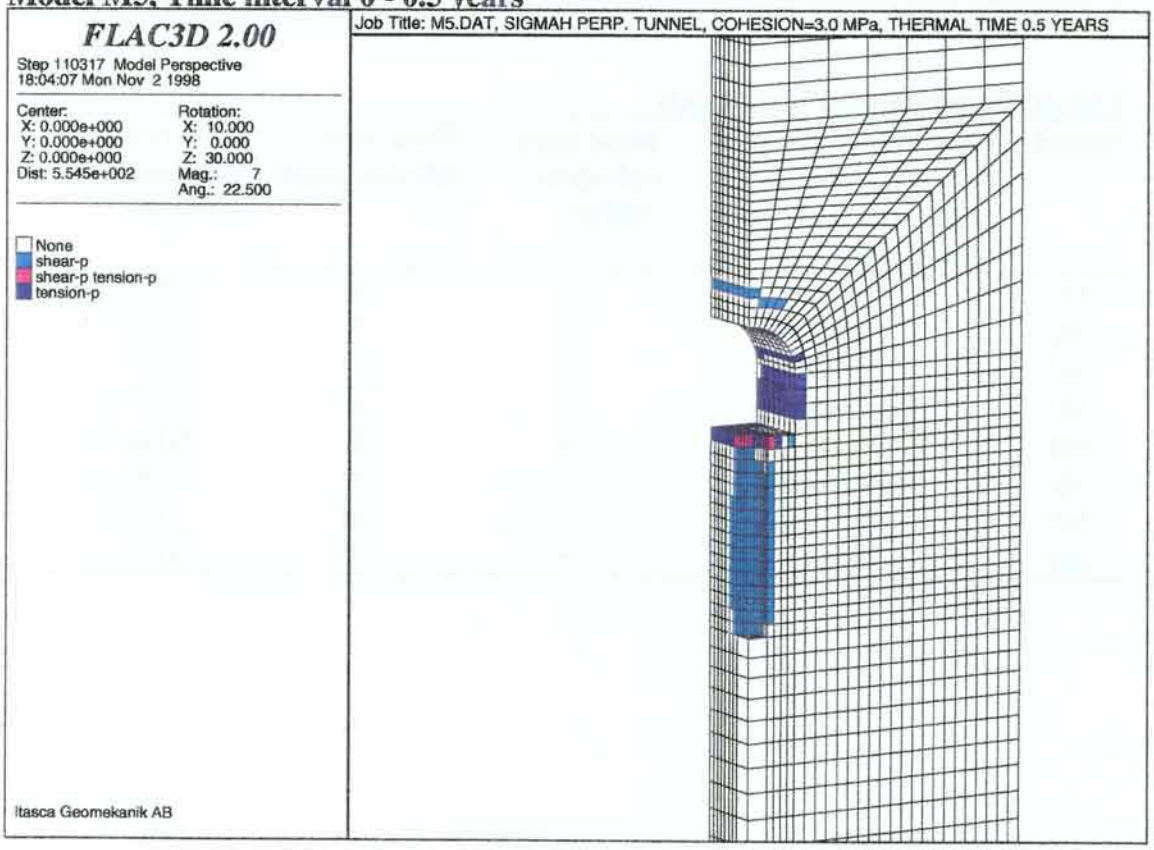

Model M5, Time interval 0.5 - 2 years

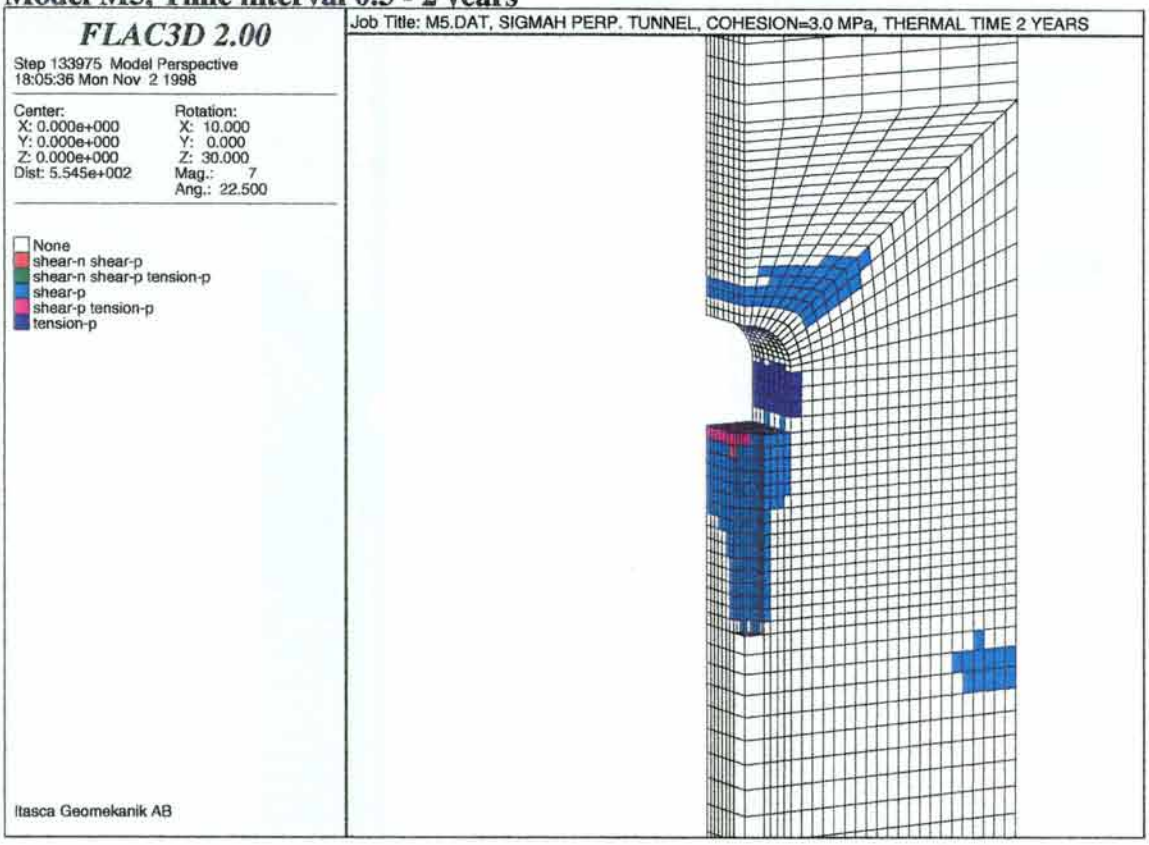

Model M5, Time interval 2 - 6 years

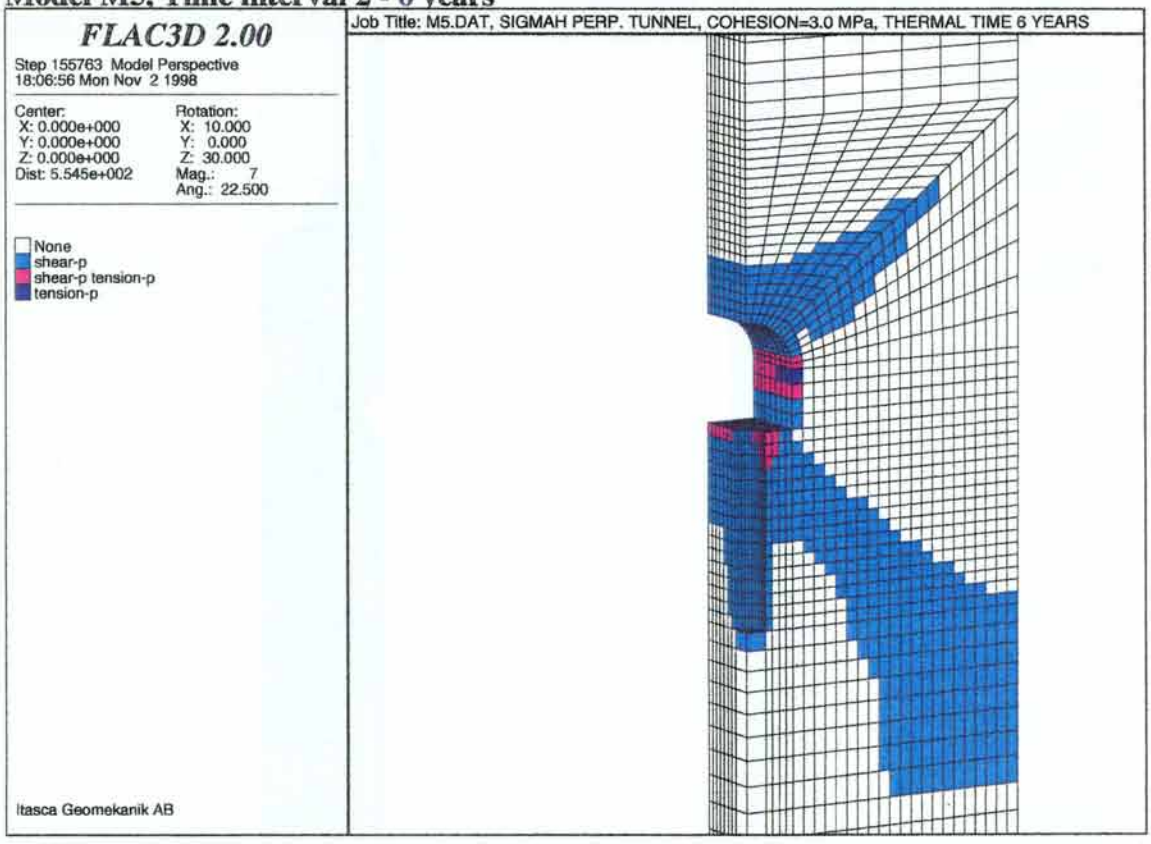

Model M5, Time interval 6 - 12 years

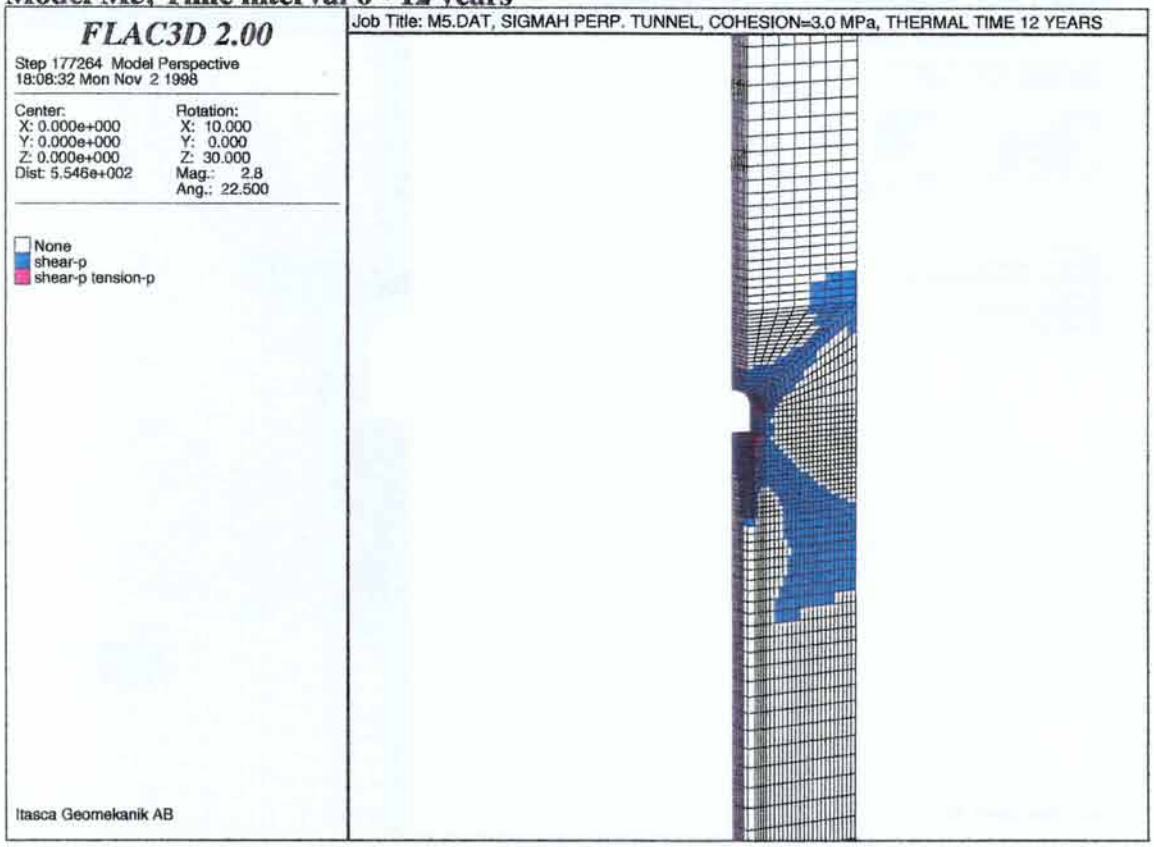

Model M5, Time interval 12 - 25 years

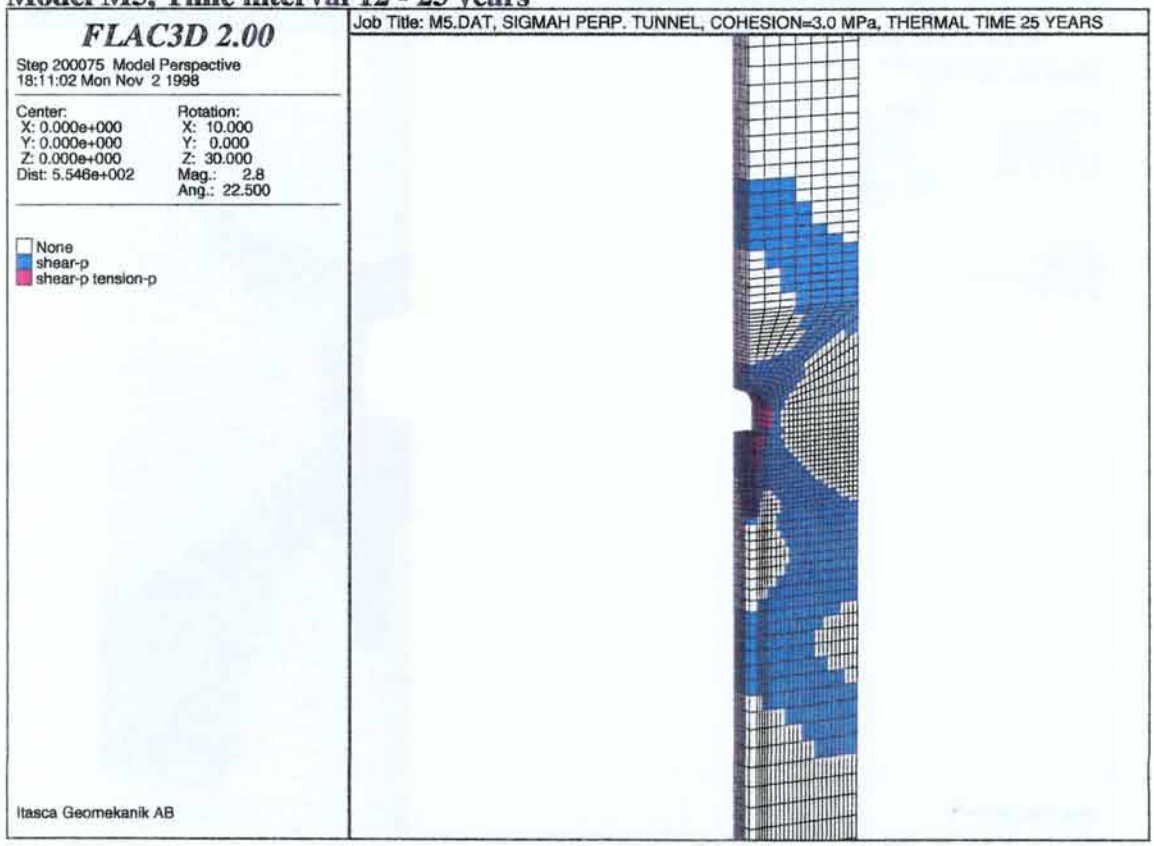

Model M5, Time interval 25 - 50 years

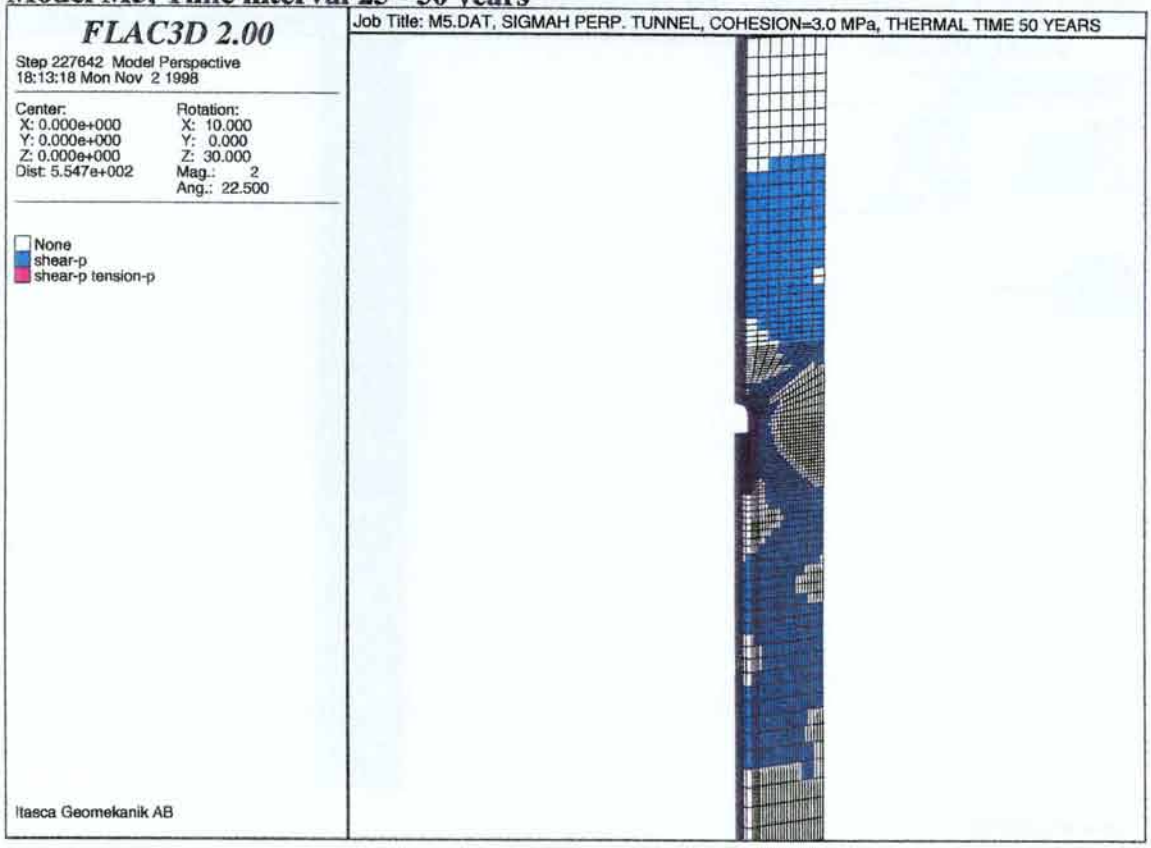

Model M5, Time interval 50 - 200 years (upper part of model)

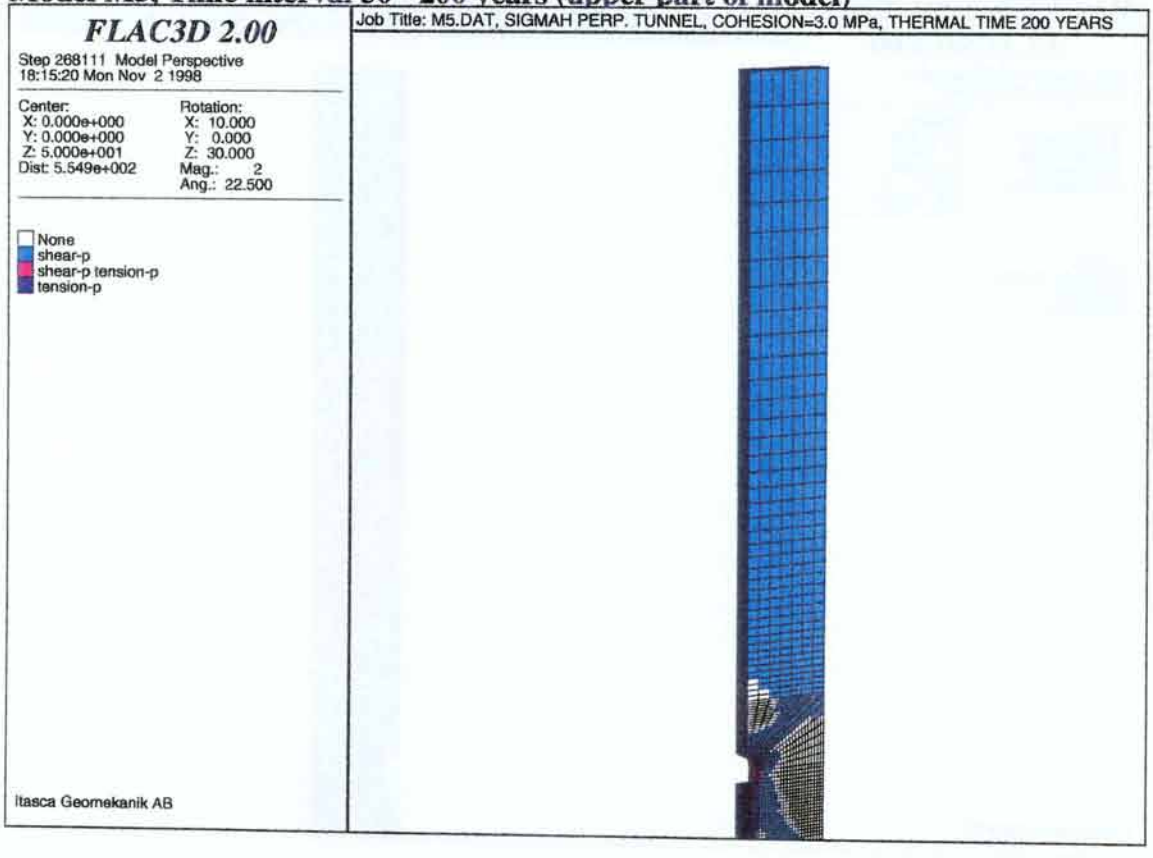

Model M5, Time interval 50 - 200 years (lower part of model)

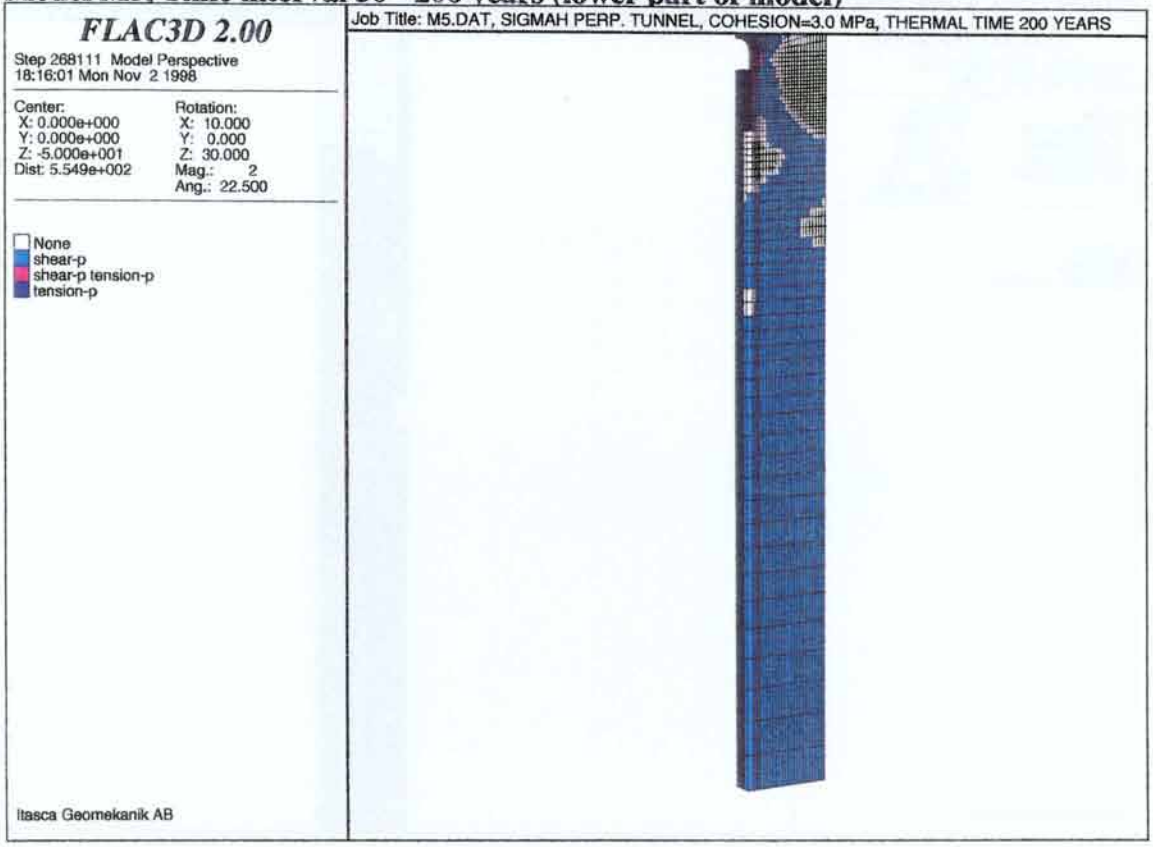

Model M5, Time interval 200 - 1 000 years (upper part of model)

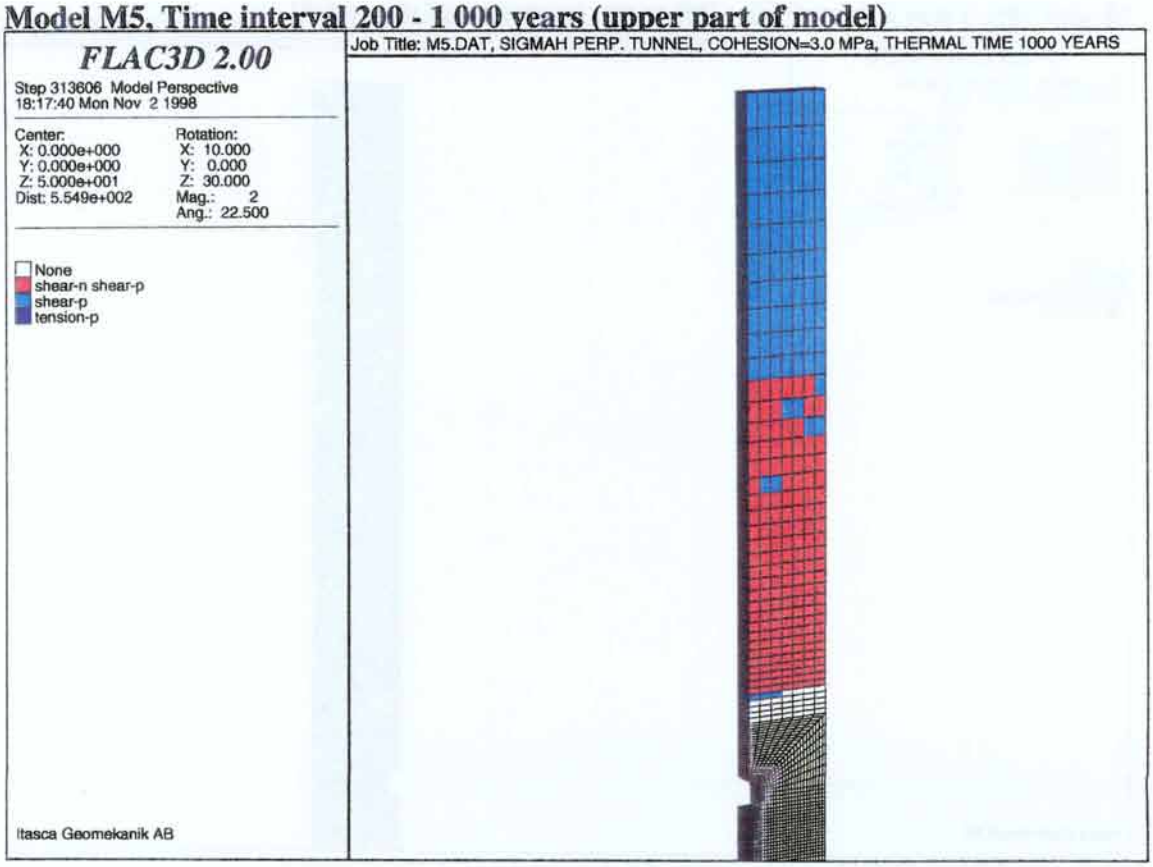

Model M5, Time interval 200 - 1 000 years (lower part of model)

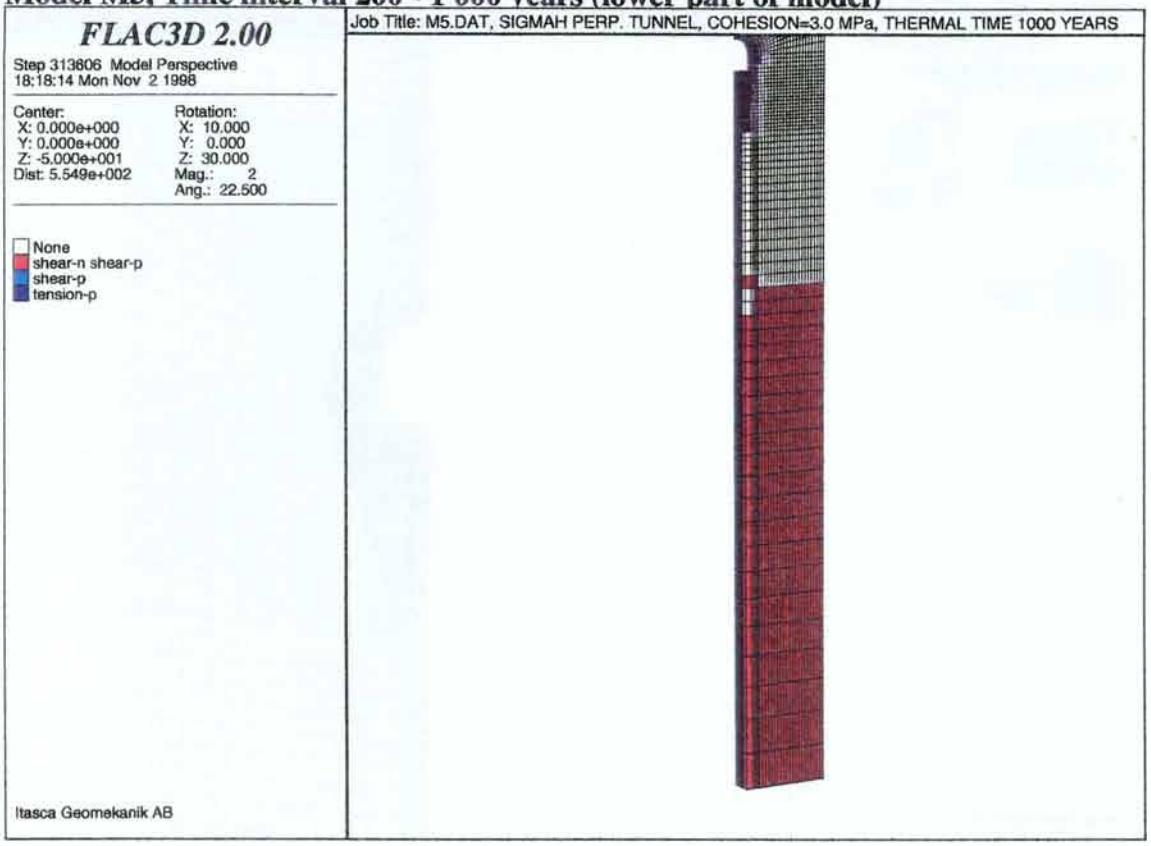

Model M5, Time interval 1 000 - 2 500 years

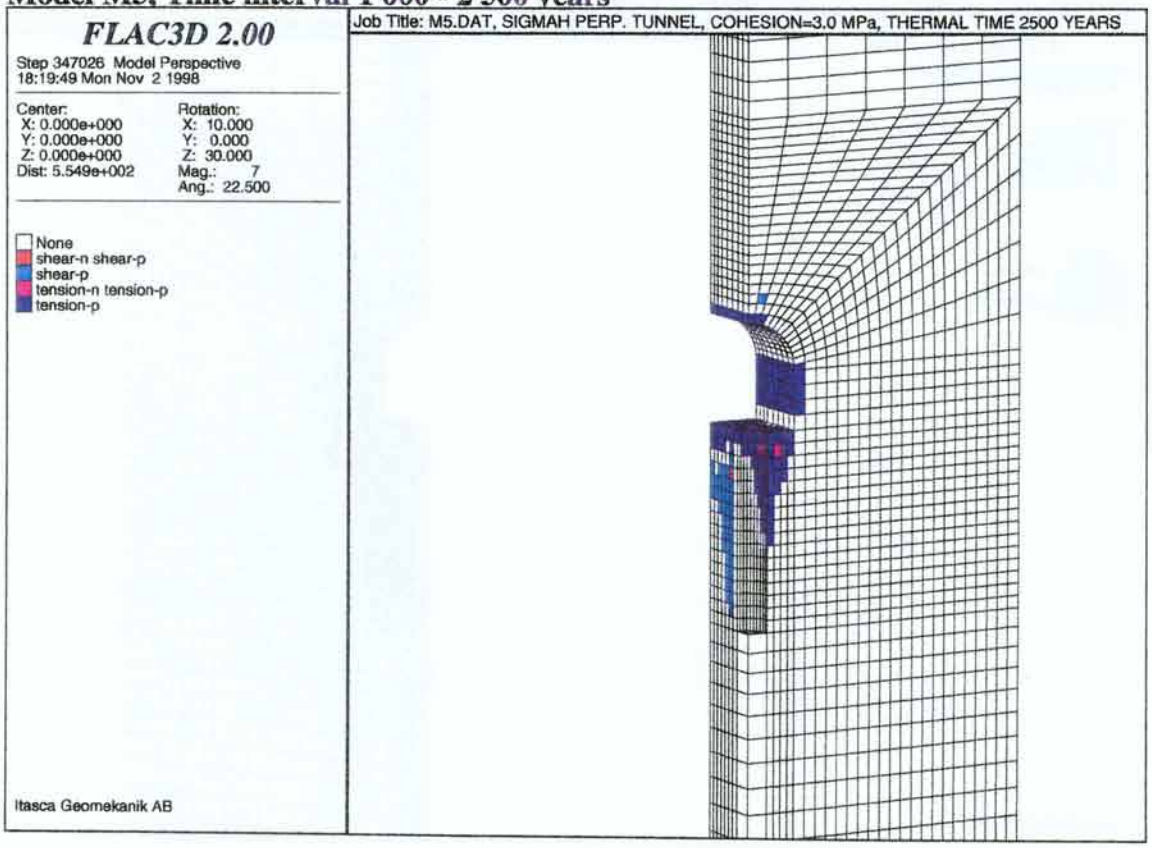

Model M5, Time interval 2 500 - 5 000 years

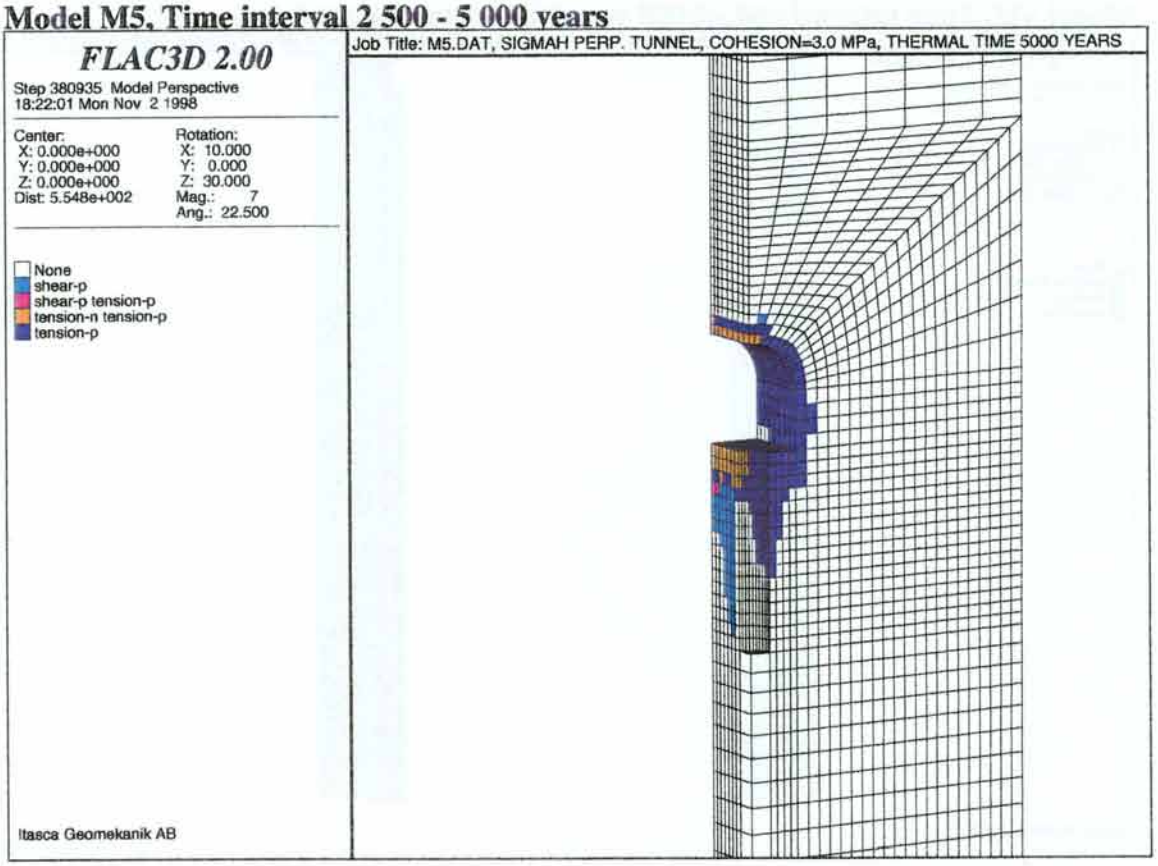

Model M5, Time interval 5 000 - 10 000 years

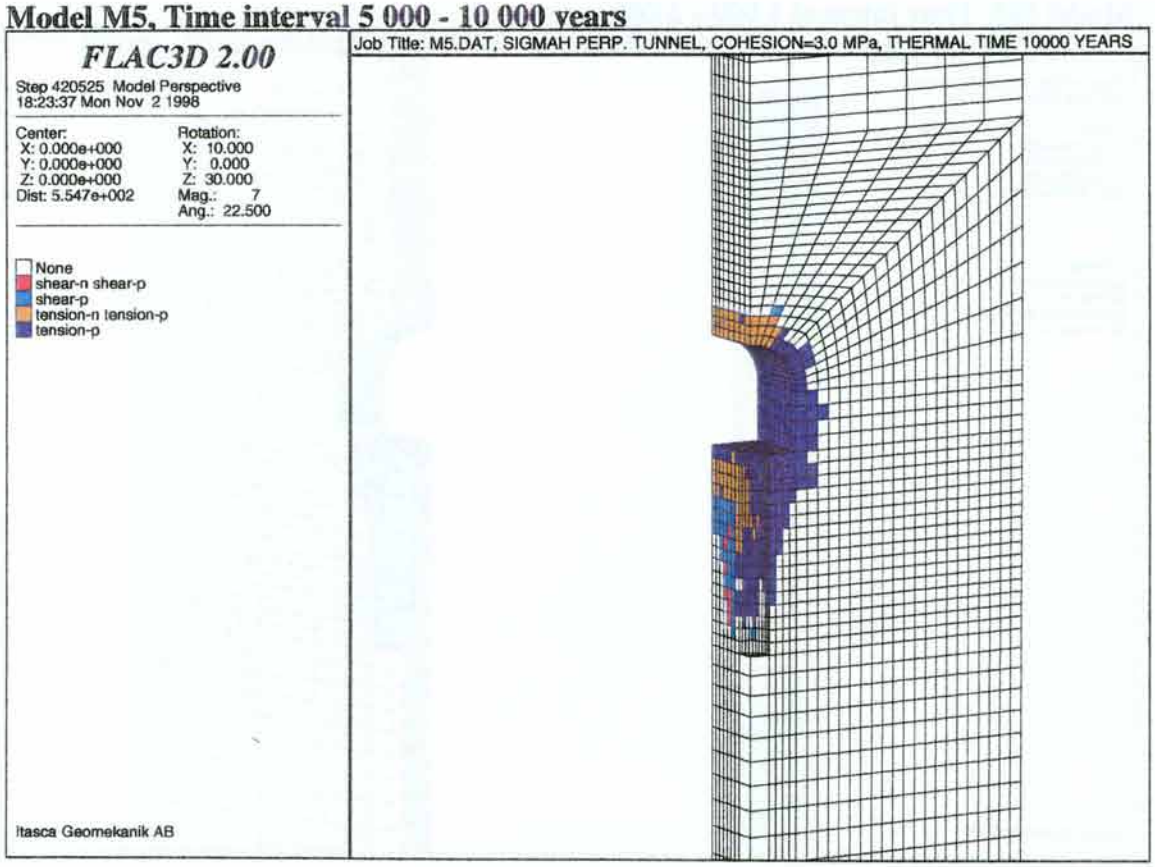

Appendix F: PLASTICITY STATE OF THE ZONES FOR MODEL M8

Plasticity state indicators for the thermo-mechanical calculations shows which zones that have been activated for that particular time interval. Thus, a zone can have state yield at one time interval and state no yield at another time interval.

In the subsequent figures, plasticity states of zones are identified by different colours with the following meaning:

None elastic,

Shear-n at shear yield now,

Shear-p elastic, but previously at shear yield,

Tension-n at tensile yield now,

Tension-p elastic, but previously at tensile yield.

These states can be combined and the combination will have its own colour (e.g. shear-p combined with tension-p).

List of thermo-mechanical models

Model	**Direction of major horizontal stress relative to repository tunnel axis**	**Rock mass cohesion [MPa]**	**Rock mass friction angle** [°]	**Effective or total stress analysis**
M1	Parallel	5	30	Effective
M2	Parallel	3	30	Effective
M3	Parallel	1	30	Effective
M4	Perpendicular	5	30	Effective
M5	Perpendicular	3	30	Effective
M6	Perpendicular	1	30	Effective
M7	Parallel	5	30	Total
M8	Parallel	5	45	Effective

Model M8, Time 0 years (Groundwater pressure initiated)

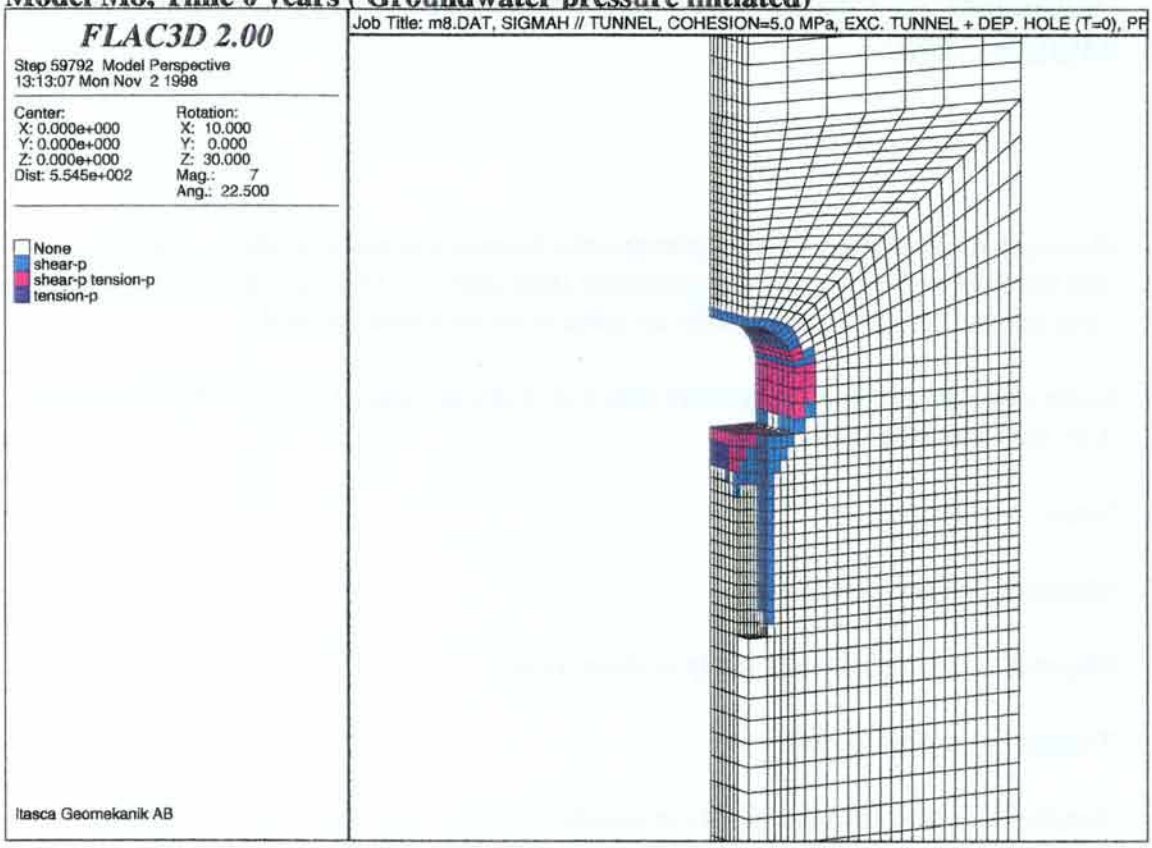

Model M8, Time interval 0 - 0.5 years

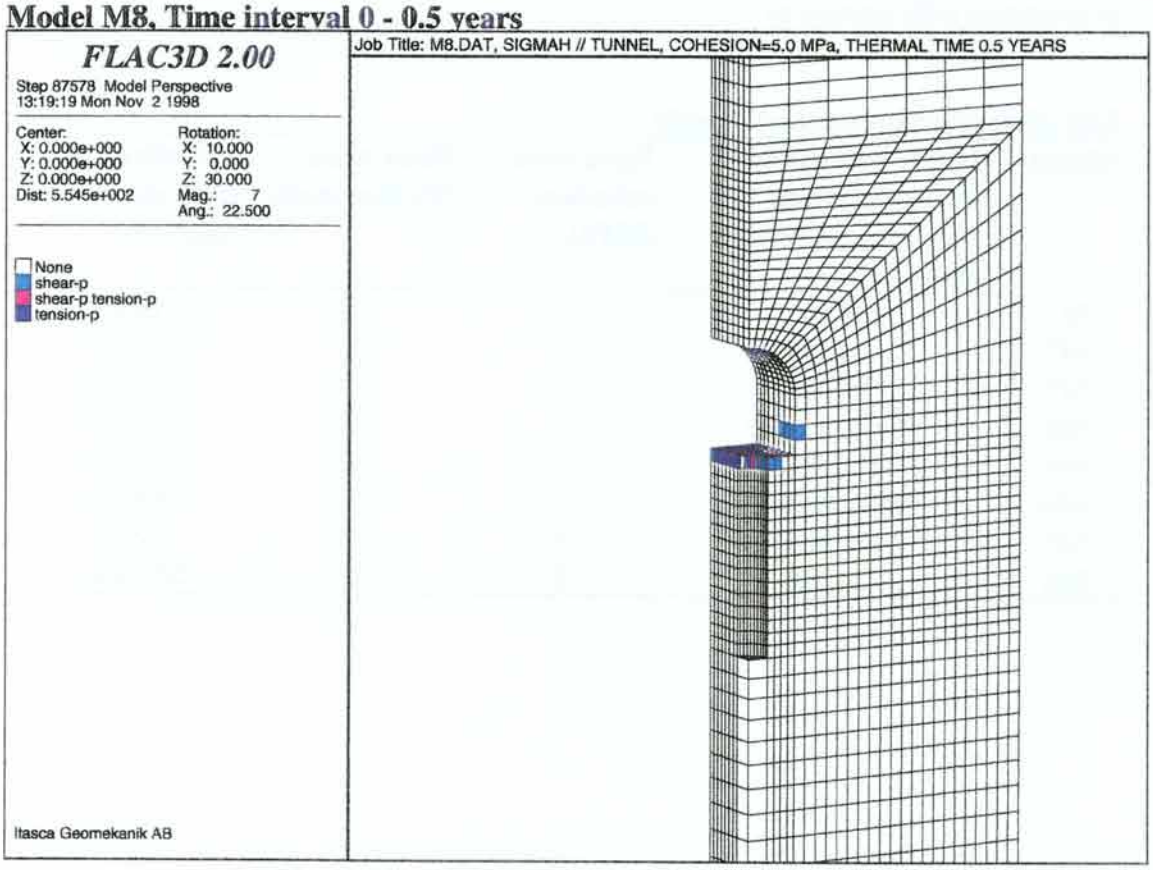

Model M8, Time interval 0.5 - 2 years

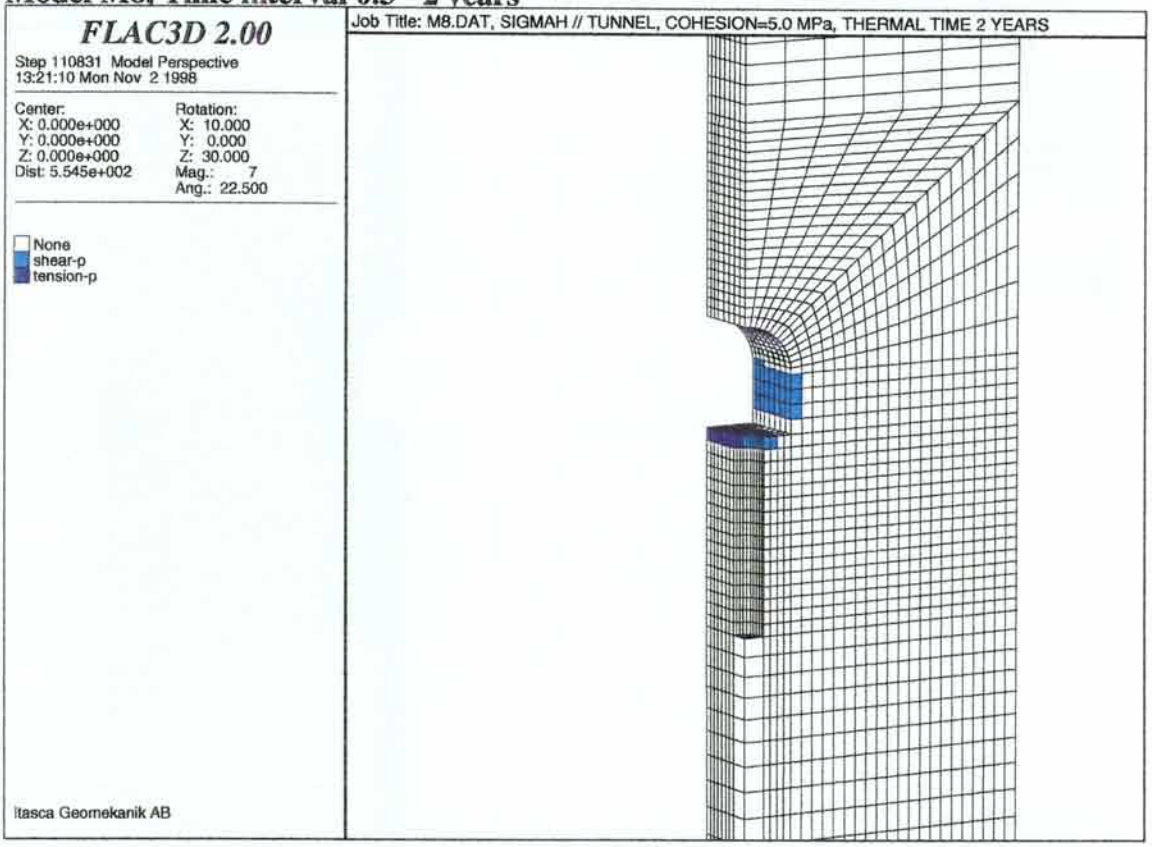

Model M8, Time interval 2 - 6 years

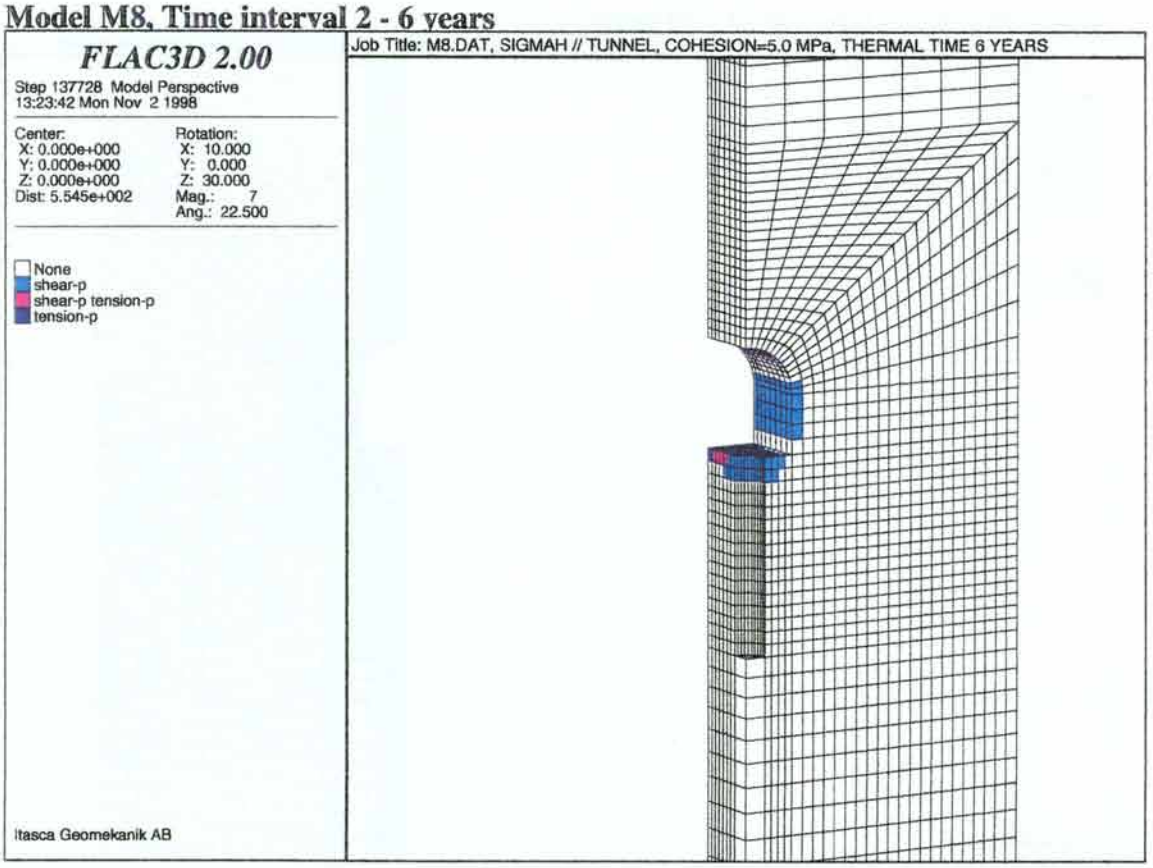

Model M8, Time interval 6 - 12 years

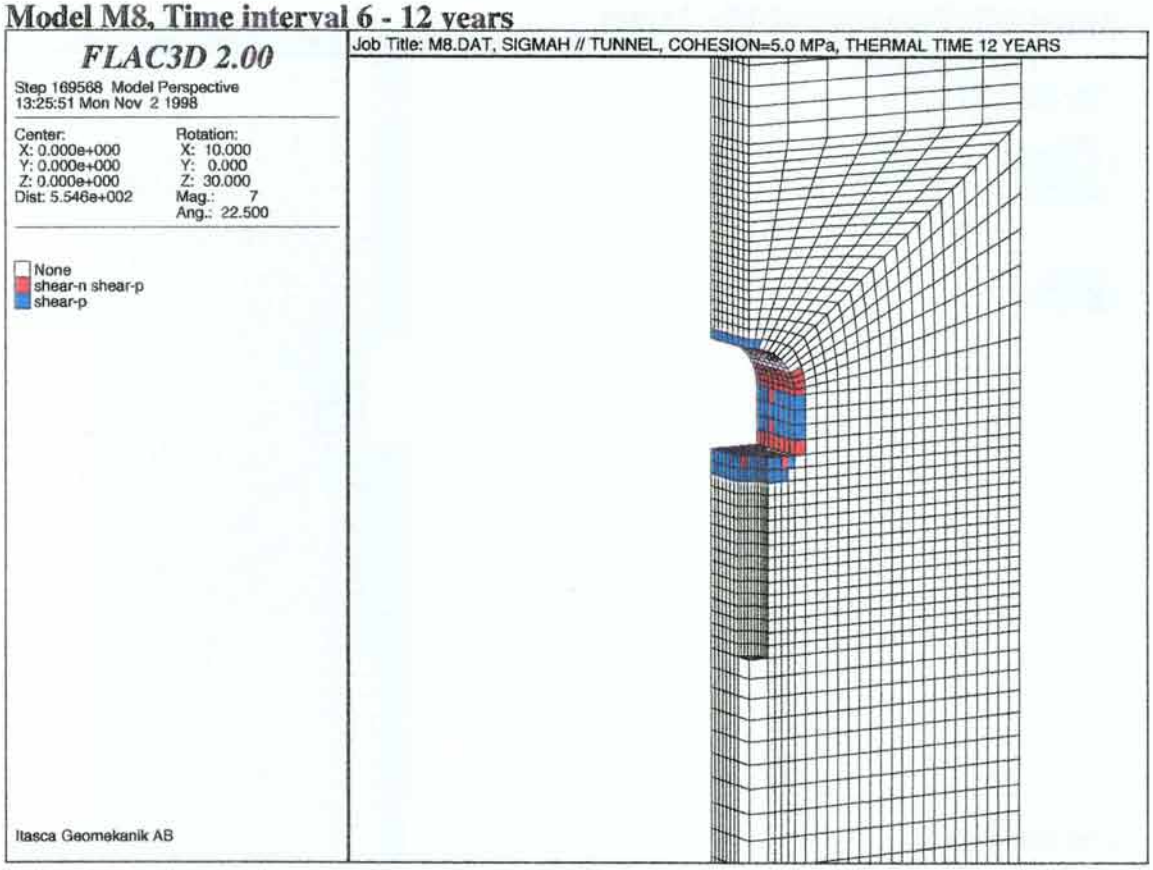

Model M8, Time interval 12 - 25 years

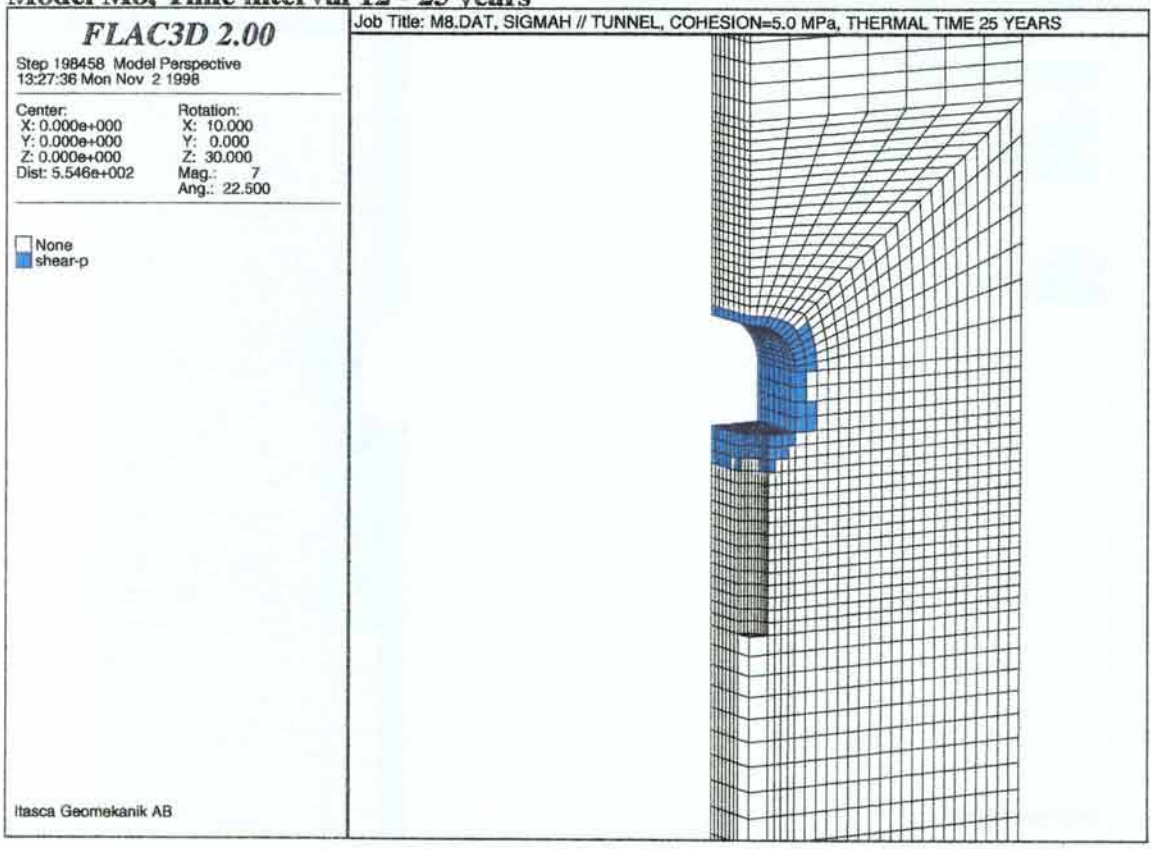

Model M8, Time interval 25 - 50 years

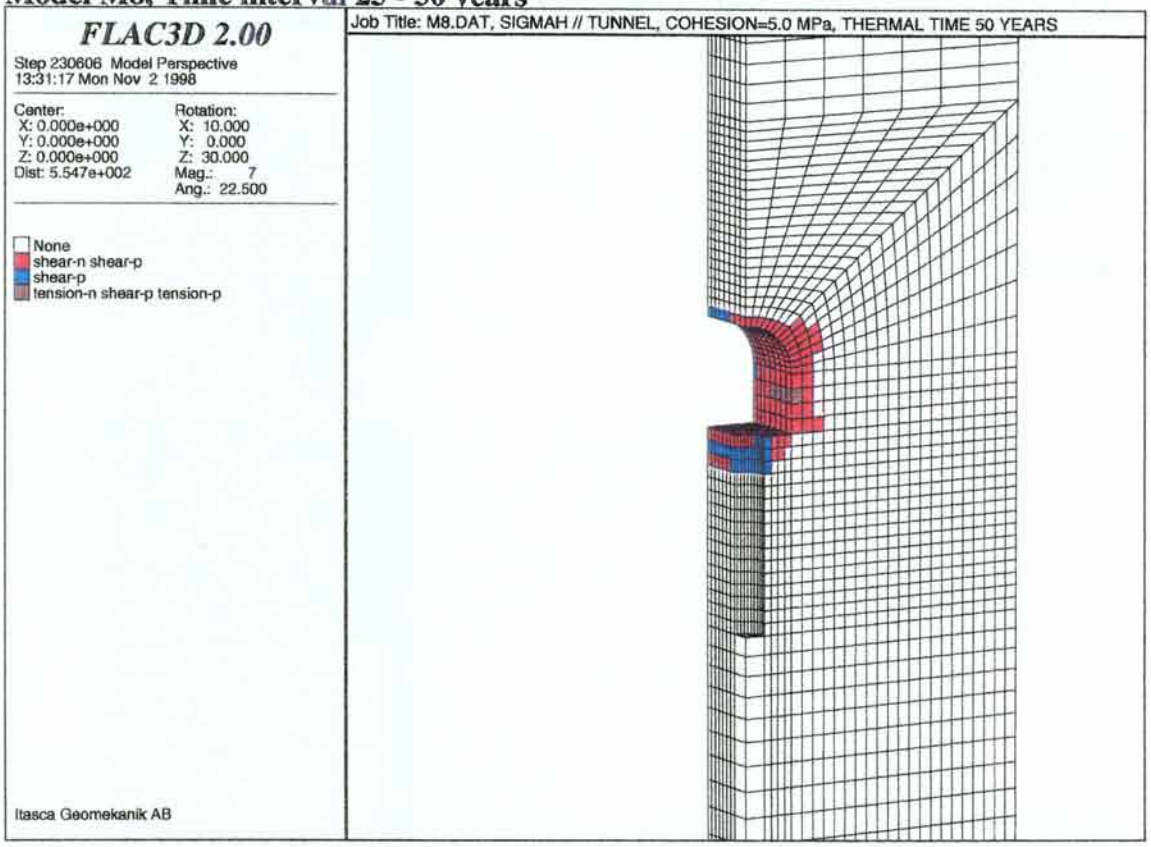

Model M8, Time interval 50 - 200 years

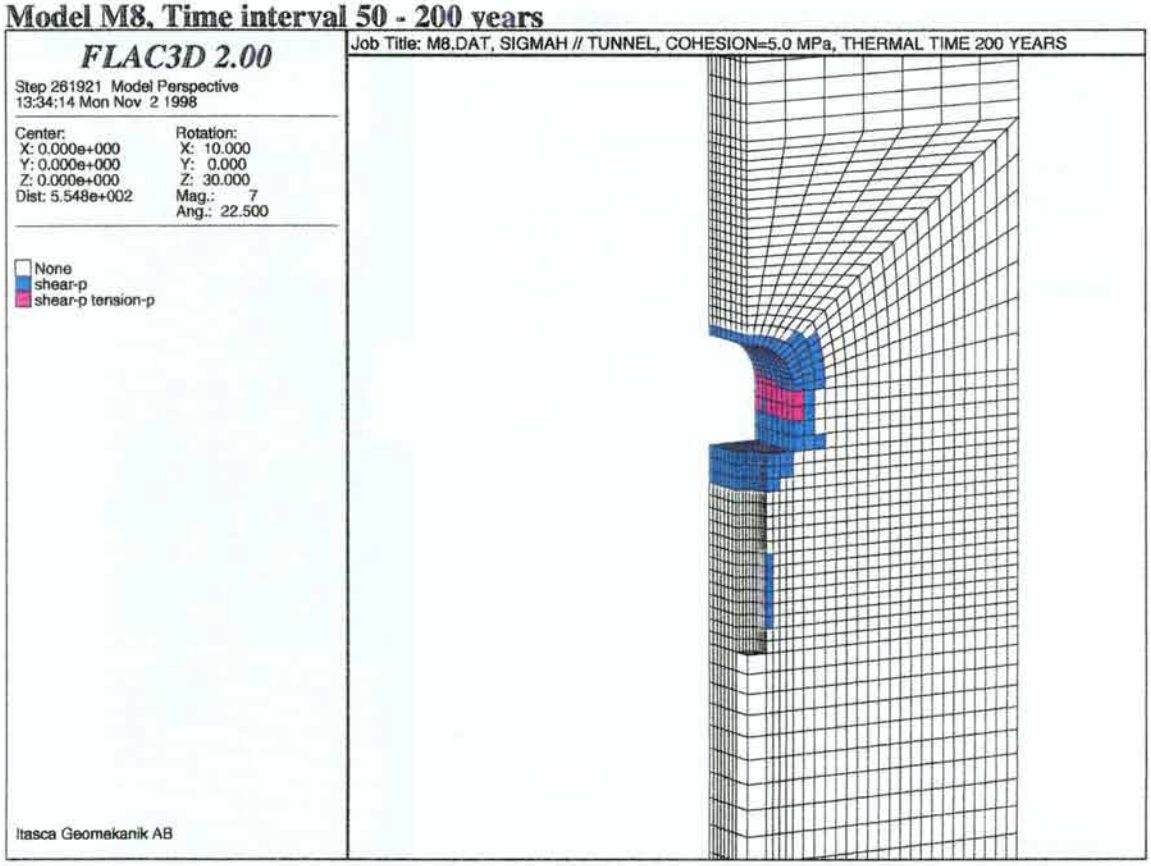

Model M8, Time interval 200 - 1 000 years

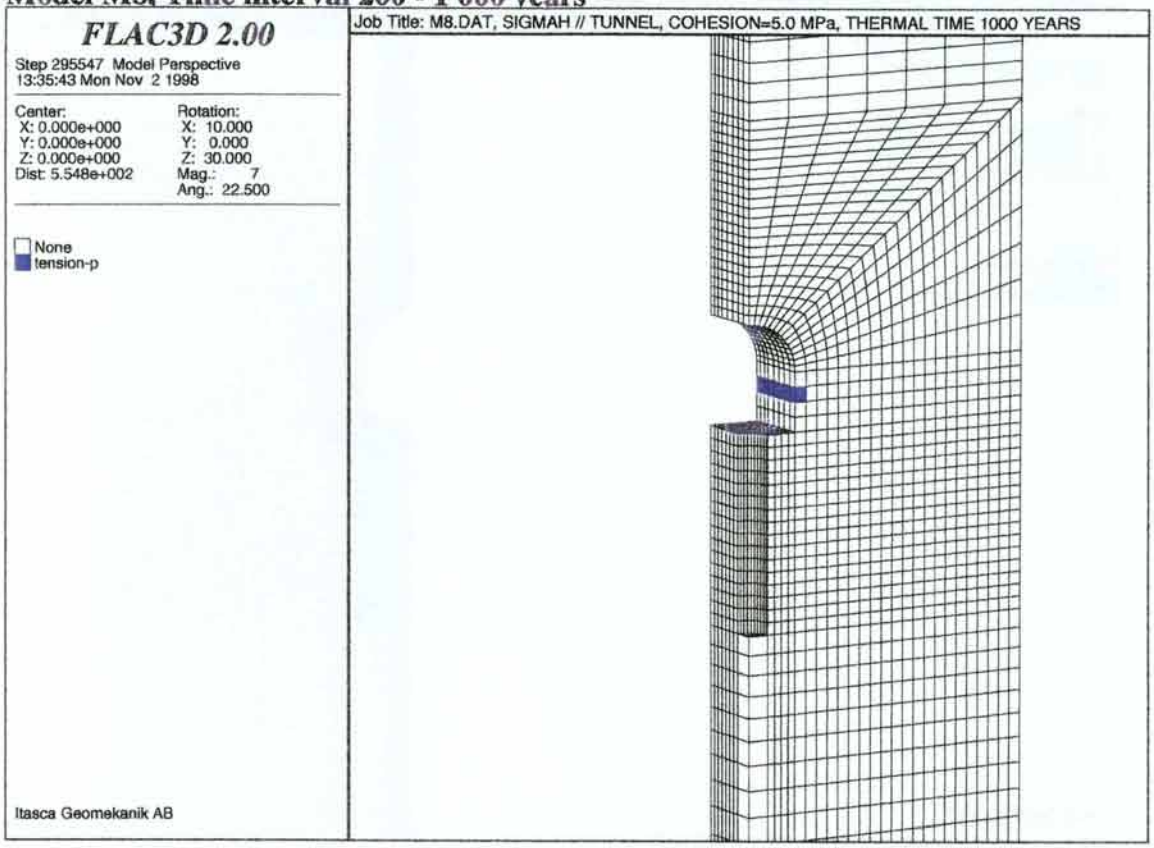

Model M8, Time interval 1 000 - 2 500 years

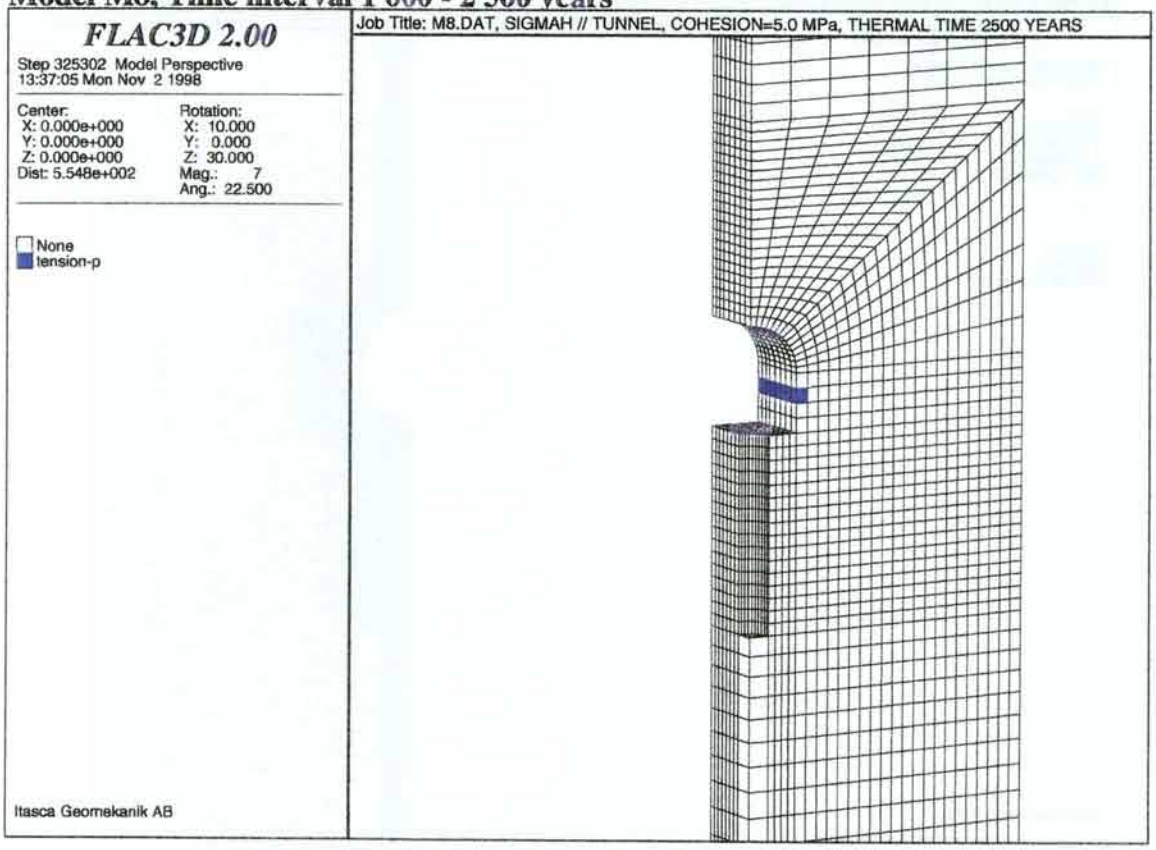

Model M8, Time interval 2 500 - 5 000 years

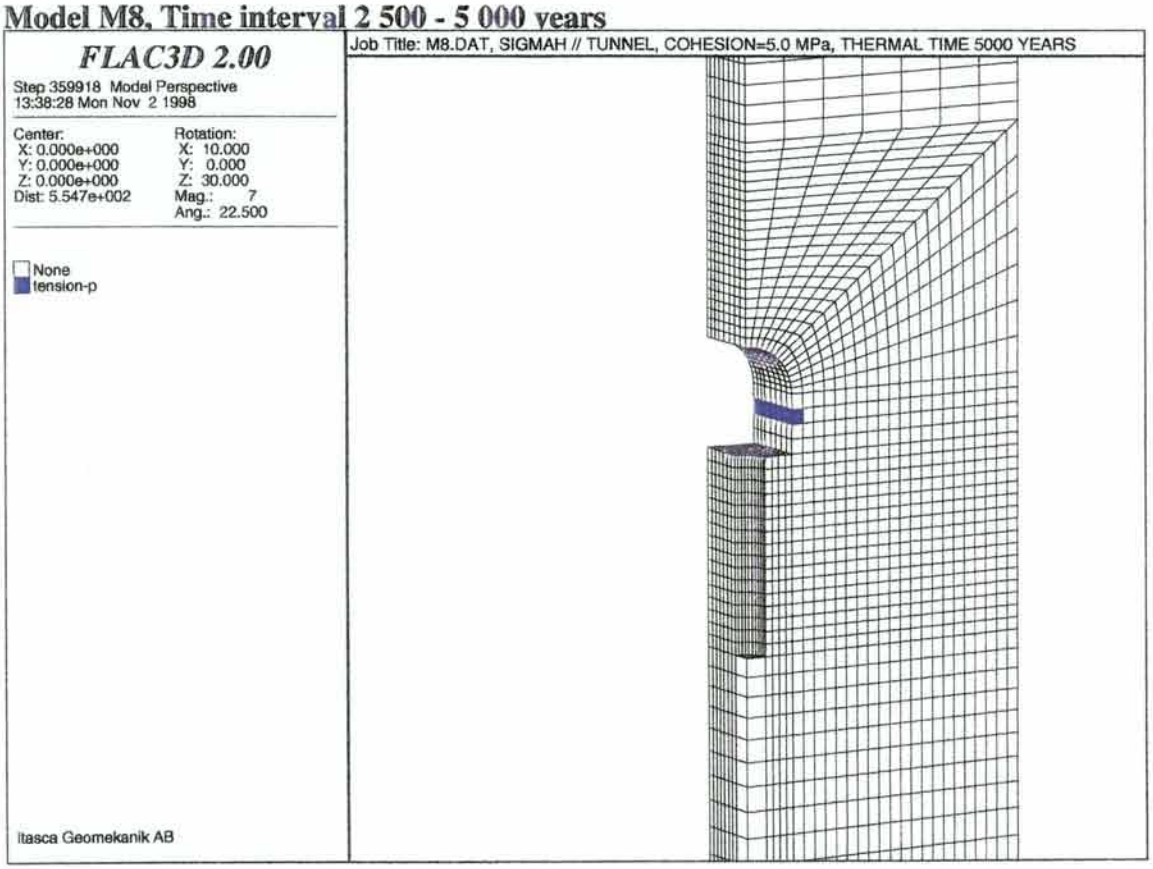

Model M8, Time interval 5 000 - 10 000 years

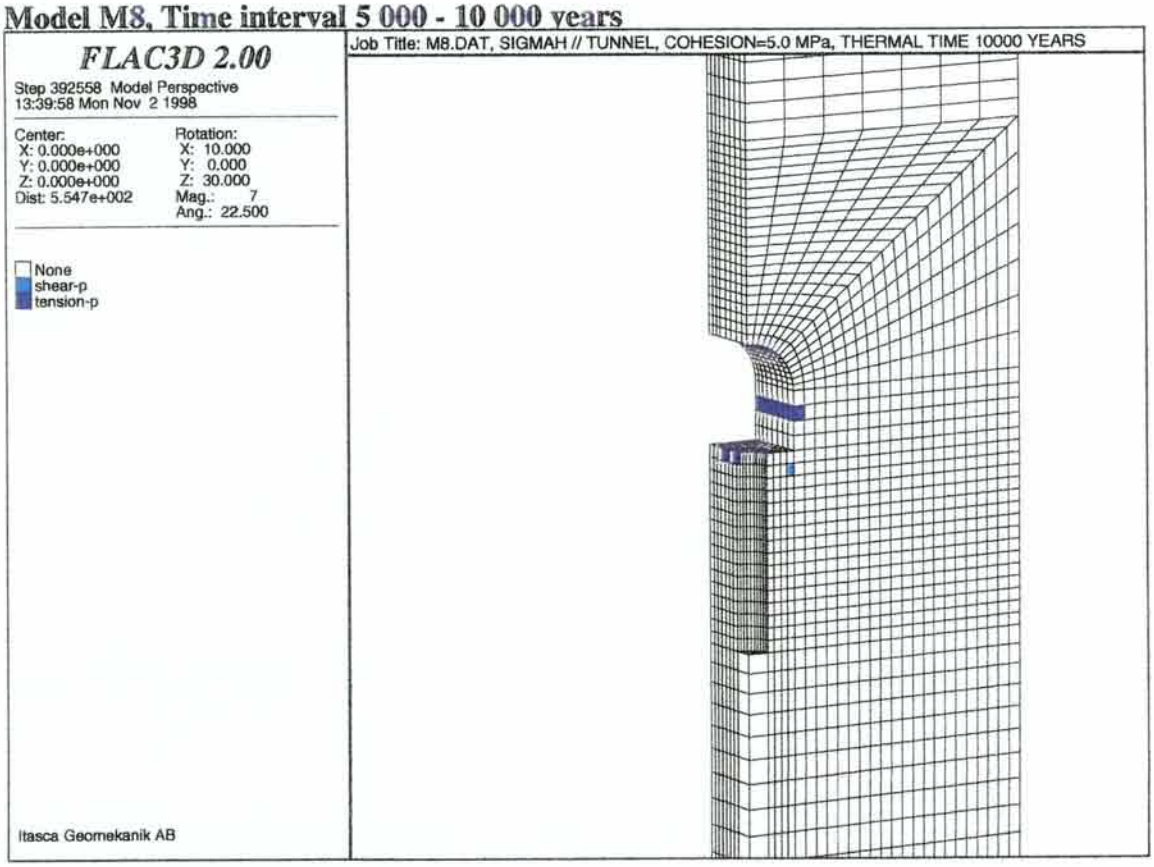

Appendix G: PLASTICITY STATE OF THE ZONES FOR MODEL M7

Plasticity state indicators for the thermo-mechanical calculations shows which zones that have been activated for that particular time interval . Thus, a zone can have state yield at one time interval and state no yield at another time interval.

In the subsequent figures, plasticity states of zones are identified by different colours with the following meaning:

None elastic,

Shear-n at shear yield now,

Shear-p elastic, but previously at shear yield,

Tension-n at tensile yield now,

Tension-p elastic, but previously at tensile yield.

These states can be combined and the combination will have its own colour (e.g. shear-p combined with tension-p).

List of thermo-mechanical models

Model	Direction of major horizontal stress relative to repository tunnel axis	Rock mass cohesion [MPa]	Rock mass friction angle [°]	Effective or total stress analysis
M1	Parallel	5	30	Effective
M2	Parallel	3	30	Effective
M3	Parallel	1	30	Effective
M4	Perpendicular	5	30	Effective
M5	Perpendicular	3	30	Effective
M6	Perpendicular	1	30	Effective
M7	Parallel	5	30	Total
M8	Parallel	5	45	Effective

Model M7, Time 0 years

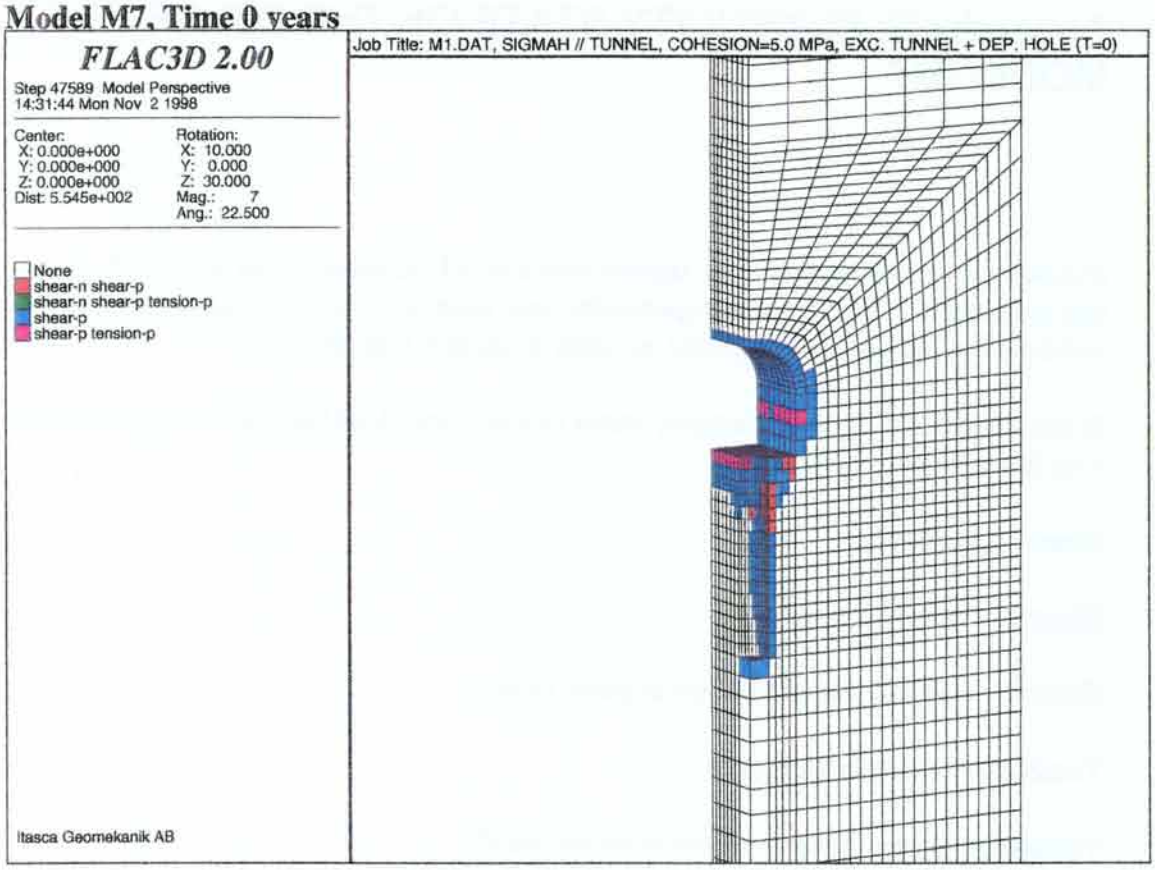

Model M7, Time interval 0 - 0.5 years

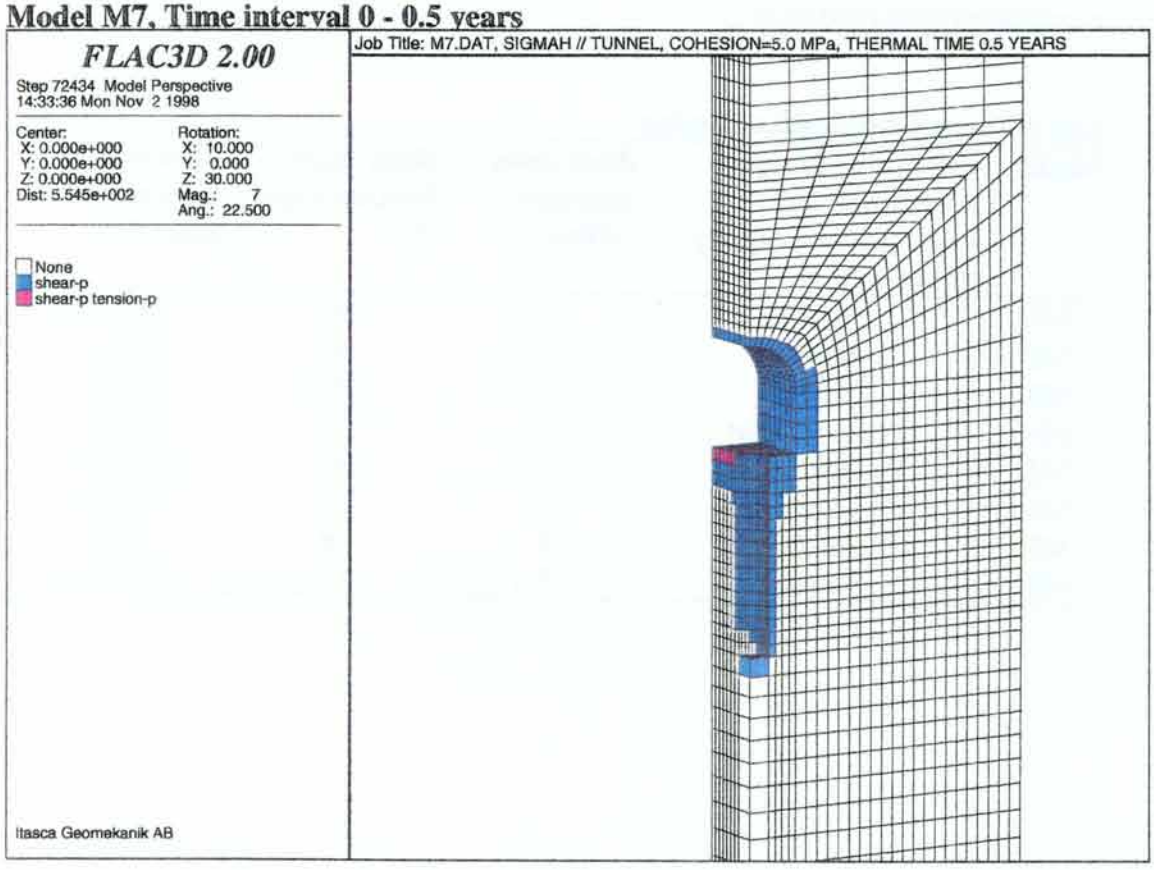

Model M7, Time interval 0.5 - 2 years

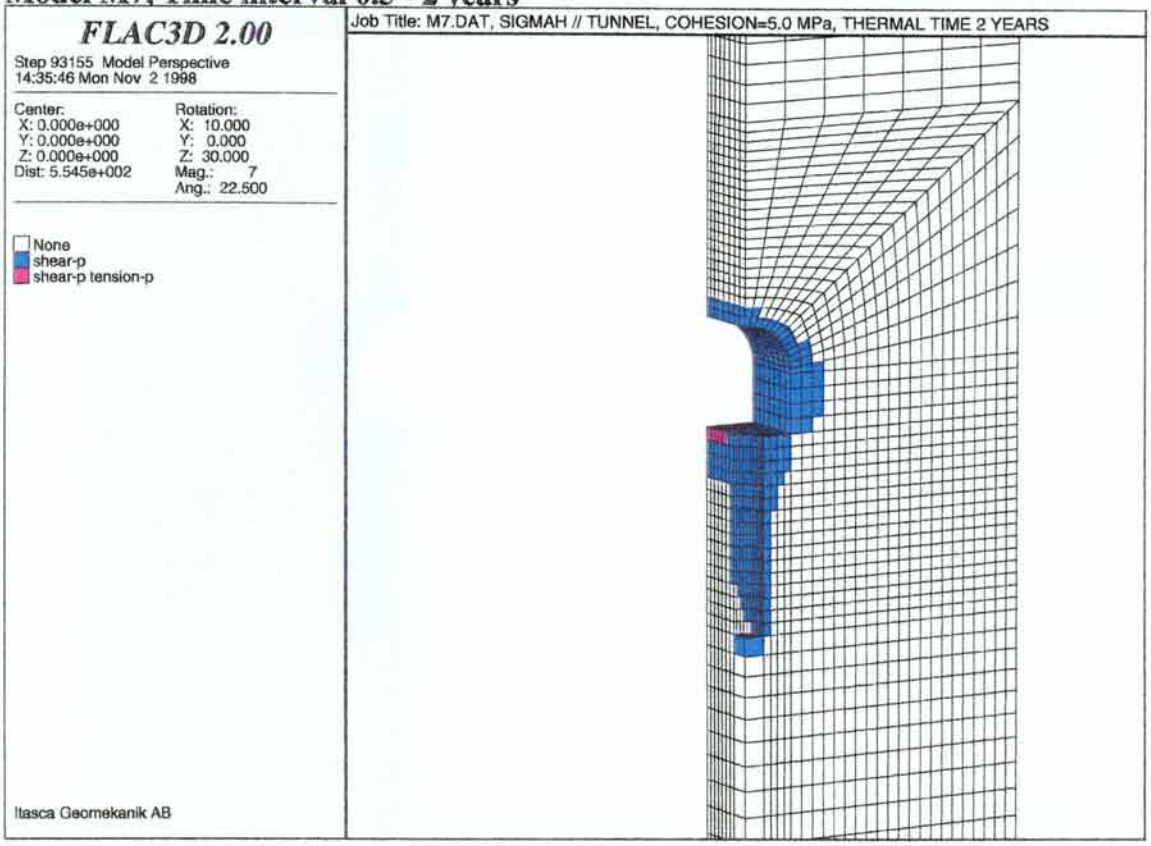

Model M7, Time interval 2 - 6 years

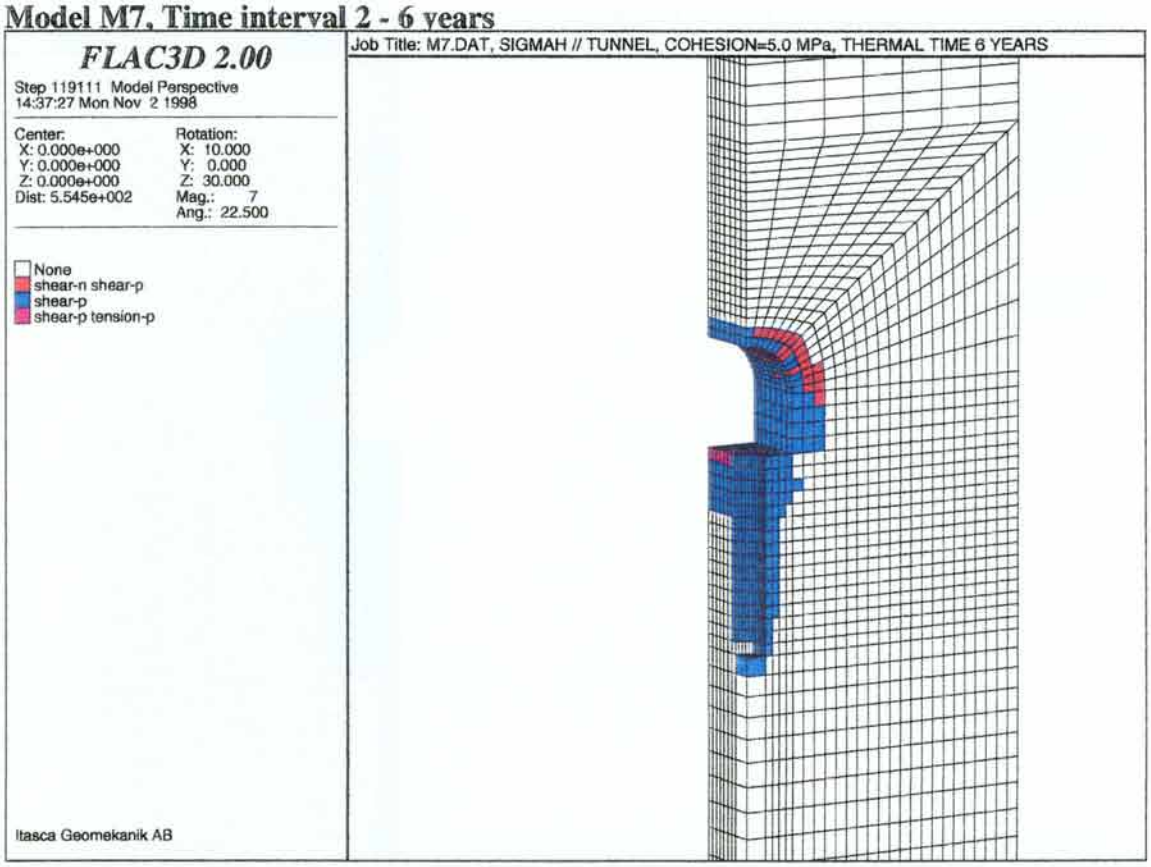

Model M7, Time interval 6 - 12 years

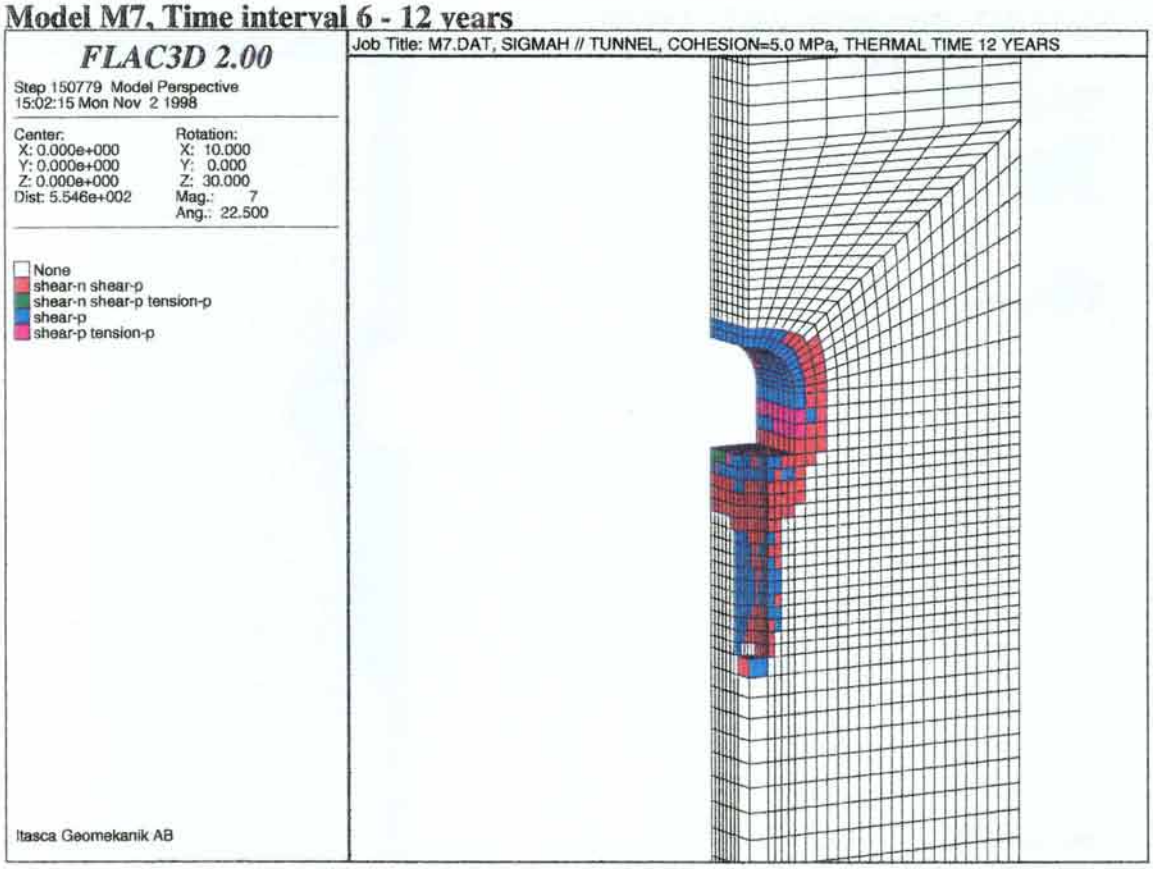

Model M7, Time interval 12 - 25 years

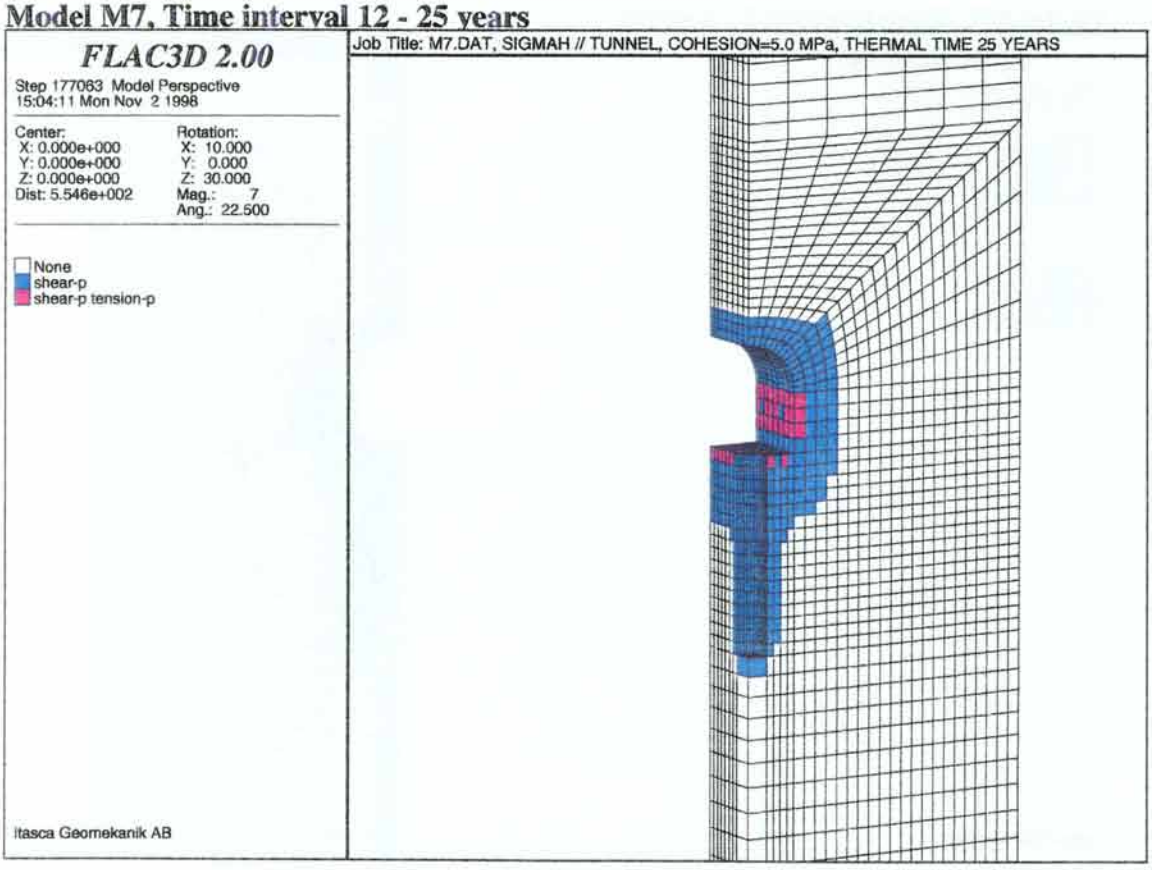

Model M7, Time interval 25 - 50 years

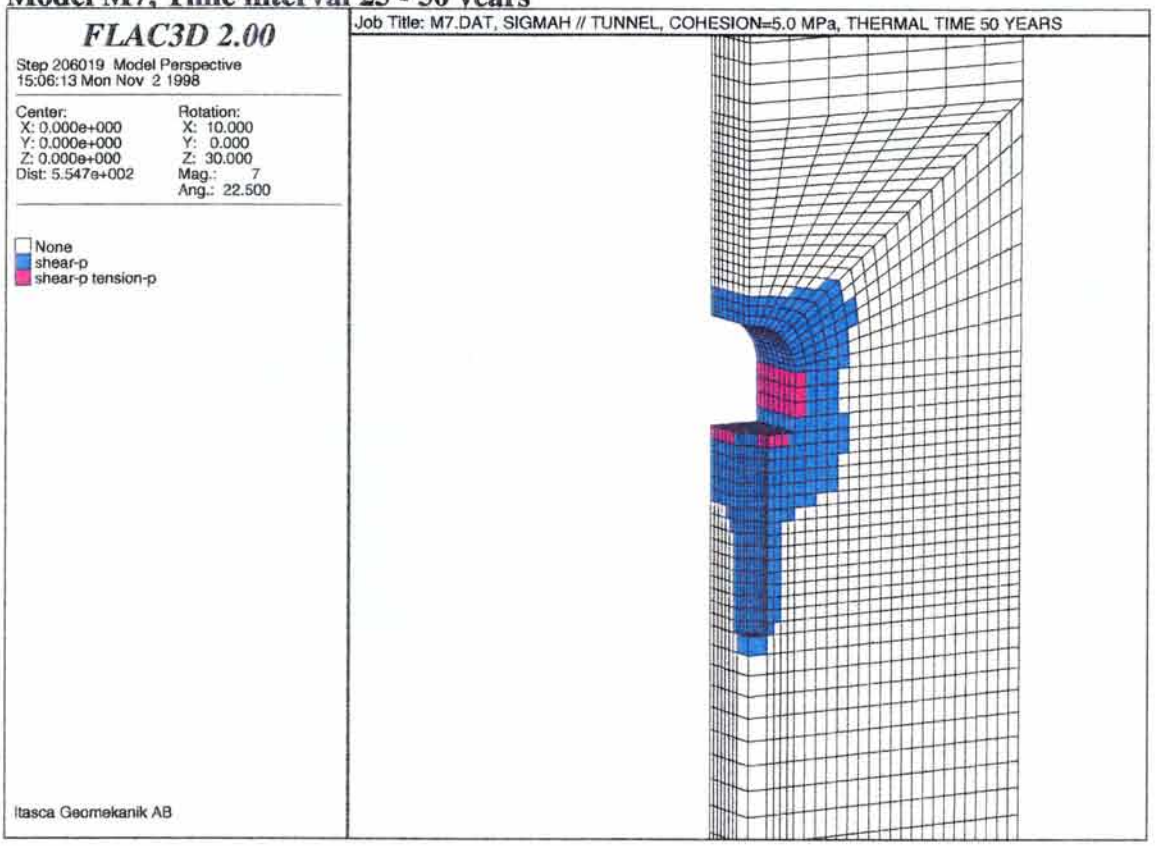

Model M7, Time interval 50 - 200 years

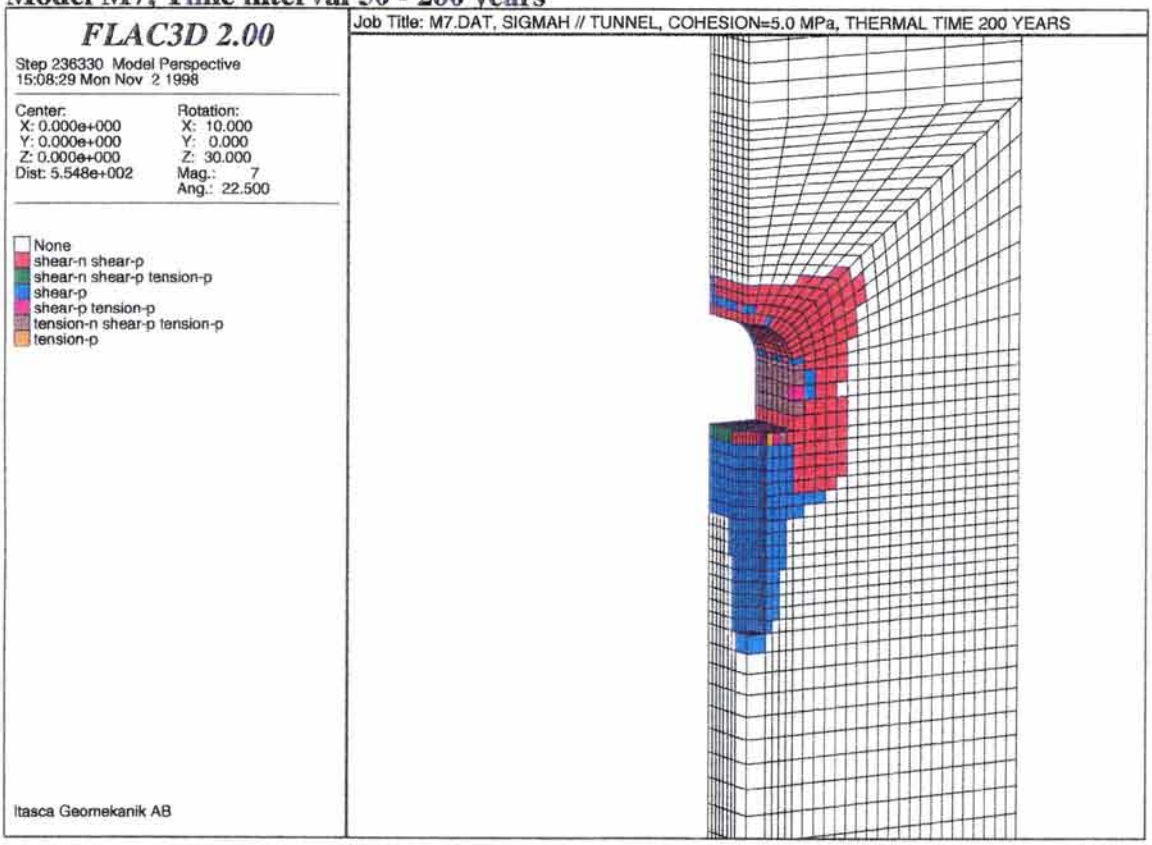

Model M7, Time interval 200 - 1 000 years

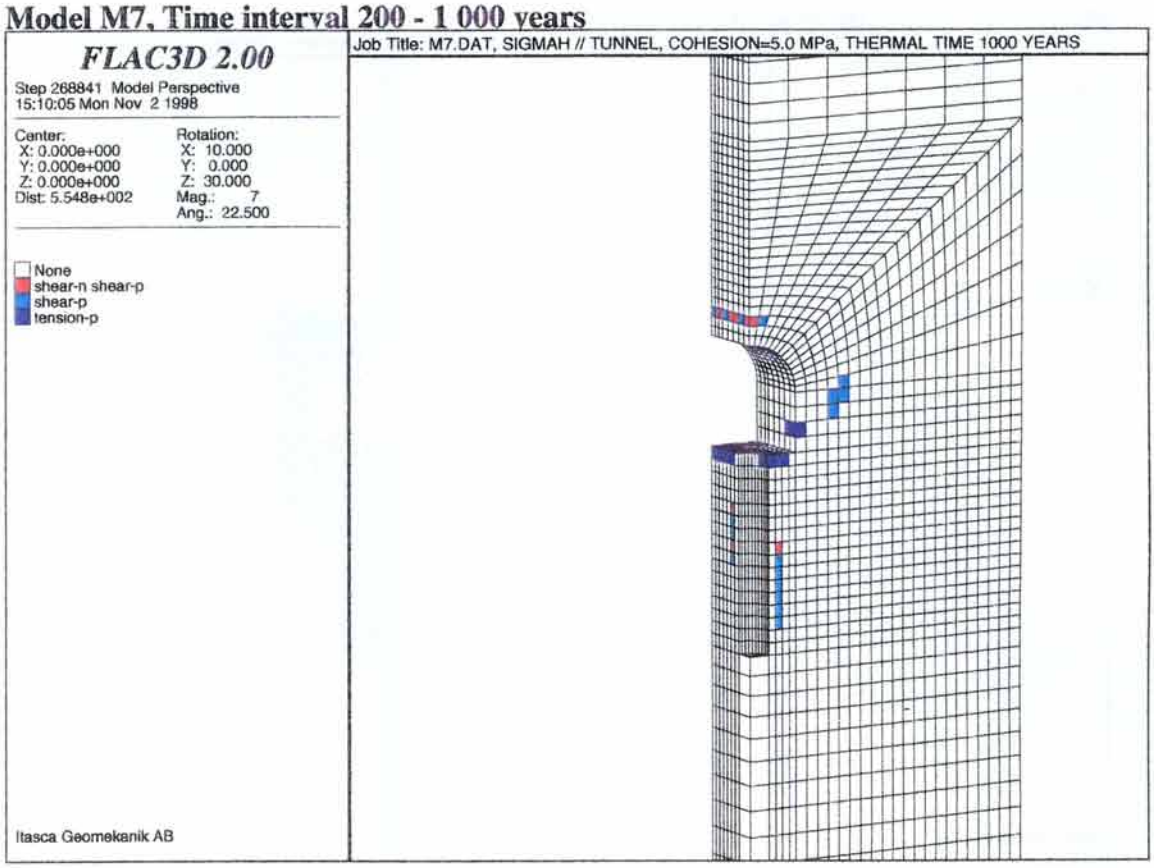

ISSN 1404-0344
CM Gruppen AB, Bromma, 1999